Masteroppgave

NTNU
Norges teknisk-naturvitenskapelige universitet
Fakultet for naturvitenskap
Institutt for bioteknologi og matvitenskap

Tor-Erik Holt Paulsen

Evaluation of Optimal Light Quality for Growing *Rhodomonas baltica*

Masteroppgave i Industriell kjemi og bioteknologi
Veileder: Olav Vadstein
Medveileder: Maren R. Gagnat
August 2021

NTNU
Kunnskap for en bedre verden

CFEED

Tor-Erik Holt Paulsen

Evaluation of Optimal Light Quality for Growing *Rhodomonas baltica*

Masteroppgave i Industriell kjemi og bioteknologi
Veileder: Olav Vadstein
Medveileder: Maren R. Gagnat
August 2021

Norges teknisk-naturvitenskapelige universitet
Fakultet for naturvitenskap
Institutt for bioteknologi og matvitenskap

NTNU
Kunnskap for en bedre verden

NTNU

TBT4900
Biotechnology, Master's Thesis

Evaluation of Optimal Light Quality for Growing *Rhodomonas baltica*

Thesis

Student
Tor-Erik H. Paulsen
tepaulse@stud.ntnu.no

Supervisors
Professor in Microbial Ecology
at NTNU
Olav Vadstein
olav.vadstein@ntnu.no
&
Research Biologist
at C-Feed AS
Maren R. Gagnat
maren@cfeed.no

31st August 2021

Preface

Due to the shared interest of improving the process of microalgae cultivation, I initiated a collaboration with the microalgae & zooplankton producer C-Feed AS. With qualified help from Professor O. Vadstein, and M. R. Gagnat at C-Feed a project was constructed. As most constructions, delays occurred. However, to the best of my knowledge the project stayed within the budget.

I want to thank my two supervisors for their helpful advise and good support. Honorable mentions goes to Amalie Johanne H. Mathisen for aiding me in the laboratory, and Charlotte Volpe for providing me with help even though her doctoral thesis was due. Finally, I want to thank friends, coworkers and loved ones for keeping me sane through five years of higher education.

Contents

Abstract

Phototrophic cultivation of microalgae using artificial light require large amounts of energy. In order to enhance economically feasibility, the production process needs to utilize optimal light qualities. With the aim of finding the combinations of monochrome light that gave the highest maximum specific growth rate (μ_{max}) for the cryptophyceae *Rhodomonas baltica* Karsten 1898, this study applied fractions of red (λ: 620-625 nm), green (λ: 522-525 nm) and blue (λ: 465-467 nm) light at a total photo flux density of 100 µmol/m^{2}s. The light composition study was conducted using a recently published method that utilized a micro-scale photo bioreactor (PBR) named Nanocosm and 96-well plates (WP). This study showed that *R. baltica* can grow at a high growth rate ($> 0.90\,\mathrm{d}^{-1}$) using different light regimes in WPs. It was found that the use of 10-30% green and 90-70% red light gave a μ_{max} 17-37% higher than 100% red light.

This study also found that the results at WP scale were comparable to observations at litre scale, thereby supporting the scalability. By using different nutrient media, this study confirmed that nutrient starvation of *R. baltica* reduced QY (quantum yield), and that nitrogen limitation cause color change related to pigment degradation. Finally, different methods of measuring biomass density and calculating μ_{max} was evaluated.

Sammendrag

Fototrof dyrking av mikroalger ved hjelp av kunstig belysning er en energikrevende prosess. For å forbredre prosessens økonomiske bærekraft bør den optimale lyskvaliteten benyttes. Med mål om å finne den kombinansjonen av monokrome lyskvaliteter som gav høyest maksimale vekstrate (μ_{max}) for svelgflagellaten *Rhodomonas baltica* Karsten 1898, ble det brukt kombinasjoner av rødt (λ: 620-625 nm), blått (λ: 465-467 nm) og grønt (λ: 522-525 nm) lys med en samlet fotonflukstetthet på 100 µmol/m^{2}s. Forsøkene med ulike lykvaliteter benyttet en nylig publisert metode ved hjelp av en mikro-skala fotobioreaktor (PBR) kalt Nanocosm og 96-brønners brett (BB). Denne studien har vist at *R. baltica* kan vokse med høy vekstrate ($> 0.90\,\mathrm{d}^{-1}$) under ulike sammensettninger av lys i et BB. Videre ble det funnet at en kombinasjon av 10-30% grønt og 90-70% rødt lys gav en 17-37% høyere μ_{max} enn ved bruk av 100% rødt lys.

Denne studien viste også at resultatene funnet i BB-skala var sammenliknbare med observasjonene gjort i liter-skala og derav underbygget at de var skalerbare. Ved å benytte ulike næringsmedier har denne studien bekreftet at næringsmangel hos *R. baltica* resulterer i redusert kvanteutbytte (QY) og at nitrogenbegrensning forutsaker en fargeendring som skyldes pigmentnedbrytning. I tillegg ble ulike metoder for måling av biomassetetteht og beregning av μ_{max} evaluert.

1 Introduction

Microalgae are not only primary producers of nutrients (fat, carbohydrates, proteins etc.) in marine food webs[1,2], but the diverse group of species[3] also play an important role as a sustainable feed for aquaculture[4]. One example is the cryptophyte genus *Rhodomonas*, that is an attractive feed for some zooplankton[5,6], for example *nauplii* of the copepode *Acartia tonsa*. Studies show that this copepode is favourable as feed to fish larva of Atlantic cod (*Gadus morhua*), and ballan wrasse (*Labrus bergylta*)[7,8]. Therefore it has become a product sold to aquaculture industry farming fish like *Gadus morhua* as first feed for fish larva[7]. To sustain the cultivation of copepodes, nutritional microalgae are provided as the main food source[5,7].

A balanced nutritional mixture with high quality is important for a healthy development of fish[5,7,8]. Therefore copepodes must be fed microalgae that provide adequate proteins and fat etc.[9]. Some microalgae are known to accumulate a high level (70%) of triacylglycerols made from form fatty acids mainly synthesized in the chloroplast[10–12]. In *Rhodomonas* sp. there is a large proportion of long chained polyunsaturated fatty acids. For *Rhodomonas* sp. these fatty acids have a good bioavailability in predators like the copepodes. Furthermore, high nutritional values have been reported in copepodes when fed with the cryptomonads *Rhodomonas baltica*[7,13], making *R. baltica* a suitable candidate as copepode feed[6]. By controlling the microalgae growth conditions, a favourable nutritional quality can be obtained[10]. One such condition is light quality and quantity. Light affect the metabolic processes and biomass composition, and hence the nutritional quality of microalgae[11,14–16].

In order to assessment of how light quality effect microalgae growth, the light quantity should be constant and in excess. Low irradiation, caused by self shading[17] or low light penetration[18] etc., cause light limitation in photosynthetic organisms[15,16]. Too high irradiation on the other hand, can cause photoinhibition[15], or non-photochemical quenching (NPQ). The latter is a photoprotective response that down-regulates the photosynthetic pathway, resulting in heat production from the excess energy[19]. By using artificial light in the form of light emitting diodes (LED), the quality (wavelength) and irradiation can be optimized for growth[15,20]. In higher plants the ratio between red and blue light affect the mode of growth and production of small metabolites[21]. How light quality and quantity affect microalgae growth[22] can be understood by studying the complexity of photosynthesis[19].

Microalgae contain complex light harvesting systems for photosynthesis that have developed over billions of years[23]. This system consists of pigments that are organised in light harvesting complexes (LHC) embedded in the thylakoid membrane. In these LHC light energy is converted into electron transport or heat (NPQ). The electron transport chain enable the production of energy carrier molecules (ATP and NADH)[19]. Wavelengths between 400 - 700 nm[24] make up the photosynthetic active radiation (PAR)[25]. The array of pigments within an organism, and their organization determine what PAR that is absorbed[19]. The pigments are divided into chlorophylls (Chl), carotenoids, and phycobilins[25]. Chl *a* for instance has a peak of absorbance in the range 450 nm to 480 nm (blue) in addition to a peak close to 700 nm (red). Carotenoids aid photosynthesis by binding to peptides in the thylakoid membrane and forming light harvesting pigment-protein, and some carotenoids have a light protective function[26]. Phycobilins are found in both blue-green algae (cyanobacteria), cryptomonads, red algae etc.[27]. One

example is the phycobilin phycoerythrin (PE) that is found in *R. baltica*. Algae containing PE can absorb light at 540-575 nm, allowing them to utilize wavelengths in the green spectrum[19,28–30].

A study performed by Lafarga-De la Cruz et al., reported that the content of Chl *a* in *Rhodomonas sp.* depends on both nutrient concentration and light quantity[31]. They showed that the amount of chlorophyll per cell was higher at lower irradiation, and that the Chl content per cell increases when adding fresh medium to a nitrogen starved culture. The regulation of Chl *a* content in algae is dynamic in order to balance the need for energy with the available light and nutrients[31]. An article by Czeczuga claims that the dynamic regulation of pigments also depends on the quality of the light. Meaning that there is an chromatic adaptation of pigment content and organization[29,32]. Another term used for dynamic regulation of pigments is photoacclimation[30]. This process enables algae to maintain photosynthetic capacity and optimize photon yield in photosystem II (PSII)[33,34]. The efficiency of PSII can be estimated by measuring fluorescence in vivo. This efficiency is proportional to the F_v/F_m ratio, where F_v is the variable fluorescence (difference between maximum and basic fluorescence in PSII) and F_m is the maximum fluorescence after dark adaptation[35].

The ratio (F_v/F_m) represents the maximum quantum yield of PSII (QY)[36,37]. This is often used as a measure of stress[38] caused by one or more stressors. These stressors force the system out of a nominal state until counteracted by homoestasis[34,39]. Non-limited microalgae have a relatively constant QY in the range 0.6 to 0.7[40]. However, QY in higher plants have been reported to average 0.8[41]. Kromkamp et al. reported that nutrient limitation result in a lower QY than for light limitation[40,42]. Stress inducing low QY, activate stress-response in the microalgae[39]. One of these protective mechanisms is lipid accumulation[43,44]. Another protective mechanism, seen in the green algae *Haematococcus pluvialis*, is the accumulation of the strong antioxidant astaxanthin[45]. By understanding how QY varies in response to nutrient limitation, light intensity and other stressors, QY become applicable when optimizing growth conditions[43].

The study performed by Vu et al. found the optimal irradiance for growing *R. baltica* and showed the relations between light, nutrients, growth, and chlorophyll composition[15]. However, Vu et al. only applied white light in their experiments[15]. It has been shown that *Nanochloropsis sp.* grown using blue light (470 nm) achieved the highest maximum specific growth rate (μ_{max}), 10% higher than using white light[22]. A different result was reported by Abiusi et al. for *Tetraselmis suecica*, here red or white light gave highest μ_{max}. Abiusi et al. also found a negative correlation between the chlorophyll content, and red light[46]. For *R. baltica* red light increase the amount of PE, but highest growth rate (turbidostat) has previously been achieved when using blue light[32]. Another factor affecting growth and pigment content, is nitrogen limitation. For *Rhodomonas* sp., nitrogen starvation lowered the protein content and increased the fatty acids content[6,42]. Furthermore, Yamamoto et al. found that PE was degraded before Chl *a* and Chl *b* when nitrogen was limiting[6]. Phosphorus also play a central biochemical role in microalgae. Phosphorus limitation has been shown to cause a metabolic shifts towards compounds that require less P[47,48]. Many studies have been performed in order to find the optimal light conditions for microalgae[15,20,22,32,46]. However, the effect of different combinations of monochromatic light on the growth of *R. baltica* has to the best of my knowledge not been studied.

Growth experiments have traditionally been performed in small (0.2 - 1 L) flasks and PBRs (photo bioreactors). This is time consuming, and expensive when testing a large array of different light conditions. One possible solution to this challenge is to screen for optimal light quality and quantity at a smaller scale. Volpe et al. recently developed a method that utilizes the technology of adjustable LEDs in combination with micro-computers, and temperature control in micro well plates (200 - 1000 µL). In doing so, they create a system capable of running multiple experiments simultaneously in a 96-well plate[49].

The goal of this study was to find the optimal mixtures of red, blue and green light for the cultivation of *R. baltica* with μ_{max} as the main criteria. The newly developed Nanocosm method (Volpe et al.) was applied[49]. Twelve different compositions of monochrome light were tested four times with a total of 240 single well experiments. Red light was the main component in the twelve compositions, as red LEDs have a higher external quantum efficiency, e.i. a greater energy fraction is converted into photons[50]. The scalability between 200 µL scale and 1.2 L scale was evaluated. At the larger scale, in addition to growth, the stress response, and adaptation of pigments during nutrient limitation was evaluated. The pigment composition in *R. baltica* was estimated using spectral deconvolution and HPLC to analyse the final biomass from small scale. This study also compared different methods for measuring biomass density and computing μ_{max}. Finally, the collected data was assessed in cooperation with C-Feed AS to find the optimal light quality for their large scale facility.

Sub-Goals

- Find the optimal light quality combination (in order to obtain the highest μ_{max}) for *R. baltica*
- Evaluate the scalability from the Nanocosm well plate cultivation system to a $\approx$ 1.2 L reactor flask
- Evaluate the response to nutrient limitation with respect to growth, QY and pigments
- Evaluate different ways of measuring and calculating the specific maximum growth rate

2 Material and Methods

The experiments were carried out at The Department of Biotechnology and Food Science at the Norwegian University of Science and Technology (NTNU) during the spring of 2021. The first part consisted of reference experiments, where the microalgae were cultured using nutrient media with different N:P ratios. The second part was a micro scale screening that tested the effect of different light qualities. All experiments were done with *Rhodomonas baltica* 5/91 cryptophyceae obtained from C-Feed AS.

2.1 Experimental Design

2.1.1 Reference Batch Study

Reproducibility assessment and optimization of setup was performed as a test experiment ($\text{batch}_{\text{test}}$) using three reactor flasks. To evaluate the scalability of results from micro scale, and study the effect of nutrient limitation, two further batch experiments at litre scale were performed using the setup shown in Figure 2.1. In the first experiment (nut_1) *R. baltica* was inoculated using different N:P ratios. Balanced medium (N:P 22 & Conwy, see Section A.2 & A.1 in Appendix A) was compared with nitrogen limited (Low-N) and phosphorus limited (Low-P) medium. A second experiment (nut_2) was a reproduction of the first, but with the CO_2 supply to maintain pH below 8.5. The biomass from these experiments provided a stock culture for all the later experiments and was used as material for control experiments.

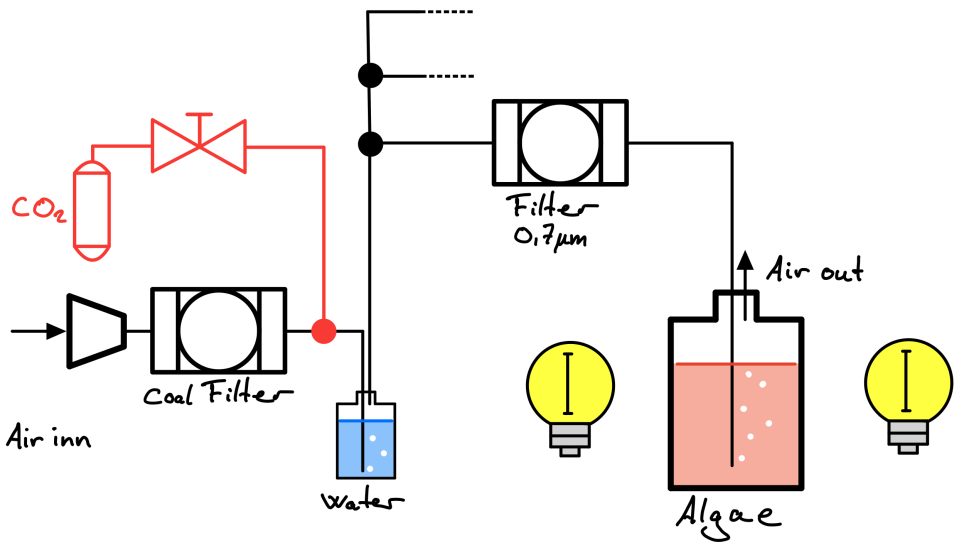

Figure 2.1: Experimental setup for batch cultivation of microalgae in reactor flasks. Compressed air was cleaned by a coal filter before entering the system. The air was humidified and distributed to three reactor flasks (2 L) where it was filtered before entry. The reactor flasks had illumination from each side from an incubator cabinet. The supply of CO_2 was provided for the second (nut_2) setup (drawn i red).

2.1.2 Light Composition Study

In order to test combinations of red, blue and green light (RGB), Nanocosm was used[49]. A versatile well plate photobioreactor allowing multiple light conditions. The plate photobioreactor consisted of a microcomputer with integrated LED lights that could be placed on top of a 96-well plate, providing each well with a adjustable light quality and quantity (Figure 2.2). A control experiment using an earlier model of the Nanocosm with white LED light was performed.

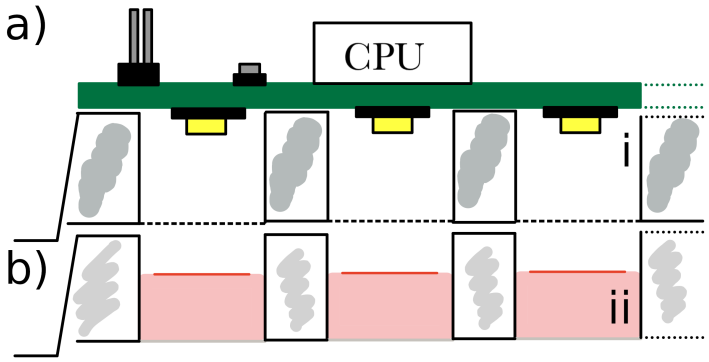

Figure 2.2: Cross section of experimental setup cultivation inn the Nanocosm micro-photobioreactor. **a)** Lid glued to the ATMEGA microcontroller with 96 individually programmable light emitting diodes (i). **b)** White well plate with transparent bottom for spectrometer and fluorescent analysis of the algae culture (ii).

Red light was set as the main component to find the optimal light combination with the lowest energy consumption. The different combinations of light had an increasing fraction of blue, green light or both (Table 2.1). The combined irradiation was adjusted to be equal for the entire study (approximately 100 µmol/m^{2}s, as this was a level used at industrial scale). (The irradiation is often stated as the photon flux density (PFD) [µmol/m^{2}s], describing the amount of photons hitting a surface per second.) Temperature was set to 22.5 °C. Passive gas exchange and reduced evaporation was facilitated by a Breathe-Easy® sealing membrane (Diversified Biotech), that was mounted on top of the 96-well plate.

Table 2.1: Names of the different light qualities. Red, Green and Blue are the amount of each color as fraction [%] of the total photon flux density (PFD). The measured PFD ± STD (standard deviation), and the calculated light intensity (I) [W/m^2] derived from Equation (2.3) and is provided for organisation a) and b) in Figure 2.3

#	Name	Red [%]	Green [%]	Blue [%]	PFD$_{a)}$ [µmol/m^{2}s]	$I_{a)}$ [W/m^2]	PFD$_{b)}$ [µmol/m^{2}s]	$I_{b)}$ [W/m^2]
1	R	100	0	0	99.8±0.8	19.2± 0.1	100.6±0.8	19.3±0.2
2	B_1	99	0	1	100.4±0.5	19.3±0.1	101.0±0.9	19.5±0.2
3	B_3	97	0	3	99.4±0.5	19.3±0.1	100.8±1.2	19.6±0.2
4	B_{10}	90	0	10	99.4±1.0	19.7±0.2	100.8±0.7	20.0±0.1
5	B_{30}	70	0	30	99.2±0.8	21.0±0.2	99.6±1.0	21.1±0.2
6	G_1	99	1	0	100.0±0.6	19.2±0.1	99.8±1.2	19.2±0.2
7	G_3	97	3	0	100.0±0.6	19.3±0.1	100.8±0.7	19.5±0.1
8	G_{10}	90	10	0	99.8±0.8	19.5±0.2	99.8±0.4	19.5±0.1
9	G_{30}	70	30	0	99.2±0.8	20.1±0.2	100.0±0.6	20.3±0.1
10	W_3	97	1.5	1.5	101.0±0.6	19.8±0.1	100.6±1.0	19.7±0.2
11	W_{10}	90	5	5	98.8±0.8	19.5±0.2	98.6±0.5	19.4±0.1
12	W_{30}	70	15	15	100.0±1.4	20.7±0.3	100.4±0.8	20.8±0.2

The distribution of light qualities was not randomized. This was to minimize the effect of crosstalk from several different light regimes, and due to the complexity of programming, calibration and data treatment of the 12 different conditions. However, two different arrangement were tested (Figure 2.3) to check for the effect of placement on the well plate, and possible edge effects. As a precaution to minimize edge effects caused by evaporation, all light mixes were placed on the 10 × 6 inner area of the well plate while water or medium was filled in all wells, see Figure 2.3.

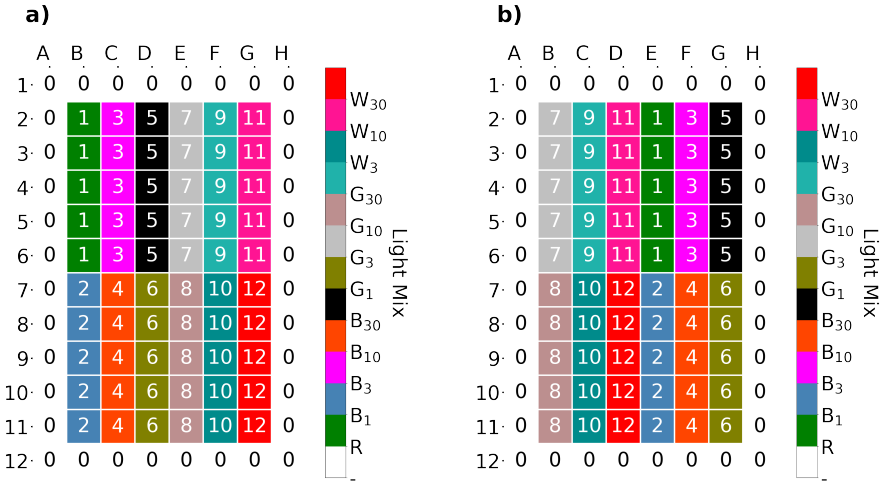

Figure 2.3: The two different organisations of light mixes. The numbers indicate the light qualities in the same order as in Table 2.1. The illustrated color for each light quality was standardized. Setup during the two first (**a**): WP-1, WP-2) and the two last experiments (**b**): WP-3, WP-4) using RGB Nanocosm.

2.2 Cultivation Method

2.2.1 Sea Water and Nutrient Media

The seawater was taken from Trondheimsfjorden at 90 m depth, filtered (VWR GF/A 1.0 µm & Whatman Polycap 36AS 0.2 µm), autocalved (AFSW), and cooled to room temperature before use.

Modified Conwy media provided nutrients (see Section A.1 in Appendix A). The Conwy medium concentrate provided by C-Feed (Conwy) had a N:P atom ratio of 10.6. This media was not optimised for *R. baltica*. A higher N:P ratio have shown to prolong the exponential growth phase, and increasing the maximum cell concentration in batch experiments[51]. Therefore an additional medium formula (N:P 22) was tested (16.5 g_N/L & 1.55 g_P/L). To obtain N and P limitation two additional modified medium concentrates were made. One of these had 10% (w/w) of the nitrate content (Low-N) and the other had 10% (w/w) of the phosphate content (Low-P), relative to the additional formula (N:P 22). These medium concentrates were diluted approximately 1:1000 in AFSW to make the nutrient media.

2.2.2 Reference Batch Study Setup and Optimization

$Batch_{test}$ was performed to assess reproducibility and optimize the cultivation setup (Table 2.2). Three 1.8 L cultures were grown in 2 L flasks with a starting concentration of less than 15 mg_{DW}/L. Two of the flasks (L_1 & L_2) were added 1.8 mL of Conwy (29.7 mg_N & 6.1 mg_P) and the third (H) 2.0 mL of Conwy (33.1 mg_N & 6.8 mg_P). The cultures were sustained until late stationary phase, before extra Conwy concentrate (1.8 mL) was added. To rule out light limitation, different PFDs (150 and 270 µmol/m^2s) were applied.

In nut_1 1 mL *R. baltica* stock culture (0.442 g_{DW}/L) and 2.0 mL medium concentrate was added to 1.8 L AFSW in 2 L flasks. For each of the three flasks different media were added (N:P 22, Low-N and Low-P). Providing circulation and gas exchange, a single air inlet (0.9 L_{air}/min) was combined with a shaking board. The air, provided by a compressor, was passed through a coal filter, humidified, and filtered (FG, 0.7 µm) (Figure 2.1). The PFD was kept continuously at 100 $µmol_{photon}/m^2s$ and the temperature was set to 22.5 °C. Irradiation was measured using a WALZ ULM-500 Universal Light Meter.

As an extension of nut_1, the Conwy medium used by C-feed was compared with the three other nutrient media (N:P 22, Low-N and Low-P). By using the similar conditions for growth as nut_1 (2 mL (0.5 g_{DW}/L) inoculum and 2.0 mL medium concentrate was was mixed with 1.8 L AFSW), it was used for cultivation in 2 L flasks.

The replication experiment nut_2 with CO_2 (1% (v/v)) was performed using 1.2 mL (0.3 g_{DW}/L *R. baltica* stock culture) and 1.2 mL medium concentrate that was mixed with 1.2 L AFSW in 2 L flasks (Table 2.2).

Table 2.2: Overview over the experiments in the batch study. Fresh medium concentrate was added to the stock culture (S.C.) and culture was harvested when required for maintenance as a semi-fed-batch. Material from S.C. was used for AFDW (ash free dry weight), OD (optical density), IVF (in vivo fluorescence), and cell count in standard curves for *R. baltica*.

Experiment	CO_2	Medium	N [mg L^{-1}]	P [mg L^{-1}]
S.C.	No	Conwy	-	-
$batch_{test}$	No	Conwy (L)	16.5	3.4
		Conwy (H)	18.2	3.8
nut_1	No	Conwy	18.2	3.7
		N:P 22	18.2	1.7
		Low-N	1.8	1.7
		Low-P	18.2	0.2
nut_2	Yes	N:P 22	16.5	1.5
		Low-N	1.7	1.5
		Low-P	16.5	0.2

2.2.3 Light Composition Study - Setup and Calibration

For cultivation, a 96-well plate (Thermo Fisher Scientific-Nunclon 96 Flat Bottom White Optical) was filled to a total volume of 200 µL AFSW per well. Row 2 - 11 contained *R. baltica* and 1 $mL_{concentrate}/L_{AFSW}$ (Conwy N:P 22 Version). Row 1 and 12 were filled with AFSW. The reservoirs between wells were added 150 µL extra liquid in all experiments except the first. This was to increase the total moisture in the system, and to ease conductive heat transfer between wells.

In total, five experiments were conducted using 96-well plates (WP) reactors as part of the light composition study (Table 2.3). The first well plate experiment (WP-1) was inoculated from an exponentially growing culture (Figure F.4 in Appendix F). The second (WP-2) was inoculated from a stationary culture (Figure F.5 in Appendix F), and cultivated at a lower temperature (20 °C), aiming to reduce evaporation. The temperature was readjusted back to 22.5 °C for the third experiment (WP-3). The inoculum used in WP-3 was in stationary phase, see Figure F.5 in Appendix F. A low light adapted (Figure F.7 in Appendix F) stock culture was used at a low initial density (Table 2.3) in the fourth experiment (WP-4), and in the white LED control experiment (WP-C) that ran simultaneously.

The micro-PBR (Nanocosm) used a programmable ATMEGA microcontroller, that ran the Arduino software, and used Adafruit NeoPixels LEDs (Figure 2.2). The LEDs emitted red (λ: 620-625 nm), green (λ: 522-525 nm), and blue (λ: 465-467 nm) light[49]. The main fraction of light was red, with blue and green light ranging from 0 to 30%. The PDF was measured (WALZ ULM-500 Universal Light Meter) 1.0 cm from each LED. Under the transparent bottoms in the WP containing cultivation medium (Figure 2.2 b)), the PDF was approximately 70% less.

The Adafruit NeoPixel allowed settings for RGB from 0 to 255 byte for each color and brightness in the same range. Byte and brightness were the two parameters used to

Table 2.3: An overview of the experiments performed to study the effect of combining different monochromatic lights. Setup refers to the organisation of light qualities (Figure 2.3). T_{set} is the temperature that the incubator cabinet was set to, Res. refers to whether the reservoirs between wells were filled with water and Inoc. is the growth state of the inoculum before inoculation, see Appendix F. The table also includes the days of duration of the experiment, the color of the surface the WP was placed on and the initial cell concentration [1×10^3 n_{cell}].

Experiment	Setup	T_{set} [°C]	Days	Res.	Surface	Inoc.	n_{cell}/mL
WP-1	a)	22.5	8.3	No	White	Exp.	$\approx 3.5 \times 10^3$
WP-2	a)	20.0	5.8	Yes	White	Stat.	$\approx 5.7 \times 10^3$
WP-3	b)	22.5	7.3	Yes	Black	Stat.	$\approx 6.7 \times 10^3$
WP-4	b)	22.5	8.9	Yes	Black	Stat.	$\approx 1.2 \times 10^3$
WP-C	-	22.5	8.9	Yes	Black	Stat.	$\approx 1.2 \times 10^3$

adjust PFD in the Arduino script. Six polynomial equations were computed that show the relation between the settings and the measured PFD. In theory this relation was exponential[49], but using an exponential equation gave an inadequate fit. The three first equations show the relation between the desired PFD (x) and the corresponding byte (Equations (2.1)). The rest show the relation between PFD and brightness for red, green and blue light (Equations (2.2)). Due to individual differences between LEDs, each LED was adjusted manually. The equations only gave an approximate value for adjusting the settings, and was based on measurements from the LEDs in position B4 and G2 (Table B.1 in Appendix B).

$$\begin{aligned} \text{byte}_{red} &= 0.0052x^2 + 0.45x - 2 \\ \text{byte}_{green} &= 0.011x^2 + 0.15x - 0.01 \\ \text{byte}_{blue} &= 0.018x^2 + 0.278x - 0.2 \end{aligned} \tag{2.1}$$

$$\begin{aligned} \text{brightness}_{red} &= 0.0024x^2 - 0.15x + 8 \\ \text{brightness}_{green} &= 0.0025x^2 - 0.17x + 9 \\ \text{brightness}_{blue} &= 0.0041x^2 - 0.25x - 13 \end{aligned} \tag{2.2}$$

The intensity of each light combination was calculated (Table 2.1). The PFD of each color in each well position was obtained using the fractions and PFD in Table 2.1. Further the intensity, I [W/m^2], was computed for each light quality using Equation (2.3) and summed up.

$$I = \frac{f \times \text{PFD} \times NA \times h \times c}{\lambda} \tag{2.3}$$

Here f is the fraction of the PFD for each color, NA is the Avogadro constant, h is the Planck constant, c is the speed of light, and λ is the average wavelength for each color[52].

2.3 Control Experiments

2.3.1 Alkaline Control by Measurement of pH

pH was monitored to assess the risk of C-limitation at too high pH levels[49]. pH was measured using 0.5 unit pH-sticks (VWR™PROLABO, PAPIER dosatest®) in the range 7.0 to 14.0.

2.3.2 Measurement of Disolved Nitrate and Phosphate

Nitrogen and phosphorus concentrations were measured to confirm the limiting effect in the different media. At the end of the batch experiment, samples were filtered (25 mm Syringe Filter w/0.2 µm Membrane) and stored at 4 °C.

Chloride cause interference with the nitrogen test kit and had to be eliminated (HACH LANGE GMBH, LCW 925), before adding the samples to the Dr. Lange Cuvette Test (HACH LANGE GMBH, LCK 339). This was performed in accordance with the manual. Next the samples were analysed using the DR3900 Laboratory Spectrophotometer (HACH).

The phosphate phosphorus and nitrate nitrogen content was also analysed at Trondhjem biologiske stasjon by Siv Anina Etter according to NS-EN-ISO6878 and NS-EN ISO 6878 respectively. The samples were analysed using a Flow Solution IV (O.I. Analytical) with a method detection limit (MDL) of 0.007 µmol L^{-1} for N in the range 0.02 to 40 µmol L^{-1}, and MDL for P of 0.009 µmol L^{-1} in the range range 0.02 to 10 µmol L^{-1}.

2.3.3 Rate of Evaporation from 96-Well Plate

The total mass was monitored and evaporation rate was calculated. The well plate was measured gravimetrically multiple times during each experiment. Homogeneous evaporation was assumed, as Volpe et al. reported insignificant variation in water loss between wells[49].

2.4 Analytical methods

2.4.1 Data Sampling and Treatment

To monitor development in the different experiments, samples were taken daily during the reference batch study. Technical duplicate ($batch_{test}$ & nut_1) or triplicate (nut_2) samples were taken form each reactor flask (Figure 2.1). These were used to measure OD, IVF, QY and pH. In addition, larger samples were taken for pigment extraction at early exponential, late exponential and stationary growth phase. In the light composition study OD and IVF was measured daily with two rows (1 and 12) as blank controls. The experiments were stopped when *R. baltica* entered the early stationary phase, and pigments were extracted for analysis.

2.4.2 Calculation of Growth Rate

Growth rate (μ) was calculated in order to evaluate the performance of the different light treatments. μ is a variable describing the doubling time per day. Let C_0 be proportional

to the population size (OD, IVF, etc.) at time t_0 [d], and C_t the population size at time t, then $\mu = (ln(C_t/C_0))/(t - t_0)$. The maximum specific growth rate (μ_{max}) was estimated from the steepest part of a sigmoid growth curve and was set as the key performance index in this study. μ_{max} was calculated by three methods; By using the equation for μ restricted to a moving mean (MM) for the time interval of highest growth (Step), logarithmic ($\log_e$) transformation and linear least-squares regression in the same time interval (LinReg), and by non-linear least square curve fitting of the growth curve (Curve Fit). The latter method solved the equation $C_t = K/(1+((K-C_0)/C_0) \times e^{-\mu_{max} t})$, where K was the carrying capacity[53]. All the methods (Step, LinReg and Curve Fit) used in the light composition study calculated the growth rate for the individual well and took the averaged for each light treatment (Section E.2 in Appendix E).

2.4.3 Estimation of Biomass

Optical Density
In order to monitor growth, the optical density (OD) was measured. Hitachi 5100 photo-spectrometer was used (at 750, 680 and 545 nm) in the largest scale batch experiments. The WP experiments used a plate scanner (TCAN - infinite M200 PRO) to quantify the development in OD at 750 nm for each well.

In Vivo Fluorescence
In vivo Chl *a* fluorescence (IVF) was measured as method for estimating biomass density. Using the plate scanner (TCAN - infinite M200 PRO), the samples were excited at 460 nm and emission was detected at 680 nm (bandwidth = 9 nm)[49].

Dry Weight
Biomass concentration was estimated by gravimetric measurements of dry biomass from a known volume. The method for ash free dry weight (AFDW) described by Zhu et al., was applied. Triplicates of precombusted (2 h, at 440 °C) glass-fibre (Whatman GF/F 25 mm, 0.7 µm) filters were used to filter 10 mL samples, that were washed with distilled water (20 mL). The filters were dried at 95 °C until constant weight, before weighing on a analytical balance (Mettler Toledo UMT2, d = 0.0001 mg). The dried filters were then ashed in a furnace (4 h, at 540 °C), cooled and weighed once more. The absolute value of the difference between the two weights normalized to the filtered volume equalled the AFDW [$g\,L^{-1}$][54].

Cell Density
To relate OD and IVF with the number of cells in the cultures, samples (100 µL @ 100 $\mu L\,min^{-1}$) were quantified to obtain standard curves. The Attune NxT flow cytometer (FCM) by Thermo Fisher was used to count the in vivo cell samples. The FCM was set to register the number of cells containing the auto fluorescent pigment Chl *a* with excitation in the blue area (460 nm) and emission in the red area (680 nm) of PAR.

2.4.4 Analysis of Pigment Content

Pigment Composition through Spectral Deconvolution
To assess the effect of light quality on pigment composition, spectral deconvolution was performed. (The computing was performed by Charlotte Volpe according to methods established by Volpe et al.[49].) Samples (10 mL) were filtered during exponential and stationary phase. These were stored in a freezer (−20 °C) before extraction in 96%

ethanol (3 mL) for 30 min in the dark at 4 °C[49]. The extract was filtered and scanned (400-750 nm) using V-1200 Spectrophotometer (VWR). This procedure was also the basis for analysing the pigments in the light composition study. Here the WPs were centrifuged at 1800 rpm for 10 min before the supernatant was discarded. The WP containing the pellet was stored in a freezer (−20 °C) before resuspension in 96% ethanol (200 µL) and 30 min extraction in the dark at 4 °C. Thereafter an absorbance scan (400-750 nm) was conducted (TCAN - infinite M200 PRO).

Pigment Content from HPLC
By using sample material from the three middle wells of R, B_{30}, G_{30} and W_{30}, well E3, F3 and G3 in WP-C and filters from N:P 22, Low-N and Low-P, a quantitative analysis of pigments by HPLC[55] was performed at Trondhjem biologiske stasjon by Siv Anina Etter.

Phycoerythrin Extraction
PE is highly soluble in water (pH = 7), but not in ethanol. Therefore a second procedure for extraction was required. In accordance with Cuellar-Bermudez et al. the extraction of PE was performed by disruption at −80 °C for 24 h before extraction into 0.1 M phosphate buffer at 4 °C for 24 h before filtering and absorbance scanning[56]. The filter samples and well plate samples were extracted using 3 mL and 200 µL PBS respectively.

2.4.5 Maximum Quantum Efficiency

Nutrient stress was monitored by a noninvasive method of quantum yield measurements. Reusing the cuvettes from the OD measurements, dark adapted (15 min for oxidation of the plastoquinone pool) samples were analysed inside a AquaPen AP 110/C (PSI)[41,43].

2.4.6 Statistical Analysis

In order to compare the results, a statistical analysis was conducted, see Figure 2.4. Initially equal variance was determined using Levene's test that has equal variance between groups as null hypothesis. This implied an assumption of homoscedasticity that was rejected if the p-value was below 0.05. In this study however, a limit of $p < 0.15$ was used as an extra precaution. Next the comparisons were analysed using One-Way ANOVA. If the ANOVA was rejected ($p < 0.05$), the Tukey multiple comparison test (MCT) was performed. The criteria for rejecting the Tukey test was set to $p < 0.05$[57]. The script in Section E.1 in Appendix E was used to perform the three statistical analysis.

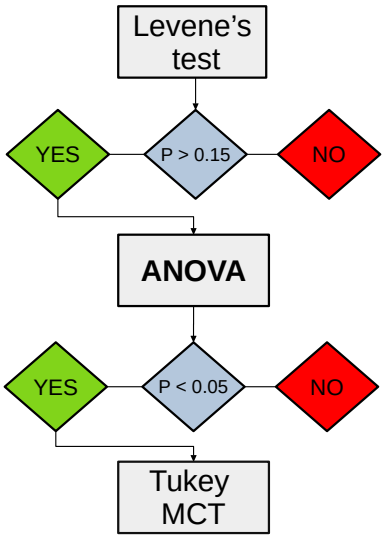

Figure 2.4: The multiple comparison test (MCT) was not performed if Levene's test or ANOVA failed.

3 Results

3.1 Control Experiments and Reliability Assessment

Batch Test Experiment and Reproducibility

The $\text{batch}_{\text{test}}$ showed parallel growth in L_1 & L_2, and that H had a longer exponential growth phase (Figure 3.1). Furthermore, it was found that L_1 & L_2 recovered from a drop in QY when supplied with more nutrients (Figure 3.2). Due to a poor resolution in the data, μ_{max} was not calculated.

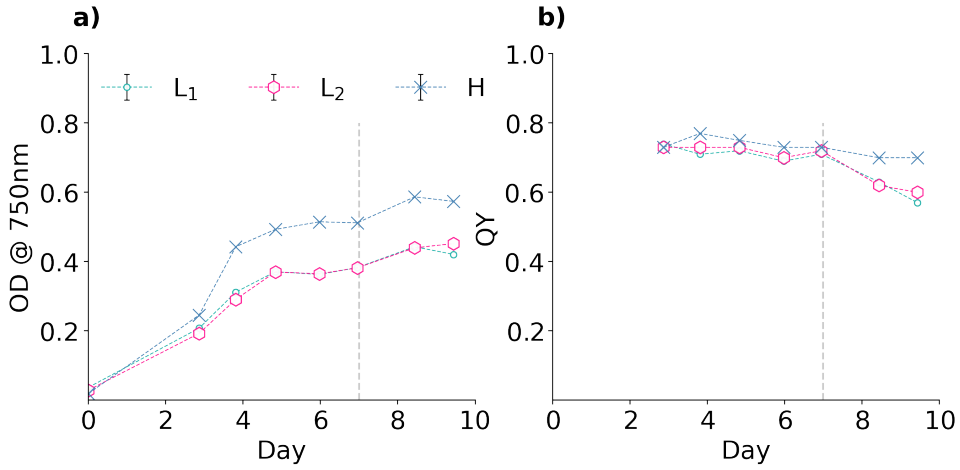

Figure 3.1: Optimization experiment $\text{batch}_{\text{test}}$ using *R. baltica* in two flask reactors with a lower nutrient concentration (L_1 & L_2), and one with a higher concentration (H). **a)** The development in OD measured at 750 nm. Dashed line indicate the time of QY drop. **b)** QY over time. Dashed line indicate the time of QY drop.

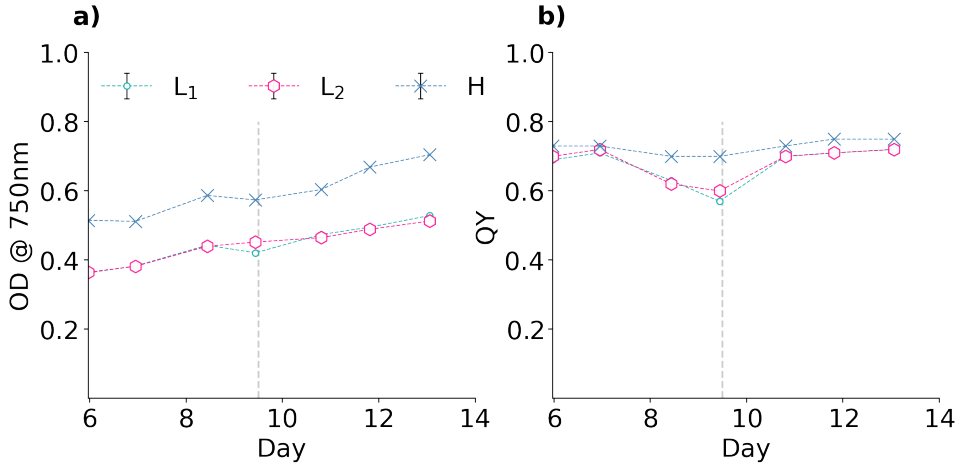

Figure 3.2: Optimization experiment $\text{batch}_{\text{test}}$ using *R. baltica* in two flask reactors with a lower nutrient concentration (L_1 & L_2), and one with a higher concentration (H). **a)** OD measured at 750 nm over time. Dashed line indicate nutrient supply. **b)** QY over time. Dashed line indicate the time of nutrient supply in the form of Conwy (C-Feed version) medium concentrate (1.8 mL).

pH in Reference Batch Study

The pH increased for three of the four cultures in nut_1 (Table 3.1). When the experiment was repeated with 1% CO_2 mixed into (nut_2) the air inlet (Figure 2.1), pH was constant (7.5) after day 0, see Table 3.1. pH was not monitored for $batch_{test}$.

Table 3.1: The measured pH values during the first (nut_1) and second (nut_2) batch experiment.

Day	Low-N	Low-P	N:P 22	Conwy
nut_1				
0	7.5	7.5	7.5	7.5
2	7.5	7.5	7.5	7.5
6	7.5	**9.0**	9.0	9.0
7	7.5	8.5	**9.5**	**9.5**
nut_2				
0	**8.0**	**8.0**	7.5	
2	7.5	7.5	7.5	
6	7.5	7.5	7.5	
7	7.5	7.5	7.5	

Comparison of Different Methods to Estimate Growth Rate

In order to estimate the maximum specific growth rate, different non-invasive measuring methods were used (Section 2.4.3), and μ_{max} was computed (LinReg and Curve Fit, Section 2.4.2). In Table 3.2 the growth was estimated by LinReg on the interval from day 3 to day 6 and Curve Fit for nut_1 Conwy. The μ_{max} calculated by LinReg was approximately 20 - 30% lower for the two set of data using OD compared with IVF based data. Growth curve fitting[53] computations of μ_{max} was the same as for LinReg for two of the data sets (Table 3.2), but OD basis from the Hitachi 5100 showed a 30% higher μ_{max} relative to LinReg, and equal to the μ_{max} based on IVF.

Table 3.2: Maximum specific growth rate [d^{-1}] in nut_1 Conwy computed from different measuring data (OD & IVF), using linear regression for all data points (mean ± SEM) and curve fitting each technical duplicate data (mean ± STD). Data consisted of two technical duplicates (Section 2.4.1).

Computation method	OD Hitachi	OD TCAN	IVF TCAN
LinReg	0.76 ± 0.04	0.88 ± 0.07	**1.07 ± 0.06**
Curve Fit	**1.09 ± 0.06**	**0.90 ± 0.01**	1.02 ± 0.04

Data from each well in the WP experiments was used to compute μ_{max}. The resulting μ_{max} was compared for the different computational techniques (Step, LinReg and Curve Fit). Step and LinReg was strongly correlated ($R^2 = 1.00$), see Figure 3.3. However, these two methods were not without bias, as the time interval was selected manually. The less biased method (Curve Fit) was compared with the linear regression. This resulted is a weaker correlation ($R^2 = 0.40$), see Figure 3.4. In most cases (both in Figure 3.4 and other WPs) the curve fitted growth rates were higher than μ_{max} found by linear regression (Table D.1 in Appendix D). The advantage of curve fitting was the use of all available data without bias and was not affected by non-synchronizes growth. This was why Curve Fit was used to estimate μ_{max} in this study.

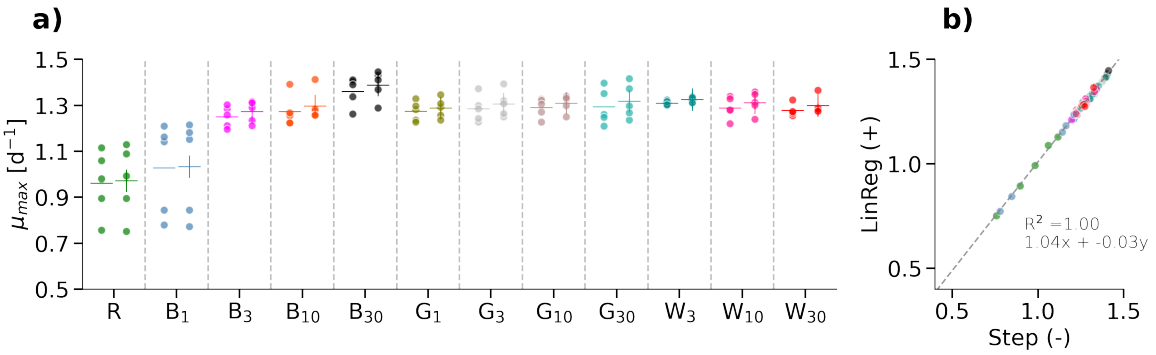

Figure 3.3: Comparison of μ_{max} for *R. baltica* for each well in WP-1 calculated using a stepwise method (−) and linear regression (+) on log-transform data. Rawdata presented in Figure 3.23. **a)** Compares the different methods and light composition. **b)** Correlation between the two calculation methods.

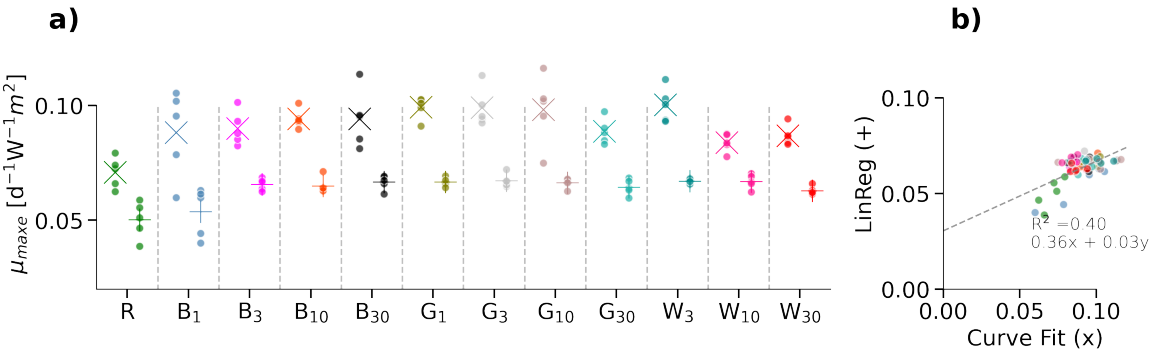

Figure 3.4: Comparison of μ_{max} per light intensity [d^{-1}W^{-1}m^2] for *R. baltica* calculated using linear regression (+) and curve fitting (×) for WP-1. **a)** Compares the different methods and light composition. **b)** Correlation plot for the linear regression and curve fitting

Distribution of Growth in Well Plates

To qualitatively evaluate the effect of organisation of the light compositions, heat map illustrations were made. These were also helpful when looking for cross talk. An indication of cross talk was growth on the WP edges (row 2 - 11, column A and H) that contained algae culture, but without a direct light source (WP-1, WP-2 and WP-3).

The distribution of growth in WP-1 (Figure 3.5) show that there were lower growth rates in row 5 to 8 column B. The light compositions R and B_1 had two wells each in this area (Figure 3.3). Growth in column A and H (not illuminated) was observed.

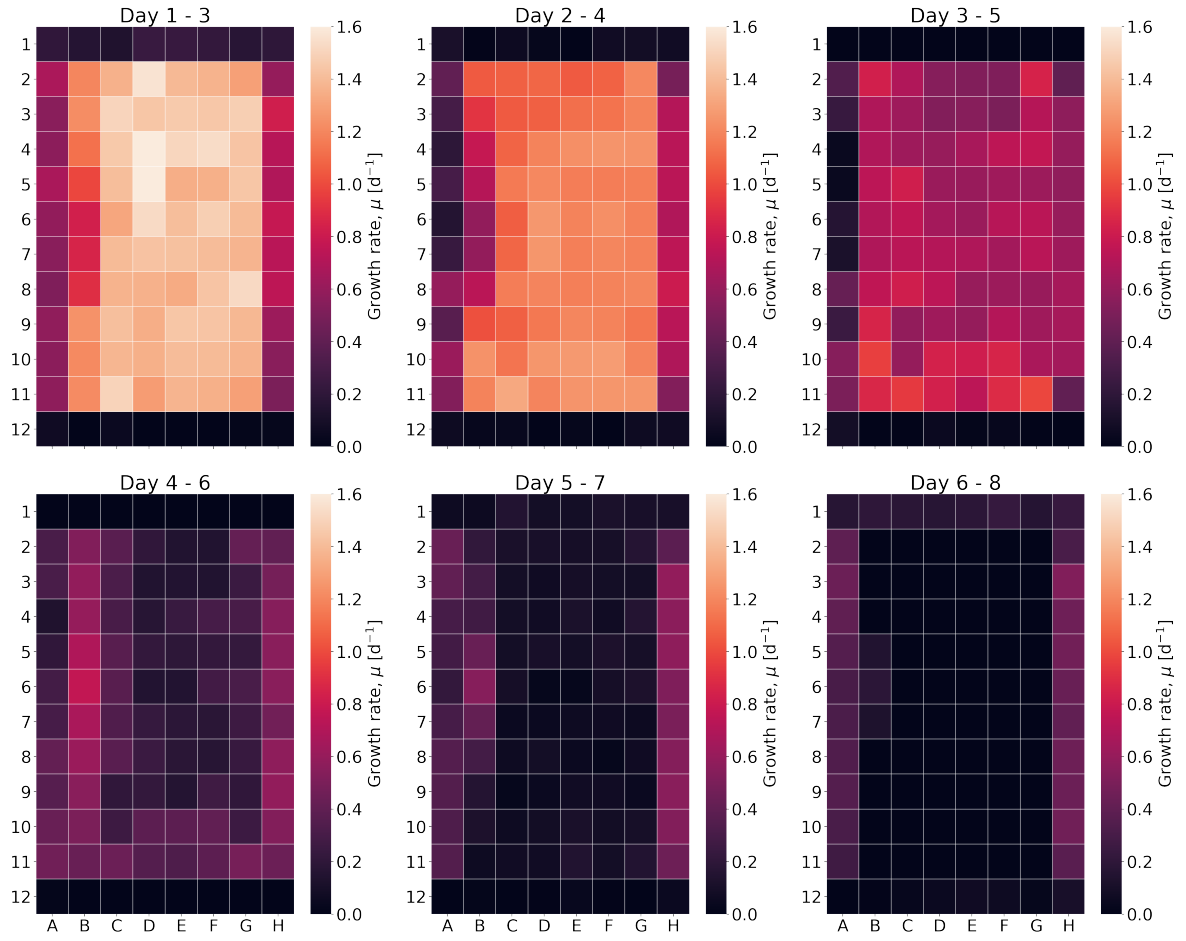

Figure 3.5: WP-1 growth rate (MM) [d^{-1}] for *R. baltica* in each well divided into periods of three days using organisation **a)** in Figure 2.3.

The experiment WP-2 had an apparent higher growth rate in the center of the well plate, see Figure 3.6. The same area that has high growth day 0 - 2 and 1 - 3 has lower growth day 3 - 5 and 4 - 6. The local low growth area observed in WP-1 (Figure 3.5) was not observed for WP-2. Growth in the no light columns A and H was observed.

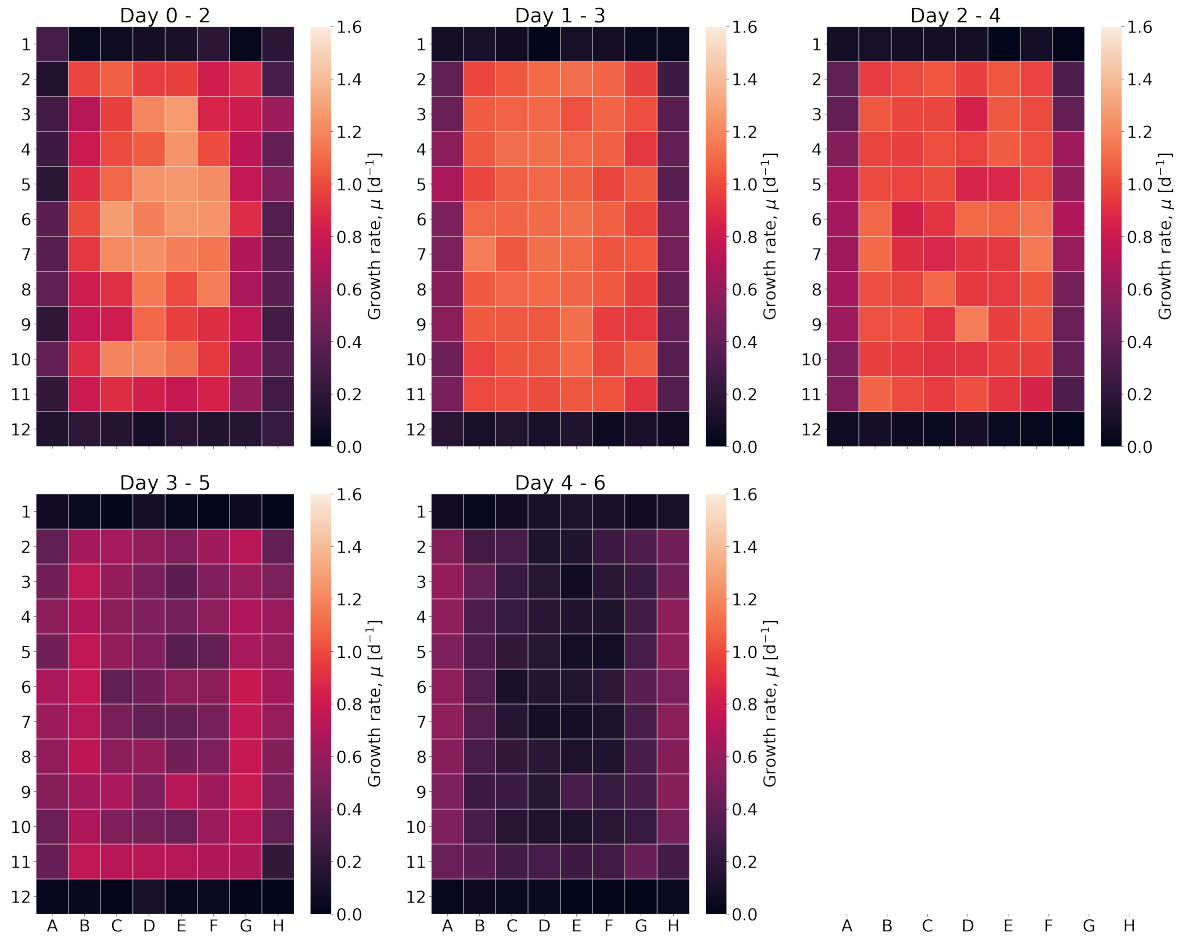

Figure 3.6: WP-2 growth rate (MM) [d^{-1}] for *R. baltica* in each well divided into periods of three days cultivated using organisation **a)** in Figure 2.3.

No growth growth was observed in the no light wells after placing the 96 well plate and Nanocosm above a black surface in WP-3 (Figure 3.7). Higher initial growth was also observed in the center of the well plate. However, the growth rate in row 7 - 10 column D appeared higher than the growth in row 3 - 6, even though they were the same distance from the edge.

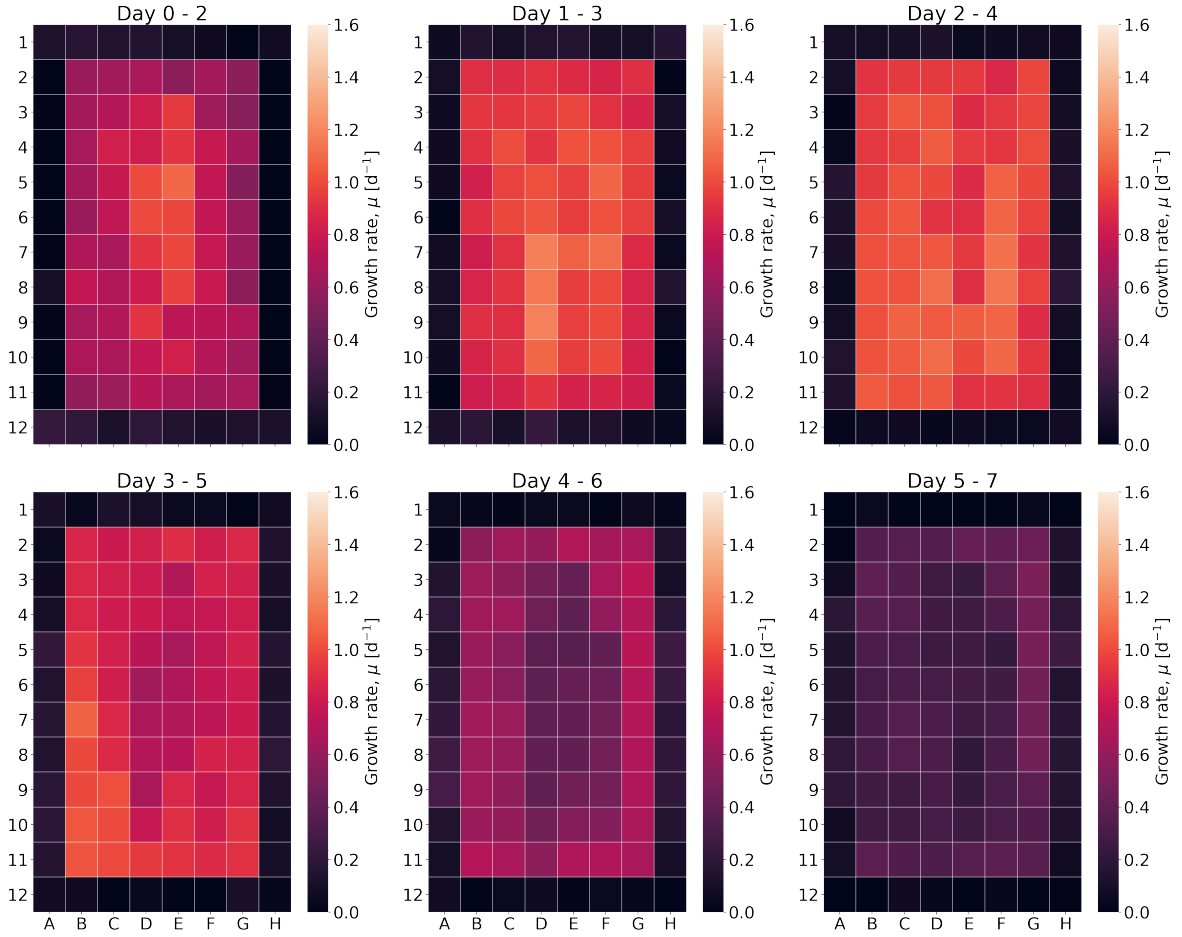

Figure 3.7: WP-3 growth rate (MM) [d^{-1}] for *R. baltica* in each well divided into periods of three days cultivated using organisation **b)** in Figure 2.3.

The PFD was set to ≈100 µmol/m²s (100% red) in the edge wells for WP-4. As an result, growth was observed in the outer wells (Figure 3.8). No obvious pattern or deviation was observed that indicated an edge effect.

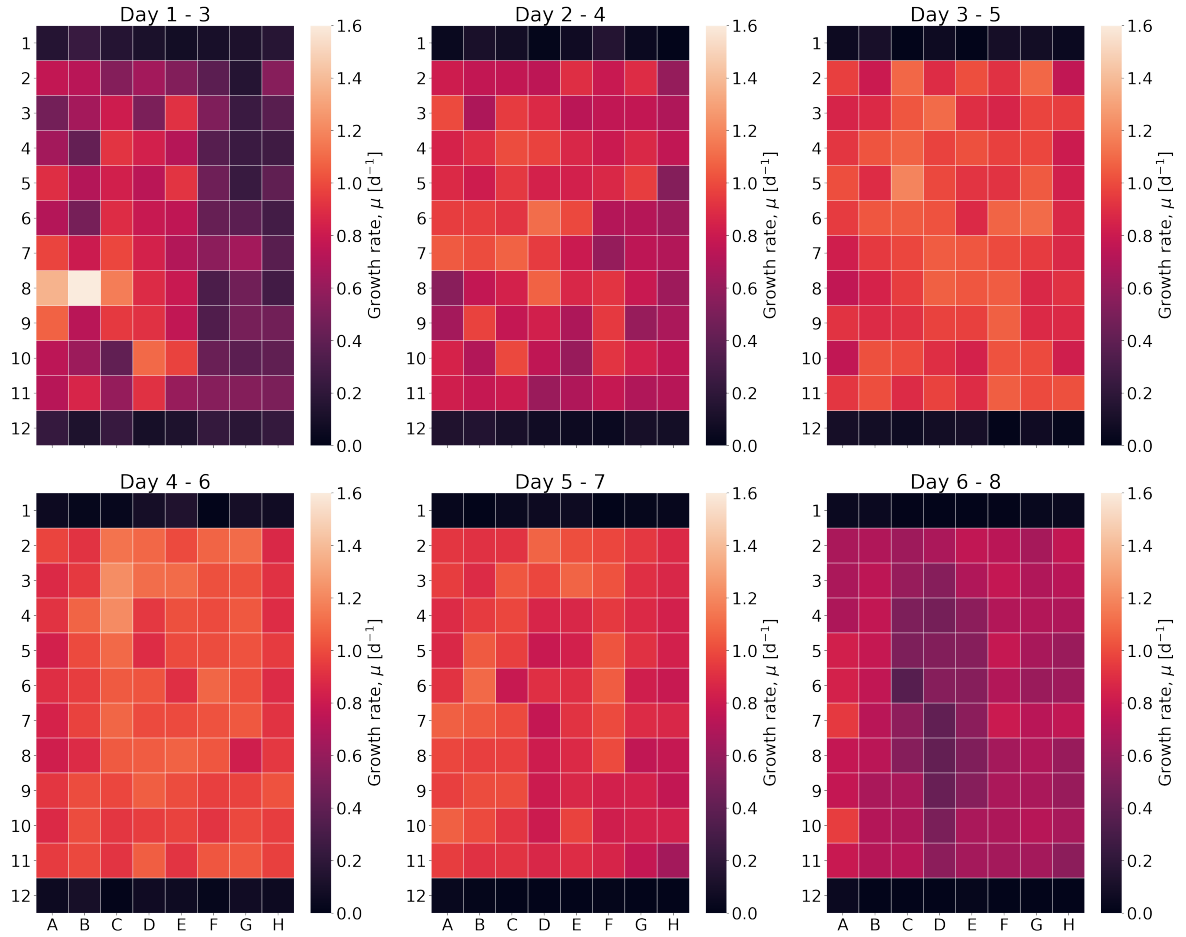

Figure 3.8: WP-4 growth rate (MM) [d^{-1}] for *R. baltica* in each well divided into periods of three days cultivated using organisation **b)** in Figure 2.3.

The control experiment WP-C was intended as a reference for growth using white light. The wells C5 and D5 had no light due to LED failure. These two wells, seen in Figure 3.9, functioned as controls for cross talk. The total growth (maximum IVF) in C5 and D5 was only 3.4% compared with the highest total growth measured.

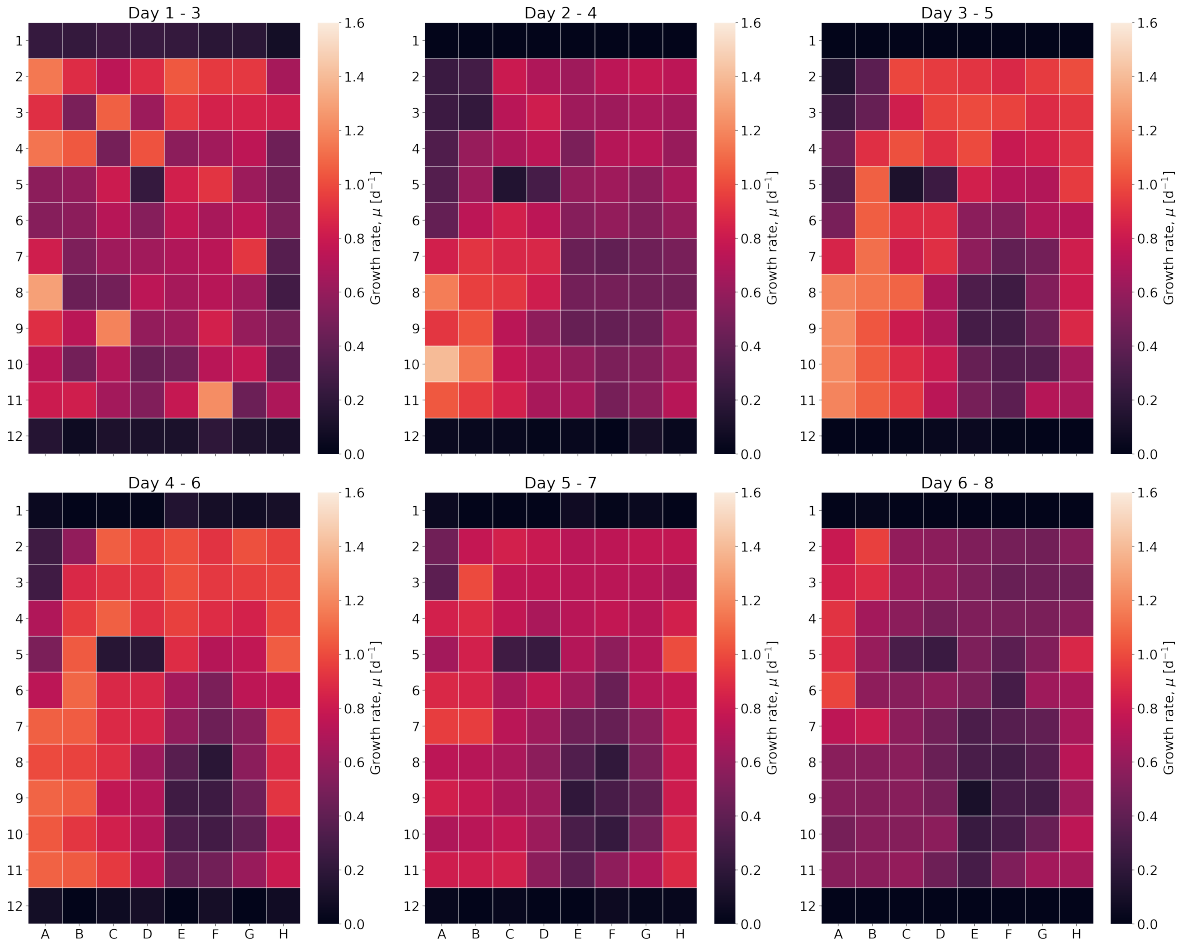

Figure 3.9: WP-C growth rate (MM) [d^{-1}] for *R. baltica* in each well divided into periods of three days.

Crosstalk

As a test to check crosstalk, the reservoirs in WP-3 were filled with the same culture as the wells day 0. This resulted in visible growth in the reservoirs by the end of the experiment (Figure 3.10). There was observed two different colors (green & red) on *R. baltica* in the reservoirs.

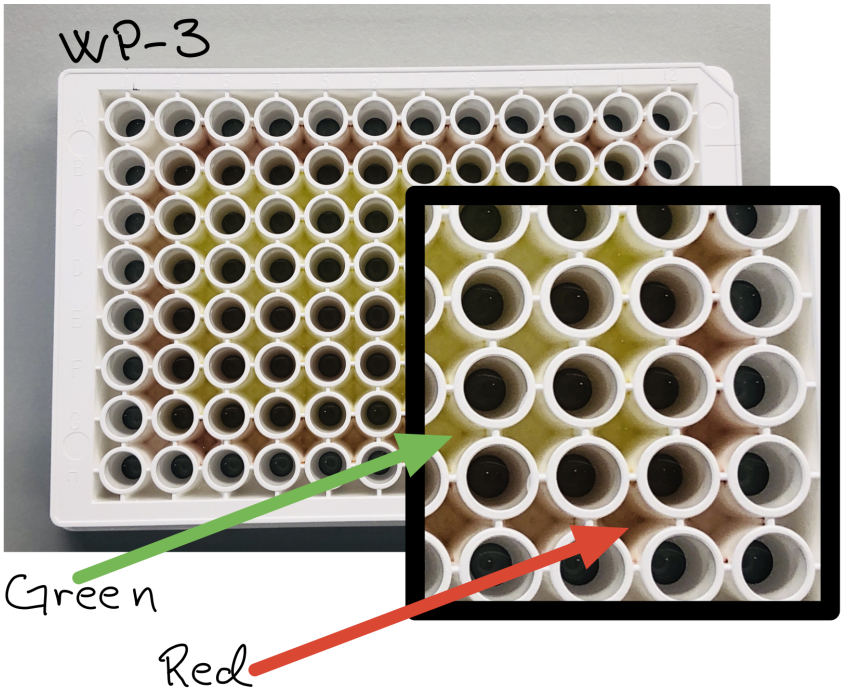

Figure 3.10: The well plate in WP-3 day 7. The inner reservoirs had a green color, while the once closes to the edge had a red color.

Effect of Membrane on Measurements of Optical Density

A control experiment was performed on each WP to evaluate the effect the Breathe-Easy® membrane had on OD measurements. The recorded values varied depending on position. This was seen in all WP experiments (WP-1: Figure 3.11). The effect of the membrane corresponded to a 30-50% reduction in OD after membrane removal.

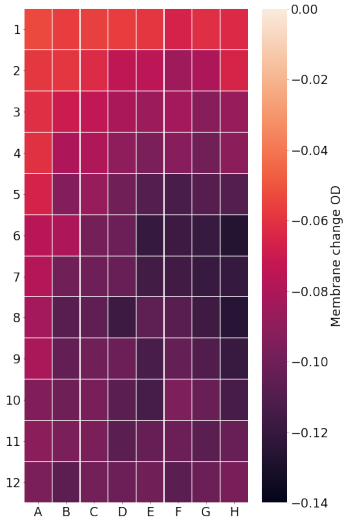

Figure 3.11: The difference in OD between before and after the Breathe-Easy® membrane was removed. The measurement was performed on the last day of cultivation.

Evaporation

The loss of water through evaporation could effect cell density and thereby impact the observed growth in the light composition study. Evaporation rate was therefore calculated using the loss of mass during the WP experiments. An experiment comparing the use of open (O) WP with a WP sealed by a membrane (M) using tap water was performed. The membrane sealed WP had a 60% lower ($p = 0.02$) evaporation rate (Table 3.3). The evaporation rate for WP-C was 97% higher ($p < 0.001$) than for WP-4. The WP-3 experiment had the highest evaporation rate among the WP experiments using the RGB Nanocosm (Table 3.3).

Table 3.3: The rate of evaporation for all well plate (WP) Nanocosm experiments. The initial volume in each of the 96 wells was 200 µL. Experiment WP-2, WP-3, WP-4, and WP-C had 150 µL extra liquid in the reservoirs. The effect of the membrane (M) could be compared with the open well plate (O), but M and O are not comparable with the remaining experiments as they had a higher light intensity. T_{set} was the temperature set in the cultivation environment. The mean evaporation rate was based on n number of rates calculated.

Experiment	T_{set} [°C]	n	Total Loss [g]/[%]	Evaporation rate [g d^{-1}]/[%/d]
WP-1	22.5	3	5.6/30	0.67 ± 0.12/3.5
WP-2	20.0	2	4.5/13	0.78 ± 0.02/2.3
WP-3	22.5	3	8.1/24	1.10 ± 0.2/3.2
WP-4	22.5	8	6.7/20	0.76 ± 0.04/2.3
WP-C	22.5	8	**13.6/40**	**1.5 ± 0.2/4.6**
O	22.5	3	-	**2.11 ± 0.5/11.0**
M	22.5	4	-	0.84 ± 0.07/4.4

Absorbance Spectra for *R. baltica*

To evaluate the content of photo-absorbing elements (chlorophylls, carotenoides and phycobiliproteins), absorbance spectra were made by different means. From the first attempt (Figure 3.12 a)), high levels of scattering were detected at the lower wavelengths. Therefore a scatter corrected absorbance curve was made and according to Johnsen et al. peak 1 was alloxanthin, 2 and 3 were phycoerythrin, peak 4 was Chl c_2 and peak 5 was Chl a[30], see Figure 3.12 b). The in vivo reading appeared 10 nm red shifted relative to the ethanol pigment extract.

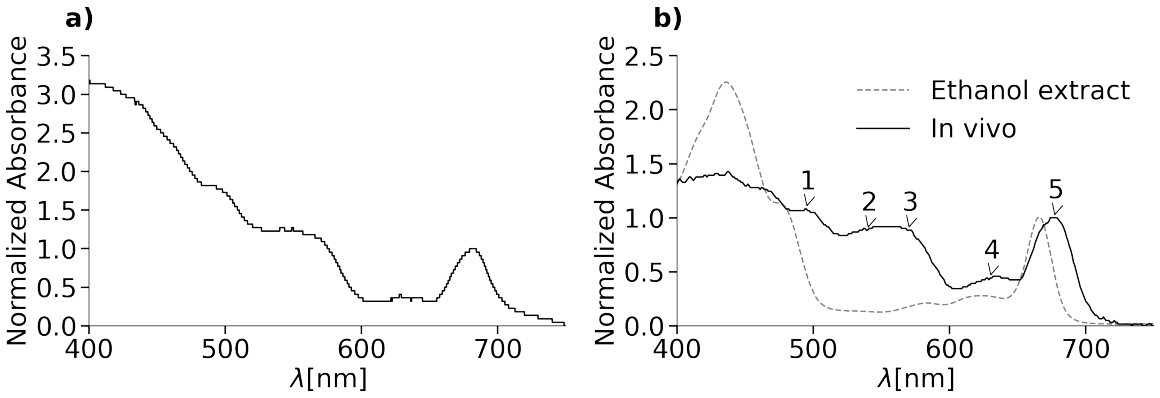

Figure 3.12: Absorbance specter of *R. baltica* (S.C.) normalized to the red peak. **a)** In vivo absorbance without correction for scattering (UV-1601PC, UV-visible Spectrophotometer, SHIMADZU). **b)** Ethanol extracted pigment, and in vivo absorbance with correction for scattering (U-3310 Spectrophotometer, HITACHI) . According to Johnsen et al. peak 1 is alloxanthin, 2 and 3 are phycoerythrin, peak 4 is Chl c_2 and peak 5 is Chl a[30].

Low Light Adaptation

The intrinsic ability for *R. baltica* to adapt to different light intensity was assessed by measuring OD at different wave lengths over time. For Low light (LL) this resulted in an increase of the relative ratios for OD_{680} and OD_{545} increased over time (Figure 3.13). This development was observed in the maintained stock culture after irradiation was lowered from 100 to 20 µmol/m^{2}s at day 0 (Figure 3.13). In the same time period OD_{750} only increased by 0.6% per day for LL due to light limitation. Prior to the reduction of PFD from 100 to 20 µmol/m^{2}s (HL) the OD_{680}/OD_{750} and OD_{545}/OD_{750} was below 1 (Figure 3.14). OD_{750} in the stock culture increased by 21% per day during HL.

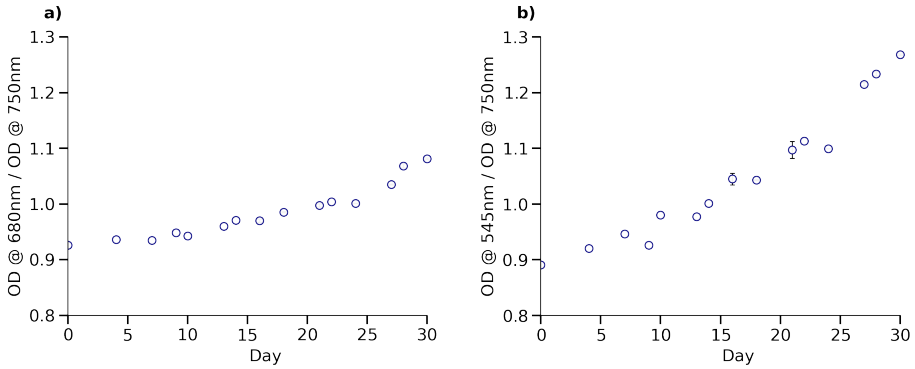

Figure 3.13: Evolution of ratio OD_{680} divided by OD_{750} (**a)**) and the ratio OD_{545} divided by OD_{750} (**b)**) for *R. baltica* in the stock culture at low irradiation (LL) (20 µmol/m^{2}s).

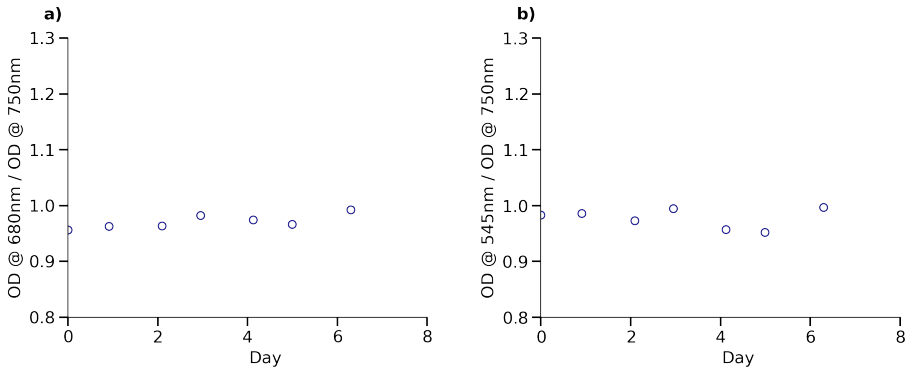

Figure 3.14: The ratio OD_{680} divided by OD_{750} (**a)**) and the ratio OD_{545} divided by OD_{750} (**b)**) for *R. baltica* in the stock culture at high irradiation (HL) (100 µmol/m^{2}s).

Standard Curves Describing the Relation Between Measuring Methods

Standard curves were computed in order to establish a relation between the non-invasive and invasive methods. The non-invasive methods measured OD and IVF, while the invasive measured AFDW (Figure 3.15) and cell concentration (Figure 3.16). Optical density was measured by two different instruments with different light paths, therefore a relation between the two was also established(Figure 3.17). All the four standard curves had a strong correlation with $R^2 > 0.97$. However, the relation between IVF and cell number (Figure 3.16) had a intercept at IVF = 198 which made it hard to estimate low cell concentrations.

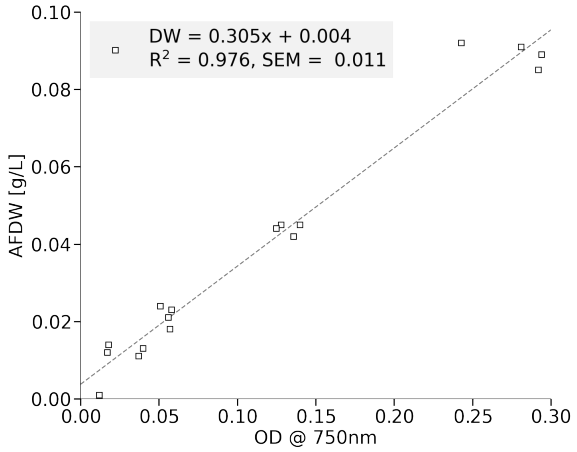

Figure 3.15: Standard curve from AFDW measurements and OD (HITACHI) for *R. baltica*. Raw data in Table C.1 in Appendix C.

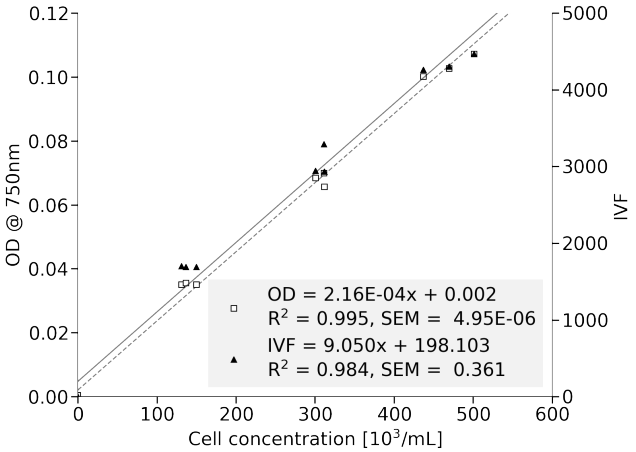

Figure 3.16: Standard curve comparing OD (empty square) at 750 nm and IVF (filled triangle) form the plate scanner (TCAN) with cell count measurements (FCM) for *R. baltica*. Raw data in Table C.2 in Appendix C.

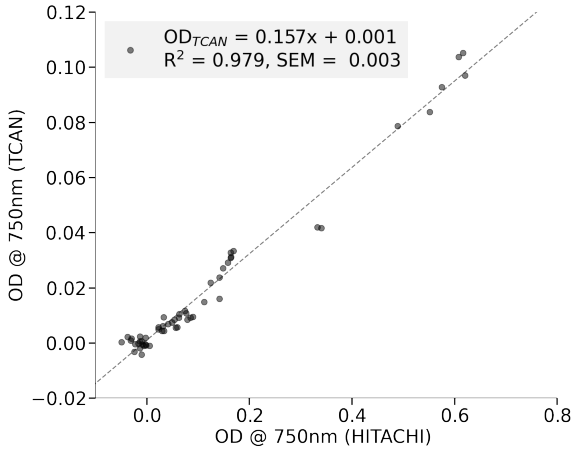

Figure 3.17: Standard curve comparing the OD at 750 nm data from two different instruments (TCAN & HITACHI) during the nut$_1$ Conwy experiment using *R. baltica*.

3.2 Reference Study at Different Initial Nutrient Levels

As a reference for the experiments in smaller scale and to evaluate the effect of nutrient limitation, a batch study was performed using four different media. As expected, the limited cultures stopped growing first (Figure 3.18 **a)**). There was no difference between the two balanced cultures (for statistics more biological replicas were required). The optical density day 9 (Figure 3.18 **a)**) corresponded to approximately 235 mg_{AFDW}/L for N:P 22 and Conwy using Figure 3.15. If nitrogen starvation for N:P 22 and Conwy occurred, the N-content would equal 7.7% (w/w).

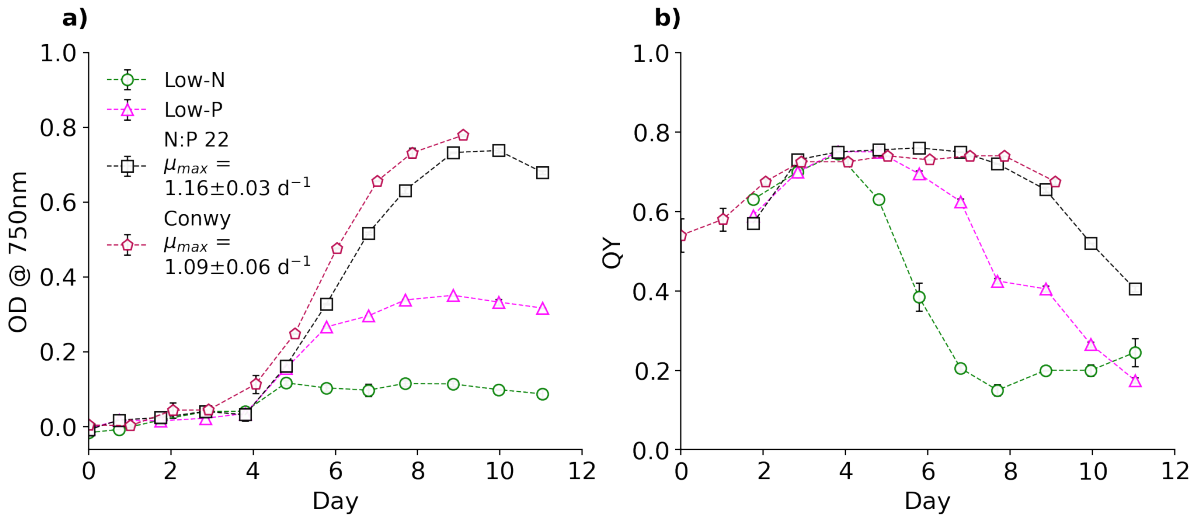

Figure 3.18: Batch experiment (nut$_1$) using *R. baltica* and different media. The four different cultures supplied with nitrogen limited (green circle), phosphorus limited (magenta triangle), balanced with N:P ratio equal 22 (black square), and standard Conwy medium supplied by C-Feed (red pentagon). **a)** OD at 750 nm over time. μ_{max} by curve fitting replica samples and provided as mean ± STD. **b)** QY over time.

In addition to different development in growth and QY (Figure 3.18), a visual differences between the cultures were observed. N:P 22 was more dense and with a stronger red color than Low-P and Low-N (Figure 3.19). The latter one got a bright green color (Figure 3.19 **a)**).

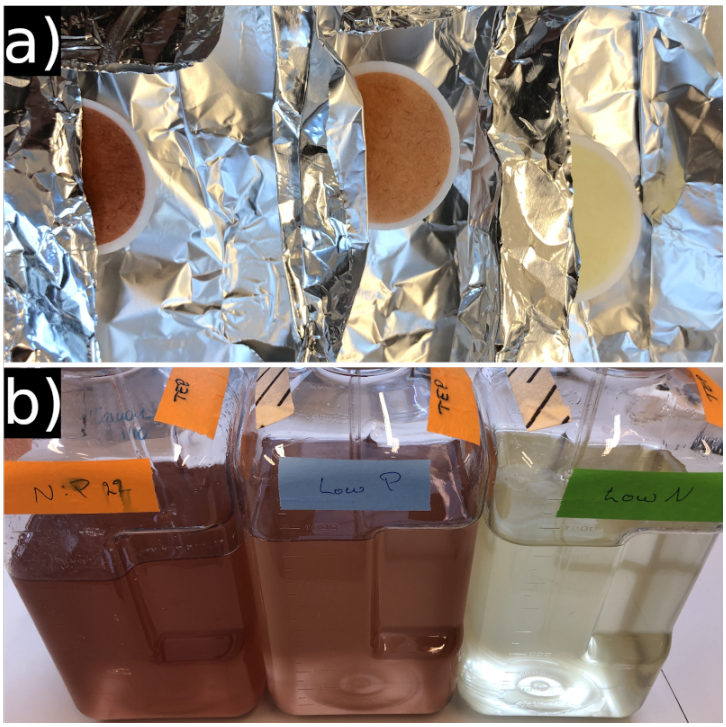

Figure 3.19: From the left the picture shows *R. baltica* supplied with: N:P 22, Low-P, and Low-N medium. **a)** Filters for pigment extraction day 7. **b)** Culture flasks day 6.

Reference Batch Experiment with Carbon Dioxide Supply

The addition of CO_2 (1% v/v) in nut_2 resulted in a stable pH (7.5) for the duration of the experiment (Table 3.1). Here μ_{max} for N:P 22 was 29% higher ($p < 0.001$) than N:P 22 in nut_1. The culture fed with Low-N medium was limited first, followed by Low-P, and the N:P 22 was the last to reach nutrient limitation, see Figure 3.20. The OD_{750} was used to estimate the biomass density of N:P 22 day 8 to be 190 mg_{AFDW}/L the equation in Figure 3.15. The N-content was estimated to be 8.6% (w/w), using the concentration of nitrogen at day 8.

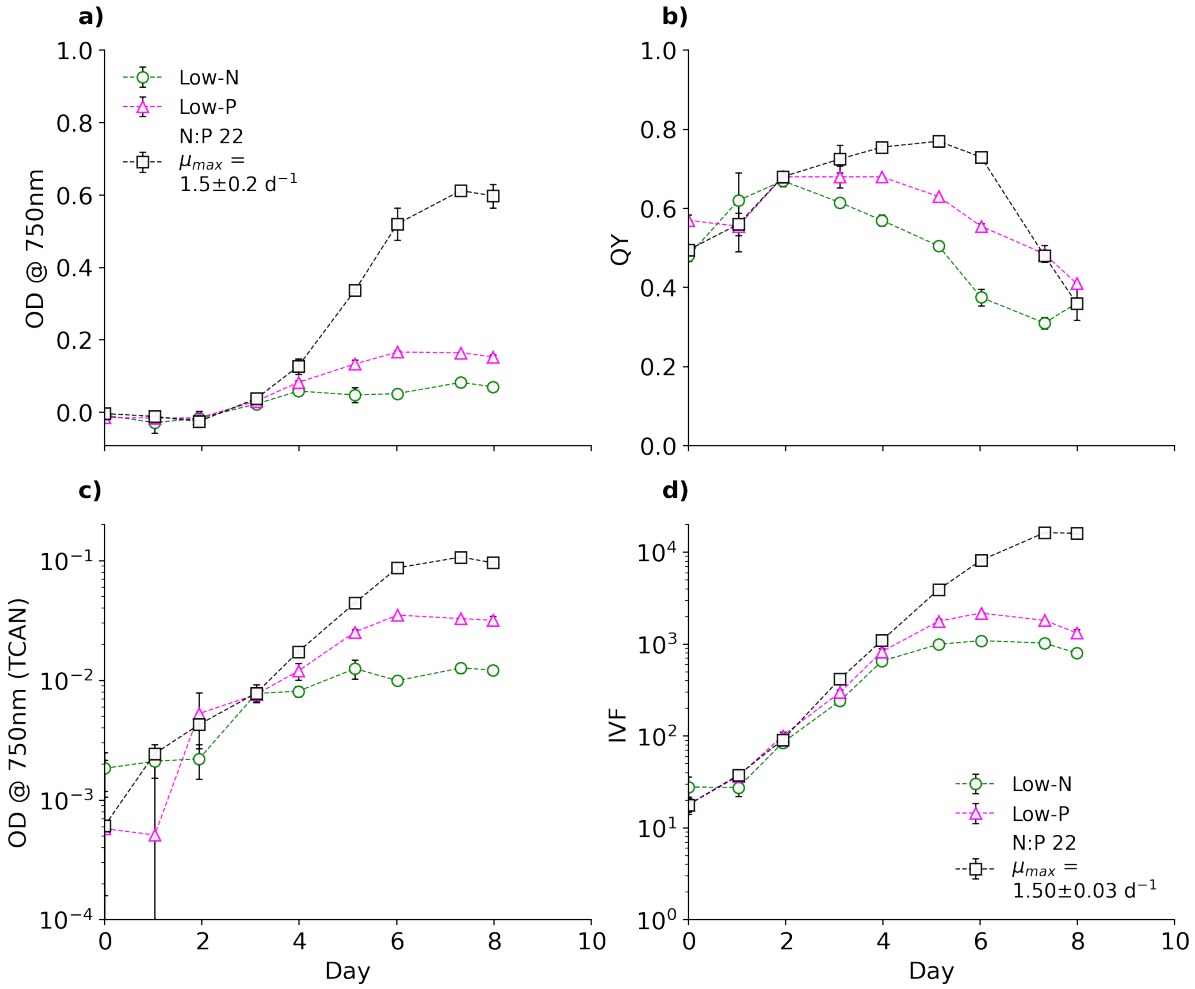

Figure 3.20: Batch experiment (nut_2) using *R. baltica*, different media and CO_2 supply. The three different cultures supplied with nitrogen limited (green circle), phosphorus limited (magenta triangle), and balanced N:P 22 (black square) medium. μ_{max} by curve fitting replica samples and provided as mean ± STD. **a)** OD at 750 nm over time (Hitachi 5100). **b)** QY over time. **c)** Log plot of OD at 750 nm over time (TCAN). **c)** Log plot of IVF over time (TCAN).

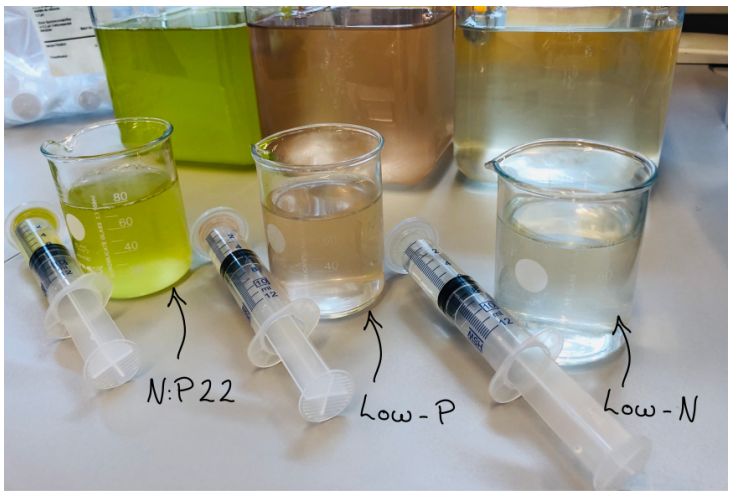

Figure 3.21: Cultures of *R. baltica* at day 8 in nut_2. From the left: N:P 22, Low-P, and Low-N.

As seen in Figure 3.21, there was visual differences between the three cultures. Low-P and Low-N, had the same appearance as nut_1 (Figure 3.19), whereas N:P 22 got a strong and bright green color. Prior to day 7 N:P 22 had a dark red color, see Figure 3.22. Note that a similar change of color was observed in WP-3 (Figure 3.10).

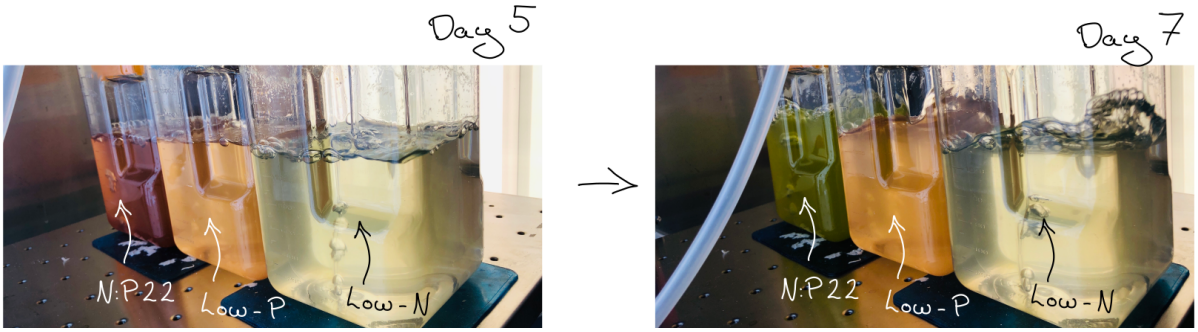

Figure 3.22: From the left the picture shows: N:P 22, Low-P, and Low-N. Pictures are taken day 5 and 7 of nut_2. There is a clear change of color for *R. baltica* cultivated in N:P 22.

Nitrogen and phosphorus concentrations were analysed in order to determine the cause of limitation in the cultures (Table 3.4). As expected, the nitrogen concentration in Low-P was the highest, but N:P 22 had the lowest remaining concentration of phosphorus. N:P 22 appeared limited by both nitrogen and phosphorus, while Low-N experienced nitrogen starvation. There was a large deviation between the two methods for determining nitrogen concentration (Table 3.4). The analysis performed at Trondhejm biologiske stasjon was ISO (International Organization for Standardization) certified and thereby the most credible for Low-N and N:P 22 as these were within the calibrated range.

Table 3.4: Final nitrogen and phosphorus concentration [$\mathrm{mg\,L^{-1}}$] in the batch experiment with CO_2 (nut_2), day 8. *Results from Trondhejm biologiske stasjon. **Outside of range.

Culture	Nitrogen [$\mathrm{mg\,L^{-1}}$]	*Nitrogen [$\mathrm{\mu g\,L^{-1}}$]	Phosphorus [$\mathrm{\mu g\,L^{-1}}$]
N:P 22	0.46	34.4	**16.5**
Low-P	2.16	**5058	**21.6**
Low-N	0.39	**2.5**	55.9

3.3 Growth in The Light Composition Study

Utilizing Nanocosm, five different experiments were performed as a part of the study assessing the effect of light quality on μ_{max}. The specific maximum growth rate in WP-1 varied more and had greater standard deviation (Figure 3.23) than the remaining WP experiments, but normally μ_{max} had a relative STD <10%. R was the only light regime that was significantly different ($p < 0.05$ and $p < 0.01$, see Figure D.3 in Appendix D), with a 23 to 32% lower μ_{max} (Figure 3.23). The μ_{max} varied from 1.37 ± 0.12 (R) to 1.98 ± 0.14 d^{-1} (W_3).

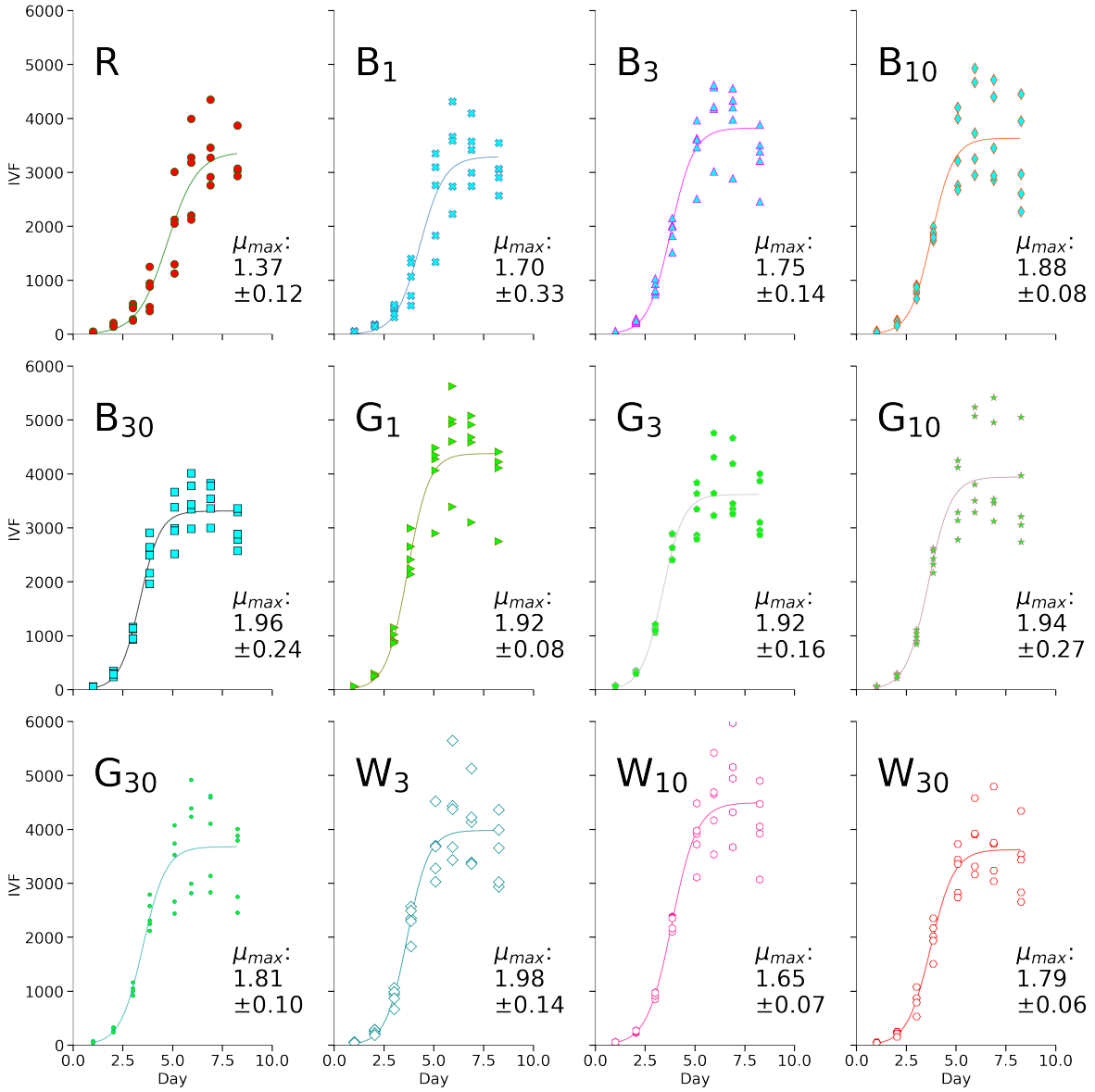

Figure 3.23: Growth and μ_{max} for *R. baltica* during WP-1 measured by IVF. μ_{max} (mean ± STD) was calculated from curve fitting each well to an individual growth curve. The growth curves in the figure uses all data points, but was not used for computing μ_{max}.

The low temperature experiment (WP-2) found no significant differences between light regimes (ANVOA, p = 0.5), and had a overall mean μ_{max} of 1.6 ± 0.1 d^{-1}. Greater differences were observed in WP-3 (Figure 3.24). R had the lowest computed μ_{max} of 0.90 ± 0.11 d^{-1}, which was 21% lower ($p < 0.01$) than B_{30}, 27% lower ($p < 0.01$) than G_{10}, and 24% lower than W_3 ($p < 0.01$, see Figure D.4 in Appendix D). The variation in growth between the five parallels of each light regime in WP-2, WP-3 and WP-4 in was smaller than in WP-1.

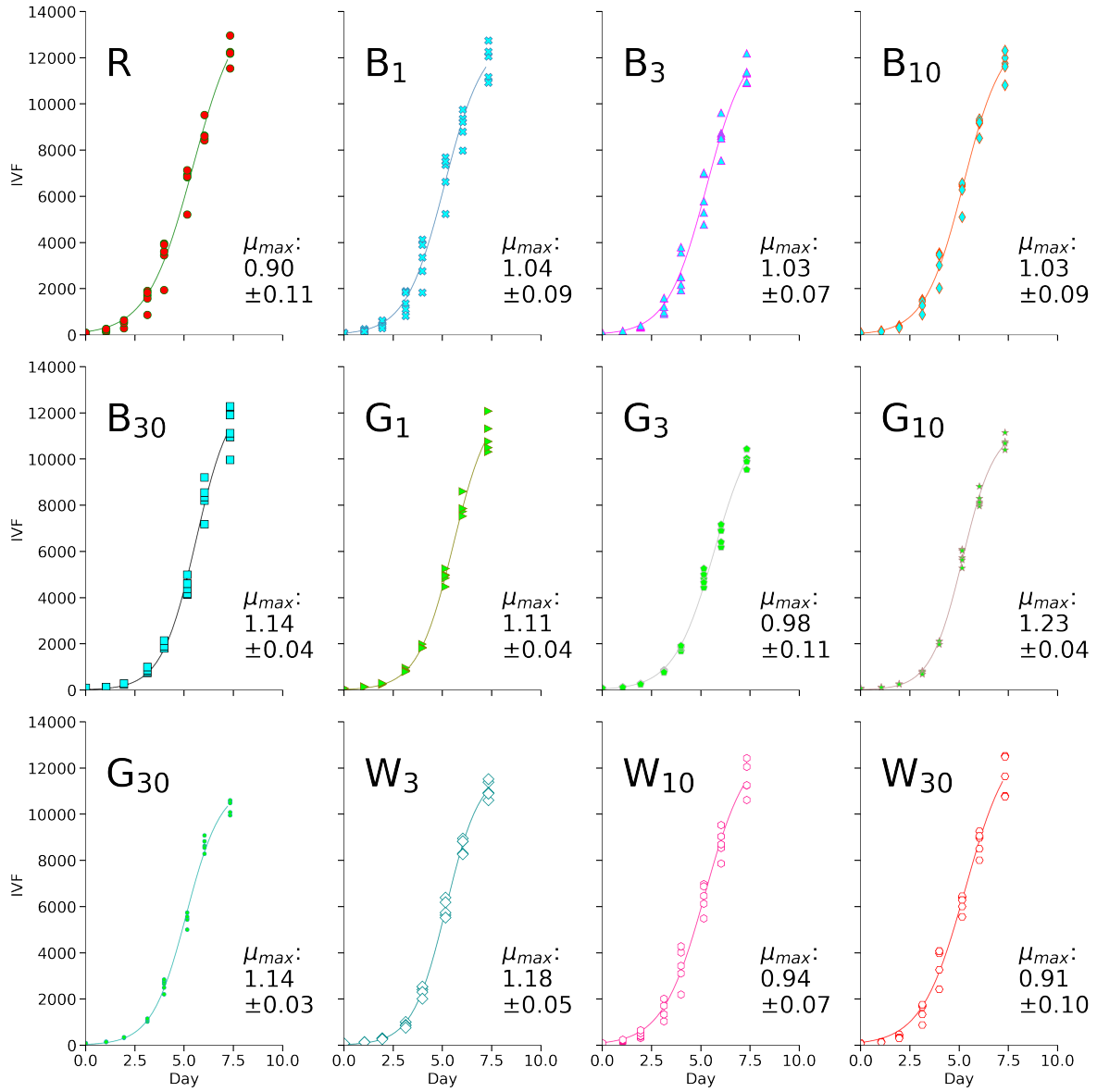

Figure 3.24: Growth and μ_{max} for *R. baltica* during WP-3 measured by IVF. μ_{max} (mean ± STD) was calculated from curve fitting each well to an individual growth curve. The growth curves in the figure uses all data points, but was not used for computing μ_{max}.

From the WP-4 experiment μ_{max} for G_{30} was $1.44 \pm 0.12\,d^{-1}$. This was the highest μ_{max} computed in WP-4, 17% higher ($p < 0.05$) than R, but surprisingly also 26% higher than B_{30}, that gave the lowest μ_{max} ($p < 0.01$, see Figure D.5 in Appendix D). WP-4 had a STD = 8% or less, which was an improvement compared with WP-1. μ_{max} from all experiments were listed in Table 3.5. Growth rates calculated using linear regression were put in Table D.1 in Appendix D.

Table 3.5: Maximum growth rate for *R. baltica*, μ_{max} [d^{-1}] (mean ± STD) calculated by curve fitting.

Light mix	WP-1	WP-2	WP-3	WP-4
R	1.37 ± 0.12	1.56 ± 0.06	0.90 ± 0.11	1.23 ± 0.08
B_1	1.70 ± 0.33	1.53 ± 0.11	1.04 ± 0.09	1.17 ± 0.04
B_3	1.75 ± 0.14	1.48 ± 0.04	1.03 ± 0.07	1.29 ± 0.06
B_{10}	1.88 ± 0.08	1.57 ± 0.09	1.03 ± 0.09	1.31 ± 0.11
B_{30}	1.96 ± 0.24	1.56 ± 0.13	1.14 ± 0.04	1.14 ± 0.06
G_1	1.92 ± 0.08	1.60 ± 0.05	1.11 ± 0.04	1.15 ± 0.07
G_3	1.92 ± 0.16	**1.66 ± 0.05**	0.98 ± 0.11	1.21 ± 0.10
G_{10}	1.94 ± 0.27	1.62 ± 0.09	**1.23 ± 0.04**	1.30 ± 0.06
G_{30}	1.81 ± 0.10	1.60 ± 0.14	1.14 ± 0.03	**1.44 ± 0.12**
W_3	**1.98 ± 0.14**	1.63 ± 0.03	1.18 ± 0.05	1.26 ± 0.07
W_{10}	1.65 ± 0.07	1.47 ± 0.12	0.94 ± 0.07	1.22 ± 0.09
W_{30}	1.79 ± 0.06	1.59 ± 0.24	0.91 ± 0.10	1.27 ± 0.06

The stepwise μ calculated as a MM developed equally for the experiments with inoculum from stationary phase (WP-2, WP-3, WP4 and WP-C, see Appendix F). The initial μ was increasing until a maximum was reached, and then gradually decreased. The time spent from initial to maximum rate varied between light regimes (Figure 3.25).

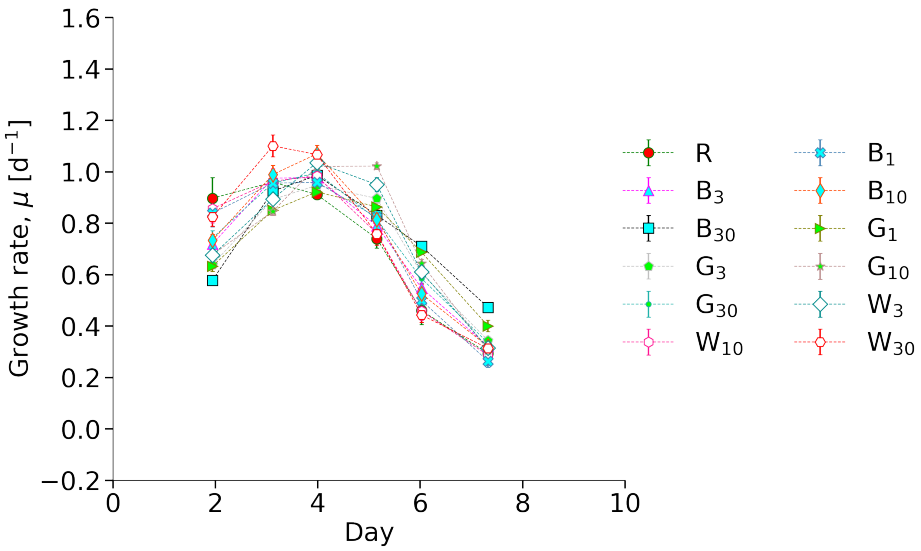

Figure 3.25: Growth rate (mean ± STD) for *R. baltica* in WP-3 calculated by Step for three day intervals (MM).

Growth Experiment, WP-C - White Control

A control experiment was conducted to compare the use of red, green and blue light with white LEDs. An older Nanocosm version with white LEDs plate used an other technology than the mixed color plates. This contained heat producing electrical components in addition to the LEDs. The growth per well was unevenly distributed (Figure 3.9). The irradiation was found to be $100 \pm 16\,\mu mol/m^2s$. However, there was no correlation between individual well irradiation and growth rate ($p = 0.89$) for WP-C. The computed μ_{max} in Figure 3.26 only include the area between column C - H and row 2 - 4, and A - D and 7 - 11, and the mean was equal to $1.6 \pm 0.3\,d^{-1}$ overlapping the median.

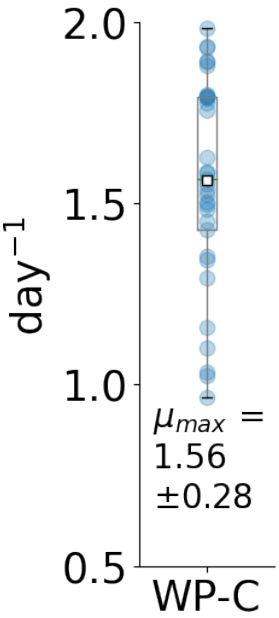

Figure 3.26: μ_{max} for *R. baltica* by linear regression using white LED light (WP-C). Wells included span the area between column C-H and row 2-4, and A-D and 7-11.

Carrying Capacity in Well Plates

The final biomass concentration of R was estimated using the standard curves (Section 3.1). The estimated AFDW of WP-3 was more than double ($p < 0.001$) that of WP-1, WP-2 and WP-4 (Table 3.6). The biomass density of the wells E3, F3 and G3 in WP-C was also estimated, but keep in mind the 40% water loss to evaporation.

Table 3.6: The final biomass [mg_{AFDW}/L] density in R for WP-1, WP-2, WP-3 and WP-4 calculated using the standard curve for the two different ODs (Figure 3.17) and the OD to DW equation (Figure 3.15) for *R. baltica*. For WP-4 the calculated biomass density was estimated for the wells E3, F3 and G3 using white light and not R.

Light mix	WP-1 [mg_{AFDW}/L]	WP-2 [mg_{AFDW}/L]	WP-3 [mg_{AFDW}/L]	WP-4 [mg_{AFDW}/L]	WP-C [$mg\,L^{-1}$]
R	90 ± 8	92 ± 18	**244 ± 8**	83 ± 8	117 ± 6

In order to compare the effect of light composition on the carrying capacity, K, the final OD in each experiment was normalized against the mean of R, see Table 3.7. Statistics showed that K was 47% higher ($p < 0.05$) in the algae treated with G_1 during WP-1 compared with R (Figure D.9 in Appendix D). No difference was found between the light regimes in WP-2 (ANOVA, $p = 0.8$). In WP-3, R was in the group of highest K. In WP-3 the G_1 resulted in 15% lower ($p < 0.01$) carrying capacity compared with R (Figure D.10 in Appendix D). For WP-4, K was 19% higher ($p < 0.05$, Figure D.11 in Appendix D) in G_{30} compared with both B_1 and B_{10}, however homogeneity assumption was weaker (Levene, $p = 0.21$), see Figure D.11.

Table 3.7: Normalized carrying capacity relative to the light regime R, K (mean ± STD), estimated from optical density at 750nm measured without membrane at the end of WP-1, WP-2, WP-3 and WP-4.

Light mix	WP-1	WP-2	WP-3	WP-4
R	1.00 ± 0.09	1.00 ± 0.20	**1.00 ± 0.03**	1.00 ± 0.09
B_1	1.02 ± 0.11	1.03 ± 0.27	0.93 ± 0.07	0.91 ± 0.02
B_3	1.32 ± 0.09	0.91 ± 0.08	0.91 ± 0.03	1.01 ± 0.02
B_{10}	1.20 ± 0.25	0.89 ± 0.04	0.91 ± 0.06	0.91 ± 0.06
B_{30}	1.23 ± 0.10	**1.29 ±0.32**	0.85 ± 0.06	0.99 ± 0.05
G_1	**1.47 ± 0.21**	1.13 ± 0.36	0.85 ± 0.06	0.99 ± 0.09
G_3	1.28 ± 0.17	1.16 ± 0.47	0.77 ± 0.02	0.98 ± 0.05
G_{10}	1.36 ± 0.22	1.12 ± 0.38	0.86 ± 0.03	1.00 ± 0.04
G_{30}	1.35 ± 0.30	1.18 ± 0.45	0.91 ± 0.03	**1.08 ± 0.02**
W_3	1.29 ± 0.17	0.94 ± 0.04	0.90 ± 0.04	0.95 ± 0.05
W_{10}	1.38 ± 0.21	1.05 ± 0.38	0.97 ± 0.08	0.99 ± 0.10
W_{30}	1.21 ± 0.19	1.06 ± 0.20	0.93 ± 0.05	0.98 ± 0.06

3.4 The Effect of Nutrients & Light Quality on Pigments

Pigments were extracted and analysed to examine the pigment composition in different growth phases and during nutrient limitations. In addition the relation between pigments and μ_{max} in the light composition study was evaluated. As shown in Figure 3.19 and Figure 3.22, the pigment composition was dependent of nutrient limitation and growth phase. This was quantified in Figure 3.27. The amount (sub-figure a), and composition (sub-figure b) varied. Note that Low-P and N:P 22 have the same relative composition during early exponential phase.

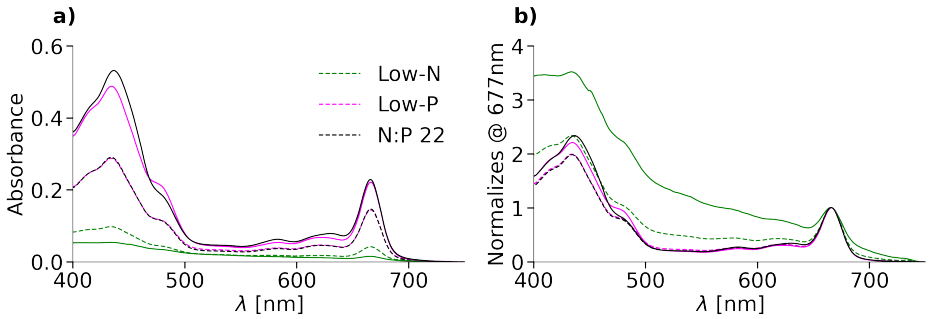

Figure 3.27: Absorbance scan of exponential phase (day 5)(dashed line) and early stationary phase (day 10)(normal line) for Low-N (green), Low-P (magenta) and N:P 22 (black) for *R. baltica*. **a)** Absorbance data. **b)** Absorbance data normalized to the red peak at 677 nm.

Pigments were extracted and analysed from WP-2, WP-3, WP-4 (Figure 3.28), and WP-C using ethanol at the end of each experiment. In WP-2, R and B_{30} had the highest blue peak for Chl *a*, while W_{30} had the lowest. B_30 also had a higher peak for Chl c_2 (Figure 3.12). In WP-3 (Figure 3.28 **b)**) R, B_{30}, G_{30}, and W_{30} were indistinguishable. The absorbance specter for WP-4 showed that G_{30} had a higher peak for alloxanthin, and a higher blue peak for Chl *a* (Figure 3.28 **c)**). WP-C had a alloxanthin peak with double the absorbance of the normalized peak at 667 nm. The median absorbance in WP-C was in general higher than in WP-4. Extraction of PE was attempted limited success, however peaks for PE (Figure 3.12) was observed in some wells (Figure D.13 in Appendix D).

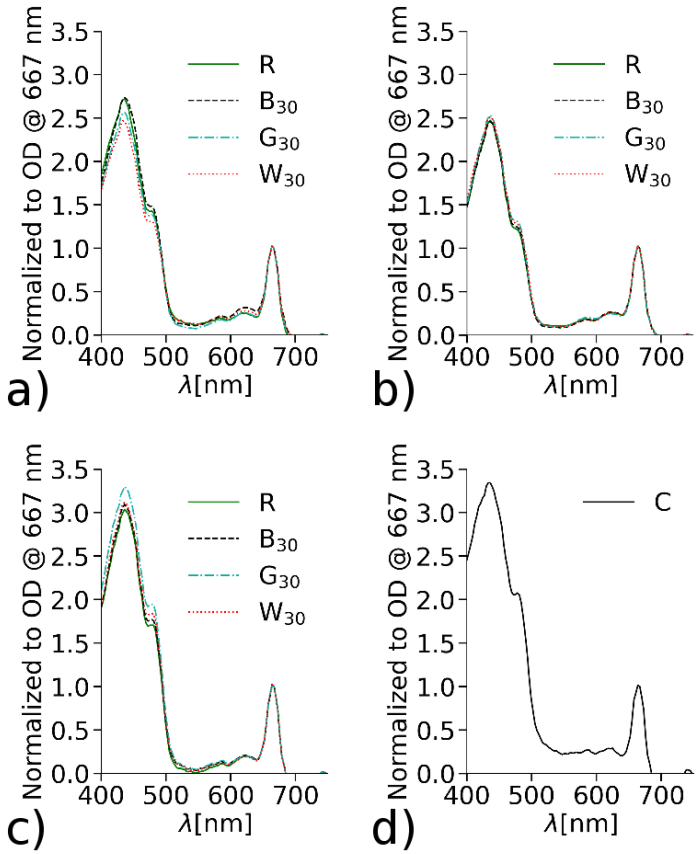

Figure 3.28: The median absorbance spectre normalized to OD at 667 nm for *R. baltica* when using the light treatments R, B_{30}, G_{30}, and W_{30}. The comparison was made for WP-2 (**a)**), WP-3 (**b)**), WP-4 (**c)**), and WP-C (**d)**).

Using spectral deconvolution, the relative composition of pigment was estimated for WP-2 (Figure 3.29), WP-3 (Figure 3.30) and WP-4 (Figure 3.29). The relative (Chl a) amount of alloxanthin and Chl c_2 was computed. Note that the sample material was taken from late exponential or stationary phase. For WP-2, there was no statistical difference in alloxanthin (Levene, p = 0.016) or Chl c_2 (ANOVA, p = 0.18) composition, see Figure 3.29. The overall mean relative content of alloxanthin was 0.51 ± 0.04, and 0.10 ± 0.01 for chl c_2.

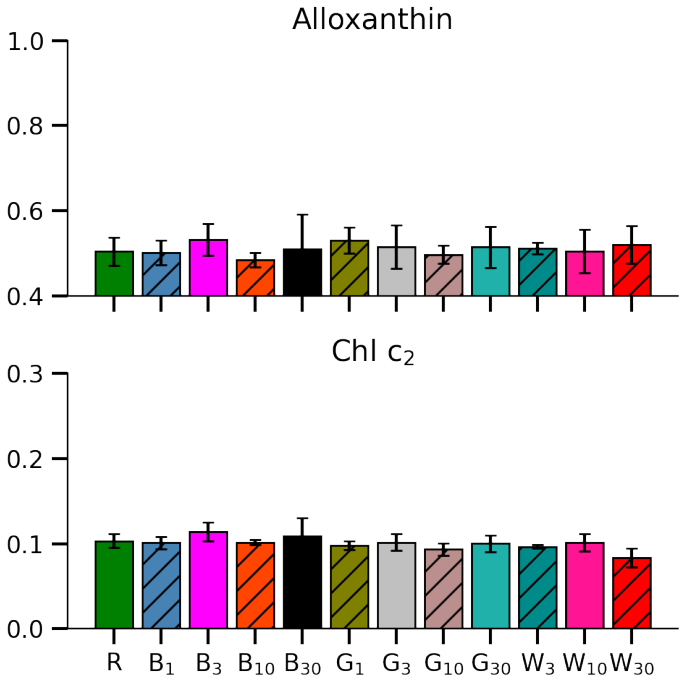

Figure 3.29: Content of alloxanthin and Chl c_2 relative to the amount of Chl a for *R. baltica* at the end of experiment WP-2. Data based on four successful extractions per light regime.

No significant difference was observed for alloxanthin (Levene, p = 0.004) or Chl c_2 (Levene: p = 0.09, ANOVA: p = 0.47) in WP-3, despite of larger variations (Figure 3.30). The overall mean content of alloxanthin was 0.46 ± 0.05 ranging from 0.42 (W_{30}) to 0.53 (G_1). Chl c_2 had an overall mean of 0.13 ± 0.01 ranging from 0.12 (B_3) to 0.14 (G_1).

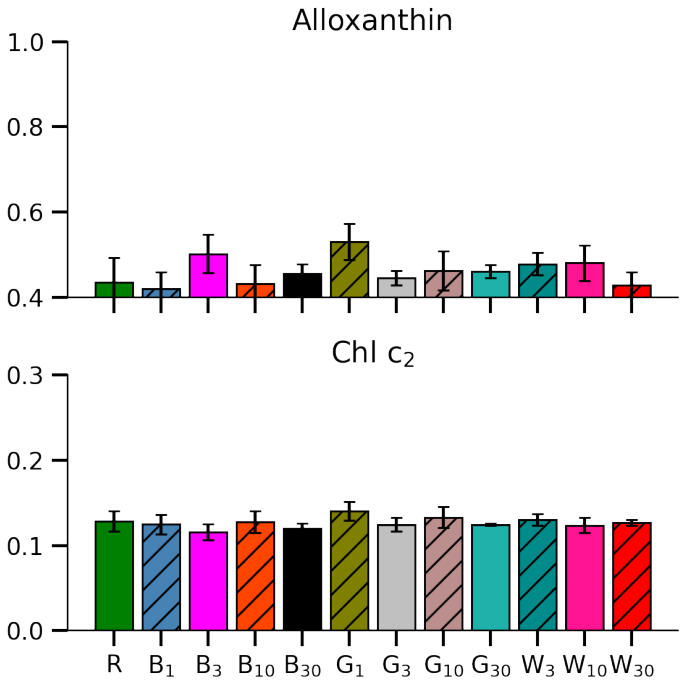

Figure 3.30: Content of alloxanthin and Chl c_2 relative to the amount of Chl *a* for *R. baltica* at the end of experiment WP-3. Data based on four successful extractions per light regime.

All extractions of pigment from WP-4 was conducted without any noise from organic matter. This contributed to a lower standard deviation within the light regimes. Here the relative content of alloxanthin in *R. baltica* treated with B_3 was 12% higher ($p < 0.001$) than the cultures treated with R, and 9% higher than G_3 ($p < 0.001$), but not higher than G_1 ($p = 0.11$). W_{30} gave the lowest relative content, 15% lower than B_3 ($p < 0.001$). The highest relative amount of Chl c_2 was obtained from G_3, and was 22% higher than G_1 that was lowest. G_3 was also 10% higher ($p = 0.0019$) than B_3, and 13% higher ($p < 0.001$) than W_3. However, there was no difference between R, B_{30}, G_{30} and W_{30}, see Figure 3.31.

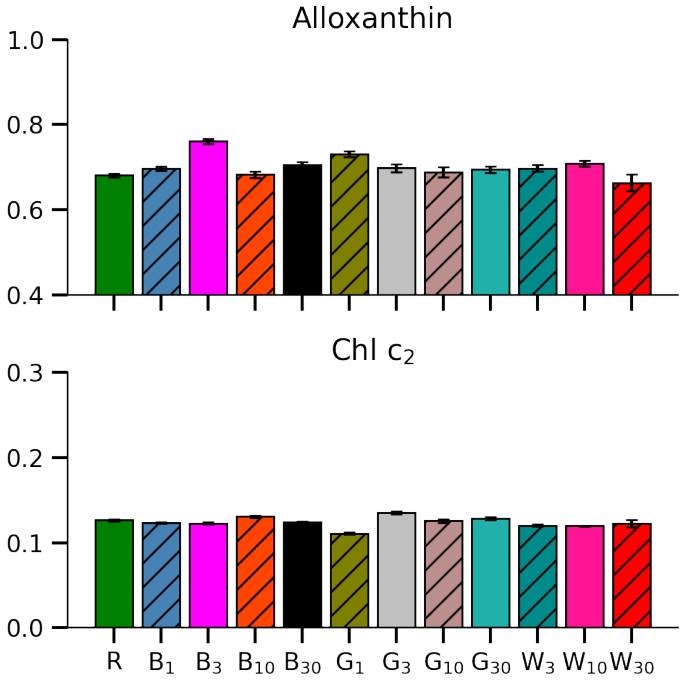

Figure 3.31: Content of alloxanthin and Chl c_2 relative to the amount of Chl *a* for *R. baltica* at the end of experiment WP-4. Data based on five successful extractions per light regime.

HPLC Results

Mixed samples from R, G_{30}, B_{30} and W_{30} were analysed with HPLC to assess the effect of light regimes on pigment content. Using the standard curves (Section 3.1) and Table 3.8, the per cell content of pigments was calculated, see Table 3.9

Table 3.8: Pigment concentration [ng µL^{-1}] from the different experiments (Exp.) using *R. baltica*. For WP-C, the mixed sample was from E3, F3 and G3. (XA = xanthin.)

Exp.	Chl c_2+c_1	AlloXA	MonadoXA	CrocoXA	Chl a	$\beta-$Carotene
WP-3						
R	**0.316**	**0.424**	0.080	**0.054**	**1.748**	0.054
B_{30}	0.304	0.419	0.082	0.048	1.413	0.040
G_{30}	0.260	**0.424**	**0.090**	0.050	1.476	**0.074**
W_{30}	0.230	0.368	0.084	0.043	1.238	0.044
WP-4						
R	**0.092**	0.190	0.030	**0.018**	0.632	0.023
B_{30}	0.082	**0.205**	0.034	0.015	**0.641**	0.043
G_{30}	0.086	0.191	**0.042**	0.017	0.561	**0.045**
W_{30}	0.089	0.190	0.038	0.023	0.602	0.028
WP-C						
C	0.055	0.105	0.026	≈ 0	0.336	0.023
nut_2						
N:P 22	0.015	0.017	0.002	0.003	0.091	0.004
Low-N	0.018	0.021	0.003	0.004	0.088	0.003
Low-P	**0.062**	**0.088**	**0.009**	**0.022**	**0.393**	**0.011**

Table 3.9: Pigment content per cell [pg/cell] in *R. baltica* from the different experiments (Exp.). The number of cells (n_{cell} $[1 \times 10^3\,mL^{-1}]$) from OD used in K estimation For WP-C, the mixed sample was from E3, F3 and G3. N:P 22 was taken in early exponential phase, while Low-N and Low-P was from stationary phase. (XA = xanthin.)

Exp.	n_{cell}	Chl c_2+c_1	AlloXA	MonadoXA	CrocoXA	Chl a	β-Carotene
WP-3							
R	554	0.570	0.764	0.145	**0.097**	**3.150**	0.097
B_{30}	499	**0.608**	**0.840**	0.164	0.096	2.830	0.080
G_{30}	526	0.493	0.805	**0.170**	0.096	2.810	**0.140**
W_{30}	533	0.431	0.691	0.157	0.081	2.320	0.082
WP-4							
R	175	**0.524**	1.090	0.171	0.104	**3.620**	0.131
B_{30}	181	0.454	**1.130**	0.188	0.081	3.550	**0.237**
G_{30}	195	0.443	0.979	0.213	0.085	2.870	0.232
W_{30}	172	0.519	1.110	**0.223**	**0.136**	3.510	0.164
WP-C							
C	265	0.207	0.398	0.098	≈ 0	1.270	0.088
nut_2							
N:P 22	214	0.071	0.080	0.011	0.015	0.426	0.021
Low-N	231	0.080	0.093	0.011	0.015	0.383	0.014
Low-P	294	**0.210**	**0.298**	**0.032**	**0.076**	**1.340**	**0.038**

4 Discussion

4.1 Control Experiments and Reliability Assessment

Reproducibility & Limiting Factors
Growth experiments in the larger scale were performed in order to obtain an understanding about the evolution in growth for *R. baltica*. This was used to plan sampling regimes for the later experiments. Reliable results in large scale experiments were desired, as the batch study was a reference to evaluate the scalability. The results for $\text{batch}_{\text{test}}$ presented in Figure 3.1 indicated reproducibility as the two cultures with identical growth medium concentration (L_1 & L_2) developed equally. A longer exponential phase and higher carrying capacity was found for H in $\text{batch}_{\text{test}}$. When comparing $\text{batch}_{\text{test}}$ and nut_1, nutrient starvation did not appear as the main limiting factor of growth in $\text{batch}_{\text{test}}$ (Figure 3.1). In nut_1 Conwy the stationary phase started at a 60% higher OD using the same nutrient concentration as H in $\text{batch}_{\text{test}}$. Albeit Lafarga-De la Cruz et al. claimed that final cell density was influenced by the initial concentration of nutrients[31]. As the cultures in nut_1 reached their carrying capacity, there was a drop in QY. This happened the same day or the day prior to observing early stationary phase. In $\text{batch}_{\text{test}}$ (that had a poor aeration by an aquatic pump) the QY dropped three days later. After the drop in QY for $\text{batch}_{\text{test}}$ L_1 and L_2, the PFD was adjusted from 150 to 270 µmol/m^{2}s to check for light limitation. This gave no increase growth and a further drop in QY for L_1 and L_2. Therefore extra Conwy was added, resulting in QY recovery to its former level (Figure 3.2), but no increase in growth rate was observed. The most probable limiting factor was therefore CO_2, as it was found that pH rose to 9.5 for nut_1 Conwy (that had good aeration) during exponential phase and thereby decreasing the available CO_2[58].

Evaluation of Measuring Method & Calculation Technique
The use of IVF measurements to calculate μ_{max} was found as the most reliable method. Not only because the membrane made it difficult to use OD during the light composition experiment (more on that later), but because of the sensitivity and precision seen in nut_2 for IVF when comparing to OD (TCAN). The curve fitting as a method for computing maximum specific growth rate was controversial[49], partly because it was a redefinition of μ_{max}. It based μ_{max} on data that was not observed, but computed using the assumption that growth followed a sigmoid curve[53]. A disadvantage of Curve Fit was the use of the data points in the post exponential phase of the experiments, that were the most affected by evaporation. The main advantage of this approach was the elimination of choice form the calculation. Each one of the 240 wells (not counting WP-C) had an individual development (Figure 3.23). Although the time interval for exponential growth was the same for several of the wells (Figure 3.3), some wells would have required individual manipulation of the time interval ($t - t_0$, Section 2.4.2) to account for non-synchronized growth. This would have been both a major source of bias and tedious work. Therefore the μ_{max} computation using curve fitting was favoured for comparing results within this study. The μ_{max} results using linear regression (Table D.1 in Appendix D) did not account for non-synchronized growth, but used the time interval where most of the wells were in exponential growth (Figure 3.3). When comparing the rates found by linear regression with the rates computed by curve fitting, the differences were large and the ranking of light regimes differed (Table 3.5. This was partly because Curve Fit probably overestimated μ_{max} on several occasions. The treatments B30, B10, and G30 were the best performing using linear regression to calculate of μ_{max}, and B30 and G30 were among the top five

best in all experiments (Table D.3, in Appendix D). Implying that the choice of method impacted the perspective on blue light, which Lafarga-De la Cruz et al. reported to have the highest productivity for *Rhodomonas* sp.[31].

Reliability of Well Plate Cultivation
Evaporation rate was reduced by the use of membrane, but varied between experiments (Table 3.3). There were several variables that had an impact on evaporation rate, but the only one monitored was the temperature in the incubator cabinet. The variation made it difficult to rationalize the observations in Table 3.3. However, the high evaporation rate from WP-C was seen in relation with heat generation from the old nancosm. As evaporation may disrupt experimental results[49] (loss of water increase OD and salinity, and can cause loss of biomass. The latter effect is occurs when algae stick to the rim of the well as a result of evaporation), the μ_{max} computation may have been affected. Yet it was assumed that evaporation was homogeneously distributed (in WP-1, WP-2, WP-3 and WP-4), as reported by Volpe et al.[49], and that the effect on comparisons with in a WP was neglected.

Although the Breathe-Easy® sealing membrane reduced evaporation (Table 3.3), it interrupted the OD measurements. The noise from the membrane was observed as a 70% difference ($p < 0.007$) in OD at 750 nm between the control row 1 and 12. In order to quantify the effect, an extra OD reading was made after removing the membrane (Figure 3.11). The difference was probably caused by the TCAN trying to read OD through the semi-transparent membrane. Attempts were made to correct for the noise created by the membrane, but the OD readings through the membrane were found to be useless.

The initial WP experiment (WP-1) had higher growth rates than WP-2, WP-3, WP-4 (Table 3.5) and WP-C (Figure 3.26). However there was a larger variation in growth than for the later experiments. WP-1 was also the only experiment with inocolum from an exponential growing culture (Figure F.4), without liquid in the reservoirs and placed on a white surface, see Table 2.3. The exponential growth at low cell densities caused more noise in the data in the start of WP-1 (Figure 3.5), as small variations have a greater impact at low densities. The distribution of growth (Figure 3.5) showed a growth rate above zero in column A and H, implying crosstalk. There were three possible sources of crosstalk. The first was directly from the LED that occurred when the Nanocosm (Figure 2.2) was misplaced relative to the wells in the WP. Secondly there was the scattering and reflection of light from the white surface underneath the WP. This was counteracted for WP-3, WP-4 and WP-C by placing the WP on a black plastic surface. The third possible way of crosstalk was if light shone trough the plastic to the neighbouring wells. As a precautionary action towards the third possibility, the microalgae was grown in white WPs as described by Volpe et al.[49]. However, crosstalk did not explain the all variation or the failed growth in row 5 to 8 column B (WP-1), see Figure 3.5, that resulted in two wells of low μ_{max} observations for R and B_1 (Figure 3.3). The cause of irregular observations in WP-1 was probably a combination of poor mixing, pipetting and crosstalk. The difference between growth in column B and G indicated that the low growth rate in R and B_1 was not only caused by the position at the edge of the WP, as both column B and G was the same distance from the edge. There might have been an increasing gradient of light crosstalk (Figure 3.10) and temperature towards the center of the WP where G_1 was located (Figure 2.3), in addition to the faulty wells (B5 & B6) that amplified the difference between R and G_1. The theory about increasing gradient of light crosstalk was

later supported by the observations made in WP-3. Here the growth in the reservoirs resulted in starvation in the inner part of the well, while the reservoirs probably had yet to reach nutrient starvation (Figure 3.11). This was seen by the color change and recognised as the same response to starvation observed in nut_2 N:P 22 (Figure 3.22). To summarize, there were several factors that should be taken into account when evaluating the results from the WP experiments.

4.2 The Effect of Nutrient Limitation & Light Quality on Growth

The Effect of Nutrient Limitation

The growth of *R. baltica* in litre scale was investigated. This provided data on growth at 100 µmol/m^{2}s that could be used to compare with the WP experiments. There was only one biological replica for each treatment, which provided limited statistical strength. However, good reproducibility was found in $batch_{test}$ (Figure 3.1) indicating that the batch experiments would provide reliable results. The use of N:P 22, Low-N, and Low-P gave the same general outcome in nut_1 and nut_2, e.i. Low-N stopped growing first, then Low-P, and last N:P 22. This was in agreement with Yamamoto et al. when they compared low and high initial concentrations of nitrogen[6]. The QY dropped before, or the same day as reduced growth was detected. The analysis of nitrogen and phosphorus at the end of nut_2 found low levels of nitrogen in Low-N and N:P 22, and low phosphorus concentration in Low-P (Table 3.4) indicating that nutrient limitation caused the drop in QY and stalling of growth.

The drop in QY was rapid for nut_1 Low-N and Low-P, which was in accordance with Kromkamp et al. and their claim that nutrient limitation cause QY to be lower than at light limitation[40]. The log transformed IVF (Figure 3.20) showed no difference in growth for nut_2 between Low-N, Low-P and N:P 22 until day 4, although QY indicated limitation day 3. When nut_2 N:P 22 became limited, the QY dropped much faster than Low-N and Low-P. This might be related to the relatively high biomass density that created a higher nutrient consumption for maintenance. The high growth rate in nut_2 N:P 22 might also explain the rapid drop in QY and color change. Continuously high growth rate, as seen in Figure 3.20 for N:P 22 until day 6 caused a sudden starvation. This was evident as N:P 22 had a color change from red to green day 6 to day 7, see Figure 3.22. This was not observed for nut_1 N:P 22. A change of color was expected for *R. baltica* when it experienced nitrogen limitation, as it has been reported to use PE as a reserve nitrogen source upon starvation[6].

Statistics using the technical duplicates and triplicates showed that the aeration with CO_2 gave higher μ_{max}. The pH in nut_1 N:P 22 was above pH = 9. A pH at this level decrease growth rate for several microalgae like in the marine diatoms *Phaeodactylum tricornutum* and *Skeletonema costatum*[59]. High pH also lowers the amount of available CO_2 which may lead to photoinhibition[58]. The increase could therefore be a consequence of lower pH during nut_2.

The Effect of Light Quality

The gradual increase in growth rate relative to R, with increasing fraction of blue light showed that both B_{10} and B_{30} gave a higher μ_{max}. However, this trend was not observed when adding green (G), and green and blue light (W). There only was 1% green light in G_1, even so the observed increase of μ_{max} from R to G_1 was 40% ($p = 0.002$). The effect of 1% green light should not be exaggerated.

The undistinguishable μ_{max} in WP-2 did not contribute when trying to answer what light combination that was optimal for growth. The 2.5 °C lower temperature was also considered to be a possible cause of the small variations in μ_{max}, as temperature may have decreased the growth potential[60] and thereby the effect of light qualities.

WP-3 and WP-4 provided significant differences and higher scores (Figure D.4 and D.5 in Appendix D) on the Levene's test relative to WP-1 (Figure D.3 in Appendix D). The results from WP-3 showed a lower μ_{max} for *R. baltica* when cultivated in R. This was in agreement with the findings of Latsos et al. and the observations in WP-1[32]. However, μ_{max} did not increase with an increasing fraction of green or/and blue light. μ_{max} obtained when using B_{30} was not higher ($p = 0.77$) than when using B_1, and G_{30} was not higher ($p > 0.9$) than G_1. The only possible correlation was found for W_3 and W_{30}, but here the computed μ_{max} was 23% lower in W_{30} than in W_3. These findings indicated that there was no direct relation between the amount of blue and green light and the growth rate. This was contradicted for G_{30} in WP-4, as it had the highest μ_{max}, and was 25% higher ($p < 0.001$) than G_1 and 19% higher ($p = 0.008$) than G_3. Although 10% green light gave the highest μ_{max} in WP-3 and 30% gave the highest in WP-4, both experiments showed improved growth from green light compared R and most other light regimes (Figure D.4 and D.5 in Appendix D). The positive effect on growth rate by green light was supported by the findings of Lafarga-De la Cruz et al. for *Rhodomonas* sp.[31], and McGee et al. for the phycobiliprotein containing rhodophyte *Rhodella* sp., but more surprisingly also for the chlorophyceae *Brachiomonas submarina*[33]. The effect of different light compositions is spices dependent[20]. A study performed by Baer et al. examined the effect of different combinations of red, green and blue light on two phycobiliprotein containing rhodophytes and found that *Galdieria sulphuraria* had highest productivity using 100% red light and the *Porphyridium purpureum* grew the fastest using 40% red, 40% green and 20% blue light[20]. When evaluating the 12 different combinations of red, green and blue tested in WP-1, WP-2, WP-3, and WP-4 all together some patterns appeared. Smaller variations between light regimes were expected, as this study uses relatively small fractions of blue and green light compared with Latsos et al. that used 100% red, blue or green light[32]. The exercise of ranking the results and putting them in a frequency table simplified the observation of small differences (Table D.3). From this it was seen that G_{10} and G_{30} were among the top five highest growth rates 7 out of 8 times. This supported the claim made earlier about the positive effect of green light.

The white control experiment showed large variations, but the mean μ_{max} from a select area in the WP had high growth compared with WP-4. The old version of the Nanocosm was not calibrated to the same extent as WP-1, WP-2, WP-3 and WP-4 (Table 2.1), but there was no correlation between the the irradiation and μ_{max}. This implied that irradiation was not the major cause of variation in growth. When qualitatively assessing the heat production from the Nanocosm, the WP-C lights was burning hot, while the multi coloured Nanocosm could be handled without the risk of burns. This might not

only have affected evaporation (as discussed earlier), but also the growth rate[60]. Having a reliable control experiment with white light would have been ideal to compare the effect of monochrome combinations of light, and the larger scale using white light.

The evaluation of optimal light quality for growing *R. baltica* was challenging. For one the impact of photoacclimation would in theory counteracted the expected outcome. Through photoacclimation the microalgae aim to maintain a high growth rate regardless of the light provided, and thereby minimizing the impact of different light treatments[30]. However, studies as the one by Baer et al. reported that best light quality gave 3.6 times higher productivity than the worst performing light treatment for *P. purpureum*[20]. The study of Baer et al. might have a weakness in its short time of acclimation (>24 h), and the continues use of the same biological replica for different light treatments. The order of testing might have affected their results, but this was not discussed. Even so, the different effects of light qualities were detectable for Baer et al. The results gained from using the nanocosm had inconsistencies, but the nanocosm could be a powerful tool using an improved experimental design and techniques[49].

Due to an unknown effect of evaporation, the carrying capacity was compared relative to the average K in R (Table 3.7), but the biomass density of R was estimated using OD (Table 3.6). As K is dependent on the nutrient supply[31], the theoretical K was equal for all wells. This was assuming that all wells received the same amount of nutrients and had a 100% biomass yield. (The doubling of biomass density for R in WP-3, was probably partly due a mistake when supplying medium concentrate.) Variations within a light regime must therefore have been due to distribution of nutrients, gas exchange, temperature, evaporation, light, and biomass loss. The results showed that WP-3 and WP-4 had less variation between the wells given the same treatment (Table 3.7). In these experiments there were only a few significant differences, but somewhat inconsistent as with μ_{max}. R had the greatest K in WP-3 (Table 3.7, and Figure D.10 in Appendix D), while G_3 had the lowest. However the use of green light gave a higher K for G_{30} in WP-4, but only significant compared with B_1 and B_{10}. This made it hard to propose that any of the light regimes allows *R. baltica* to spend more nutrients on growth and less on maintenance. However, it was interesting to note an overlap between the highest K and μ_{max} calculated using LinReg in WP-2 and WP-4 (Table 3.7, Table D.1 in Appendix D). As nutrient starvation was an assumption when estimating K, the values presented may also have reflected the average biomass productivity.

4.3 Scalability of Micro Scale Experiments

The larger scale experiment nut_1 showed that pH arose to a CO_2-limiting level within 6 days of exponential growth (Table 3.1) and in the poorly aerated $batch_{test}$ exponential growth stopped day 4. Lafarga-De la Cruz et al. reported an increase from 7.7 to 9.9 within 4 days for a similar batch experiment. It was therefore probable that CO_2 limitation occurred in the small scale WP study, as only passive gas exchange was facilitated. Apart form CO_2, nutrient starvation was a probable cause of limitation (Table 3.4). As QY began dropping at the same time as growth declined (day 5) for nut_2 N:P 22 (Figure 3.20), it was assumed that nutrient starvation would occur before light limitation in both scales. Several of the light treatments in WP-2, WP-3 and WP-4 had a μ_{max} in the size range between the two μ_{max}-observations for N:P in nut_1 and nut_2. This was not taking into account factors like evaporation, gass exchange and temperature that may

have created noise in the smaller scale. Other studies working with *Rhodomonas* sp. have reported μ_{max} in the range 0.73 to 0.96 d^{-1}[15,31,32]. This was lower than the estimations of μ_{max} in this study, however Step was used to calculate μ_{max} in these studies. The calculations of μ_{max} using LinReg (which correlates with Step, see Figure 3.3), in WP-2, WP-3 and WP-4 ranged between 0.92 ± 0.04 and $1.14 \pm 0.07\,d^{-1}$ (Table D.1 in Appendix D), which is close to, but higher than previously reported results for μ_{max}. The results obtained through using Nanocosm was scalable to a litre scale, taking into account that the results from WP-1 had the most sources for error, and was discarded in relation to scalability.

4.4 The Effect of Nutrients & Light Quality on Pigments

The composition and content of pigments were analysed to assess if chromatic adaptation[29] occurred in *R. baltica*. There was a great interest to see how the presence of PE was related to growth when using green light, but this study failed to provide results for that discussion (Figure D.13 in Appendix D). However, the method of spectral deconvolution and HPLC provided information about the pigments dissolved in ethanol. A weakness of the analysis was that the cultures were in early stationary phase (as samples could not be extracted sooner), where they were expected to become nutrient limited. According to the Yamamoto et al. pigments are degraded upon nutrient limitation[6]. This degradation was observed visually in the reference batch study (Section 3.2) for the N-limited cultures, and for nut_2 N:P 22 at day 7 (Figure 3.22). The degradation of pigments probably occurred in the WP experiments as a color change was observed in the reservoirs of WP-3 (Figure 3.10). This might have affected the PE extraction (Figure D.13 in Appendix D).

The absorbance at 545 nm is proportional to the amount of PE when subtracting absorbance (scattering) at 750 nm[6,32]. The relation between OD at 680 nm and OD at 750 nm indicate the chlorophyll content, as 680 nm is associated with Chl *a* (Figure 3.12). These two relations were used to observe photoacclimation in the LL maintained stock culture (Figure 3.13), compared with the stock culture when it was treated with HL (Figure 3.14). The relative absorbance showed a steady increase in Chl and PE content over a time period of 30 days, meaning that *R. baltica* was adapting to LL by producing more pigments.

In the initial assessment of pigments, the absorbance spectrum was created and the peaks for alloxanthin, PE, Chl c_2 and Chl *a* were identified, see Figure 3.12. The apparent redshifted peak (Figure 3.12) has previously been reported by Johnsen et al. as a measure to absorb more of the available light[30]. Later observations found no significant difference in the content of the pigments alloxanthin, and Chl c_2 relative to Chl *a* for WP-2 and WP-3. This was mainly due to large standard deviation, which could be related to poor extraction technique. The extraction from WP-4 provided statistically stronger results and showed light regimes as B_3 and G_3 to have elevated content of alloxanthin and Chl *c*2 respectively. However, none of the most radically different light regimes (R, G_{30}, B_{30} or W_{30}) showed a difference in pigment composition (Figure 3.31), and only minor differences in the median absorbance spectra (Figure 3.28). Using the mixed samples analysed by HPLC (Table 3.8) to calculate the relative amount of alloxanthin, and Chl c_2 gave a result that deviated 35-40 percent points (pp) for alloxanthin, and 1-3pp for Chl c_2 compared with spectral deconvolution. However, the HPLC analysis did not show any

large difference in composition between R, G_{30}, B_{30} or W_{30}. This implied no observed correlation between pigment composition and μ_{max}.

The pigment content in Low-P was more than double that of Low-N in stationary phase, with the exception of β-Carotene (170% higher). This was in agreement with the absorbance specter (Figure 3.27), visual observations (Figure 3.19), and the low florescent intensity observed for Low-N in the microscope (Figure D.15 in Appendix D). The Chl c_2+c_1 and a cell content was approximately the same for Low-P and WP-C, see Table 3.9. However, the content of alloxanthin, manadoxanthin and β-carotene was measured to be lower in Low-P. This might be due to the limitation on phosphorus for Low-P, as Lovio-Fragoso et al. reported that P limitation has a negative influence on alloxanthin and β-carotene in diatoms.

5 Conclusion

This study showed that *R. baltica* had the ability to adapt to different light qualities while maintaining a high maximum specific growth rate. However, the study struggled to find consistent results describing the relation between light qualities and maximum specific growth rate (μ_{max}). Results between well plate (WP) experiments using the Nanocosm varied, both when comparing within and between experiments. WP-1 found that R gave 23 - 32% lower growth than the mixes of monochrome light. WP-2 showed no significant differences in μ_{max} for any of the light regimes. WP-3 also found R to have the lowest μ_{max} ($0.90 \pm 0.11\,\mathrm{d}^{-1}$), that B_{30} gave a 21% higher, and that G_{10} gave the highest μ_{max} of $1.23 \pm 0.04\,\mathrm{d}^{-1}$. WP-4 showed that μ_{max} was greatest for G_{30} ($1.44 \pm 0.12\,\mathrm{d}^{-1}$), 17% higher than R. The overall results found that the use of G_{10} and G_{30} gave the highest μ_{max} compared with R e.i. the use of a green and red light combination facilitates for higher μ_{max} than only red light. The effect of blue light fraction, and a combination of blue and green require further investigation.

The use of the Nanocosm as a tool for evaluating different combination of monochrome light is possible, but the experimental design and set-up require further improvements to reduce noise and increase reproducibility. In general, small scale experiments are more sensitive to variations. This study showed that the specific maximum growth rates observed in the 96-well plate were within a reasonable range of the once obtained at a litre scale, thereby confirming the scalability of the setup.

Using nutrient medium with different N:P ratios, it was found that the QY of *R. baltica* drop when nutrient starvation occurs, or the day prior to starvation. Further, it was shown that nitrogen starvation causes a color change from red to green, due to the phycobilin phycoerythrin (PE) being degraded.

In vivo chlorophyll fluorescence was found to be the preferred method for monitoring growth when using the Nanocosm setup by Volpe et al. The application of curve fitting to determine μ_{max} was efficient as it used all available data points from each reactor flask or well without the need for manual adjustments. The inclusion of all data points was also a disadvantage, as the undesired effect of evaporation become more pronounced over time. The use of curve fitting provided larger variations in μ_{max} between light regimes than calculations using the traditional approach of log-transformation and linear regression, but also a different outcome.

6 Improvements and Recommendations

It is my recommendation that C-Feed AS continue the work on optimizing their light quality for cultivation of *R. baltica*. This study, in combination with existing literature suggest that light quality effect μ_{max} of *R. baltica*, and that correct application can increase the productivity while lowering the energy consumption.

Further I have the following suggested improvements and recommendations based on my empirical knowledge and experience gained through this study.

- Gain control of the actual temperature in the algae culture when using a WP for cultivation. This implies measuring the liquid temperature and taking actions to ensure that the temperature is equal for all wells
- Create a better mount for the Nanocosm that locks it in the correct position above the 96-well plate, thereby decreasing crosstalk
- Avoid evaporation by increasing the moisture surrounding the area of cultivation, or reduce the overall temperature and/or light intensity
- Perform multiple control experiments using monochrome light and equal irradiation on the entire well plate to evaluate the effect of position on the WP
- Perform a control experiment where there are rows without light separating the illuminated wells, and observe for growth in the adjacent wells without light
- Perform a control using white light, where the nanocosm has a cooling system installed
- Place the white WP on a black surface with low reflection to avoid indirect cross talk
- Look for other methods than Nile Red staining for lipid analysis and use a FCM for analysis
- Acclimate the microalgae to the light regime used in the experiments or create a semi-steady state by harvesting and feeding the cultures in the WP
- Use a more advanced form of curve fitting that is custom made for estimation of microbial growth when computing μ_{max}
- Use LEDs that have a peak wavelength more relevant for *R. baltica*
- Supply the medium used in well plates with carbonate $NaHCO_3$ to avoid CO_2 limitation
- Perform WP-1 and WP-2 once more with stationary culture, 22.5 °C, water in reservoirs and with a black surface underneath the WP
- Perform the light composition experiment at lower PFD to increase the sensitivity of light quality
- Improve the method for PE-extraction, or send samples directly to an external laboratory
- Standardize the acclimatization and state of the inoculum prior to the experiments

References

[1] Chauton, M. S., Reitan, K. I., Norsker, N. H., Tveterås, R. and Kleivdal, H. T. (2015). A techno-economic analysis of industrial production of marine microalgae as a source of EPA and DHA-rich raw material for aquafeed: Research challenges and possibilities. *Aquaculture* 436, pp. 95–103. DOI: 10.1016/j.aquaculture.2014.10.038.

[2] Field, C. B., Behrenfeld, M. J., Randerson, J. T. and Falkowski, P. (1998). Primary Production of the Biosphere: Integrating Terrestrial and Oceanic Components. eng. *Science (American Association for the Advancement of Science)* 281.5374, pp. 237–240. DOI: 10.1126/science.281.5374.237.

[3] Heimann, K. and Huerlimann, R. (2015). «Chapter 3 - Microalgal Classification: Major Classes and Genera of Commercial Microalgal Species». *Handbook of Marine Microalgae*. Ed. by S.-K. Kim. Boston: Academic Press, pp. 25–41. DOI: https://doi.org/10.1016/B978-0-12-800776-1.00003-0.

[4] Enamala, M. K. et al. (2018). Production of biofuels from microalgae - A review on cultivation, harvesting, lipid extraction, and numerous applications of microalgae. eng. *Renewable & sustainable energy reviews* 94, pp. 49–68. DOI: 10.1016/j.rser.2018.05.012.

[5] Brown, M., Jeffrey, S., Volkman, J. and Dunstan, G. (1997). Nutritional properties of microalgae for mariculture. eng. *Aquaculture* 151.1, pp. 315–331. DOI: 10.1016/S0044-8486(96)01501-3.

[6] Yamamoto, S., Bossier, P. and Yoshimatsu, T. (2020). Biochemical characterization of Rhodomonas sp. Hf-1 strain (cryptophyte) under nitrogen starvation. eng. *Aquaculture* 516, p. 734648. DOI: 10.1016/j.aquaculture.2019.734648.

[7] Øie, G. et al. (2017). Effect of cultivated copepods (Acartia tonsa) in first-feeding of Atlantic cod (Gadus morhua) and ballan wrasse (Labrus bergylta) larvae. eng. *Aquaculture nutrition* 23.1, pp. 3–17. DOI: 10.1111/anu.12352.

[8] Gagnat, M. R., Wold, P.-A., Bardal, T., Øie, G. and Kjørsvik, E. (2016). Allometric growth and development of organs in ballan wrasse (Labrus bergylta Ascanius, 1767) larvae in relation to different live prey diets and growth rates. eng. *Biology open* 5.9, pp. 1241–1251. DOI: 10.1242/bio.017418.

[9] Drillet, G. et al. (2011). Status and recommendations on marine copepod cultivation for use as live feed. eng. *Aquaculture* 315.3, pp. 155–166. DOI: 10.1016/j.aquaculture.2011.02.027.

[10] Schenk, P. M. et al. (2008). Second Generation Biofuels: High-Efficiency Microalgae for Biodiesel Production. eng. *Bioenergy research* 1.1, pp. 20–43. DOI: 10.1007/s12155-008-9008-8.

[11] Cecchin, M. et al. (2020). Improved lipid productivity in Nannochloropsis gaditana in nitrogen-replete conditions by selection of pale green mutants. eng. *Biotechnology for biofuels* 13.1, pp. 78–78. DOI: 10.1186/s13068-020-01718-8.

[12] Siaut, M. et al. (2011). Oil accumulation in the model green alga Chlamydomonas reinhardtii: Characterization, variability between common laboratory strains and relationship with starch reserves. eng. *BMC biotechnology* 11.1, pp. 7–7. DOI: 10.1186/1472-6750-11-7.

[13] Salveson, E. (2013). *Effects of copepod density and water exchange on the egg production of Acartia tonsa Dana (Copepoda: Calanoida) feeding on Rhodomonas baltica (Master's thesis, NTNU)*. eng.

[14] Alboresi, A. et al. (2016). Light Remodels Lipid Biosynthesis in Nannochloropsis gaditana by Modulating Carbon Partitioning Between Organelles. eng. *Plant physiology (Bethesda)* 171.4, pp.00599.2016–2482. DOI: 10.1104/pp.16.00599.

[15] Vu, M. T. T., Douëtte, C., Rayner, T. A., Thoisen, C., Nielsen, S. L. and Hansen, B. W. (2015). Optimization of photosynthesis, growth, and biochemical composition of the mi-

croalga Rhodomonas salina—an established diet for live feed copepods in aquaculture. eng. *Journal of applied phycology* 28.3, pp. 1485–1500. DOI: 10.1007/s10811-015-0722-2.

[16] Sánchez, J. F., Fernández-Sevilla, J. M., Acién, F. G., Cerón, M. C., Pérez-Parra, J. and Molina-Grima, E. (2008). Biomass and lutein productivity of Scenedesmus almeriensis: influence of irradiance, dilution rate and temperature. eng. *Applied microbiology and biotechnology* 79.5, pp. 719–729. DOI: 10.1007/s00253-008-1494-2.

[17] Kwon, G. et al. (2020). Effects of light and mass ratio of microalgae and nitrifiers on the rates of ammonia oxidation and nitrate production. eng. *Biochemical engineering journal* 161, p. 107656. DOI: 10.1016/j.bej.2020.107656.

[18] Reyna-Velarde, R., Cristiani-Urbina, E., Hernández-Melchor, D. J., Thalasso, F. and Cañizares-Villanueva, R. O. (2010). Hydrodynamic and mass transfer characterization of a flat-panel airlift photobioreactor with high light path. eng. *Chemical engineering and processing* 49.1, pp. 97–103. DOI: 10.1016/j.cep.2009.11.014.

[19] Larkum, A. W. D. (2020). «Light-Harvesting in Cyanobacteria and Eukaryotic Algae: An Overview». eng. *Photosynthesis in Algae: Biochemical and Physiological Mechanisms*. Advances in Photosynthesis and Respiration. Cham: Springer International Publishing, pp. 207–260. DOI: 10.1007/978-3-030-33397-3_10.

[20] Baer, S., Heining, M., Schwerna, P., Buchholz, R. and Hübner, H. (2016). Optimization of spectral light quality for growth and product formation in different microalgae using a continuous photobioreactor. eng. *Algal research (Amsterdam)* 14, pp. 109–115. DOI: 10.1016/j.algal.2016.01.011.

[21] Ouzounis, T., Fretté, X., Rosenqvist, E. and Ottosen, C.-O. (2014). Spectral effects of supplementary lighting on the secondary metabolites in roses, chrysanthemums, and campanulas. eng. *Journal of plant physiology* 171.16, pp. 1491–1499. DOI: 10.1016/j.jplph.2014.06.012.

[22] Das, P., Lei, W., Aziz, S. S. and Obbard, J. P. (2011). Enhanced algae growth in both phototrophic and mixotrophic culture under blue light. eng. *Bioresource technology* 102.4, pp. 3883–3887. DOI: 10.1016/j.biortech.2010.11.102.

[23] Cardona, T. (2018). Early Archean origin of heterodimeric Photosystem I. eng. *Heliyon* 4.3, e00548–e00548. DOI: 10.1016/j.heliyon.2018.e00548.

[24] Kume, A. et al. (2011). Erratum to: The ratio of transmitted near-infrared radiation to photosynthetically active radiation (PAR) increases in proportion to the adsorbed PAR in the canopy. eng. *Journal of plant research* 124.1, pp. 107–107. DOI: 10.1007/s10265-010-0365-y.

[25] Mascoli, V., Novoderezhkin, V., Liguori, N., Xu, P. and Croce, R. (2020). Design principles of solar light harvesting in plants: Functional architecture of the monomeric antenna CP29. eng. *Biochimica et biophysica acta. Bioenergetics* 1861.3, pp. 148156–148156. DOI: 10.1016/j.bbabio.2020.148156.

[26] Takaichi, S. (2011). Carotenoids in algae: Distributions, biosyntheses and functions. eng. *Marine drugs* 9.6, pp. 1101–1118. DOI: 10.3390/md9061101.

[27] Manirafasha, E., Ndikubwimana, T., Zeng, X., Lu, Y. and Jing, K. (2016). Phycobiliprotein: Potential microalgae derived pharmaceutical and biological reagent. eng. *Biochemical engineering journal* 109, pp. 282–296. DOI: 10.1016/j.bej.2016.01.025.

[28] Carruthers, T. J., Longstaff, B. J., Dennison, W. C., Abal, E. G. and Aioi, K. (2001). «Chapter 19 - Measurement of light penetration in relation to seagrass». *Global Seagrass Research Methods*. Ed. by F. T. Short and R. G. Coles. Amsterdam: Elsevier Science, pp. 369–392. DOI: 10.1016/B978-044450891-1/50020-7.

[29] Czeczuga, B. (1985). Studies on phycobiliproteins in Algae. VI. Light-harvesting phycobiliprotein pigments in some Rhodophyta from the Adriatic Sea. eng. *Acta Societatis Botanicorum Poloniae* 54.4, p. 443. DOI: 10.5586/asbp.1985.038.

[30] Johnsen, G. and Sakshaug, E. (2007). Biooptical characteristics of PSII and PSI in 33 species (13 pigment groups) of marine phytoplankton, and the relevance for pulse-amplitude-modulated and fast-repetition-rate fluorometry. eng. *Journal of phycology* 43.6, pp. 1236–1251. DOI: 10.1111/j.1529-8817.2007.00422.x.

[31] Lafarga-De la Cruz, F., Valenzuela-Espinoza, E., Millán-Núñez, R., Trees, C. C., Santamaría-del-Ángel, E. and Núñez-Cebrero, F. (2006). Nutrient uptake, chlorophyll a and carbon fixation by Rhodomonas sp. (Cryptophyceae) cultured at different irradiance and nutrient concentrations. *Aquacultural Engineering* 35.1, pp. 51–60. DOI: 10.1016/j.aquaeng.2005.08.004.

[32] Latsos, C., Houcke, J. van, Blommaert, L., Verbeeke, G. P., Kromkamp, J. and Timmermans, K. R. (2021). Effect of light quality and quantity on productivity and phycoerythrin concentration in the cryptophyte Rhodomonas sp. eng. *Journal of applied phycology* 33.2, pp. 729–741. DOI: 10.1007/s10811-020-02338-3.

[33] McGee, D., Archer, L., Fleming, G. T. A., Gillespie, E. and Touzet, N. (2020). Influence of spectral intensity and quality of LED lighting on photoacclimation, carbon allocation and high-value pigments in microalgae. eng. *Photosynthesis research* 143.1, pp. 67–80. DOI: 10.1007/s11120-019-00686-x.

[34] Finazzi, G. and Minagawa, J. (2014). «High Light Acclimation in Green Microalgae». eng. *Non-Photochemical Quenching and Energy Dissipation in Plants, Algae and Cyanobacteria*. Advances in Photosynthesis and Respiration. Dordrecht: Springer Netherlands, pp. 445–469. DOI: 10.1007/978-94-017-9032-1_21.

[35] Van Wijk, K. J. and Van Hasselt, P. R. (1990). The quantum efficiency of photosystem II and its relation to non-photochemical quenching of chlorophyll fluorescence; the effect of measuring-and growth temperature. eng. *Photosynthesis research* 25.3, pp. 233–240. DOI: 10.1007/BF00033164.

[36] Baker, N., Harbinson, J. and Kramer, D. (2007). Determining the limitations and regulation of photosynthetic energy transduction in leaves. eng. *Plant, cell and environment* 30.9, pp. 1107–1125. DOI: 10.1111/j.1365-3040.2007.01680.x.

[37] Figueroa, F. L., Jerez, C. G. and Korbee, N. (2013). Use of in vivo chlorophyll fluorescence to estimate photosynthetic activity and biomass productivity in microalgae grown in different culture systems/Uso de la fluorescencia de la clorofila in vivo para estimar la actividad fotosintetica y productividad de la biomasa en microalgas crecidas en diferentes sistemas de cultivo. eng. *Latin american journal of aquatic research* 41.5, p. 801. DOI: 10.3856/vol41-issue5-fulltext-1.

[38] Ibaraki, Y. and Murakami, J. (Jan. 2007). «Distribution of chlorophyll fluorescence parameter Fv/Fm within individual plants under various stress conditions». *XXVII International Horticultural Congress - IHC2006: International Symposium on Advances in Environmental Control, Automation and Cultivation Systems for Sustainable, High-Quality Crop Production under Protected Cultivation*. Vol. 761, pp. 255–260. DOI: 10.17660/ActaHortic.2007.761.33.

[39] Power, M. (1998). Introduction Recovery in Aquatic Ecosystems: Considerations for definition and measurement. eng. *Journal of aquatic ecosystem stress and recovery* 6.3, pp. 179–180. DOI: 10.1023/A:1017284215776.

[40] Kromkamp, J. and Peene, J. (1999). Estimation of phytoplankton photosynthesis and nutrient limitation in the Eastern Scheldt estuary using variable fluorescence. eng. *Aquatic ecology* 33.1, pp. 101–104. DOI: 10.1023/A:1009900124650.

[41] Vonshak, A., Torzillo, G. and Tomaseli, L. (1994). Use of chlorophyll fluorescence to estimate the effect of photoinhibition in outdoor cultures of Spirulina platensis. eng. *Journal of applied phycology* 6.1, pp. 31–34. DOI: 10.1007/BF02185901.

[42] Kolber, Z., Zehr, J. and Falkowski, P. (1988). Effects of Growth Irradiance and Nitrogen Limitation on Photosynthetic Energy Conversion in Photosystem II 1. eng. *Plant physiology (Bethesda)* 88.3, pp. 923–929. DOI: 10.1104/pp.88.3.923.

[43] White, S., Anandraj, A. and Bux, F. (2011). PAM fluorometry as a tool to assess microalgal nutrient stress and monitor cellular neutral lipids. eng. *Bioresource technology* 102.2, pp. 1675–1682. DOI: 10.1016/j.biortech.2010.09.097.

[44] Courchesne, N. M. D., Parisien, A., Wang, B. and Lan, C. Q. (2009). Enhancement of lipid production using biochemical, genetic and transcription factor engineering approaches. eng. *Journal of biotechnology* 141.1, pp. 31–41. DOI: 10.1016/j.jbiotec.2009.02.018.

[45] Domínguez, A., Pereira, S. and Otero, A. (2019). Does Haematococcus pluvialis need to sleep? *Algal Research* 44. cited By 0. DOI: 10.1016/j.algal.2019.101722.

[46] Abiusi, F. et al. (2014). Growth, photosynthetic efficiency, and biochemical composition of Tetraselmis suecica F&M-M33 grown with LEDs of different colors. eng. *Biotechnology and bioengineering* 111.5, pp. 956–964.

[47] Mühlroth, A. et al. (2017). Mechanisms of Phosphorus Acquisition and Lipid Class Remodeling under P Limitation in a Marine Microalga. eng. *Plant physiology (Bethesda)* 175.4, pp. 1543–1559. DOI: 10.1104/pp.17.00621.

[48] Lovio-Fragoso, J. P., Jesús-Campos, D. de, López-Elías, J. A., Medina-Juárez, L. Á., Fimbres-Olivarría, D. and Hayano-Kanashiro, C. (2021). Biochemical and molecular aspects of phosphorus limitation in diatoms and their relationship with biomolecule accumulation. eng. *Biology (Basel, Switzerland)* 10.7, p. 565. DOI: 10.3390/biology10070565.

[49] Volpe, C., Vadstein, O., Andersen, G. and Anddersen, T. (2021). Nanocosm: a well plate photobioreactor for environmental and biotechnological studies. eng. *Lab on a Chip*. DOI: 10.1039/d0lc01250e.

[50] Yam, F. and Hassan, Z. (2005). Innovative advances in LED technology. eng. *Microelectronics Journal* 36.2, pp. 129–137. DOI: 10.1016/j.mejo.2004.11.008.

[51] Liu, Y., Li, L. and Jia, R. (2011). The Optimum Resource Ratio (N:P) for the Growth of Microcystis Aeruginosa with Abundant Nutrients. *Procedia Environmental Sciences* 10. 2011 3rd International Conference on Environmental Science and Information Application Technology ESIAT 2011, pp. 2134–2140. DOI: 10.1016/j.proenv.2011.09.334.

[52] Gauglitz, G. (2003). «Chapter 2 - Photophysical, Photochemical and Photokinetic Properties of Photochromic Systems». *Photochromism*. Ed. by H. Dürr and H. Bouas-Laurent. Amsterdam: Elsevier Science, pp. 15–63. DOI: 10.1016/B978-044451322-9/50006-3.

[53] Sprouffske, K. and Wagner, A. (2016). Growthcurver: An R package for obtaining interpretable metrics from microbial growth curves. eng. *BMC bioinformatics* 17.1, pp. 172–172. DOI: 10.1186/s12859-016-1016-7.

[54] Zhu, C. J. and Lee, Y. K. (1997). Determination of biomass dry weight of marine microalgae. eng. *Journal of applied phycology* 9.2, pp. 189–194.

[55] Fernandes, A. S., Petry, F. C., Mercadante, A. Z., Jacob-Lopes, E. and Zepka, L. Q. (2020). HPLC-PDA-MS/MS as a strategy to characterize and quantify natural pigments from microalgae. eng. *Current Research in Food Science* 3, pp. 100–112. DOI: 10.1016/j.crfs.2020.03.009.

[56] Cuellar-Bermudez, S. P., Aguilar-Hernandez, I., Cardenas-Chavez, D. L., Ornelas-Soto, N., Romero-Ogawa, M. A. and Parra-Saldivar, R. (2015). Extraction and purification of high-value metabolites from microalgae: essential lipids, astaxanthin and phycobiliproteins. eng. *Microbial biotechnology* 8.2, pp. 190–209.

[57] Lee, S. and Lee, D. K. (2018). What is the proper way to apply the multiple comparison test? eng. *Korean journal of anesthesiology* 71.5, pp. 353–360. DOI: 10.4097/kja.d.18.00242.

[58] Larsson, C. and Axelsson, L. (1999). Bicarbonate uptake and utilization in marine macroalgae. eng. *European journal of phycology* 34.1, pp. 79–86. DOI: 10.1017/S0967026299001936.

[59] TARALDSVIK, M. and MYKLESTAD, S. M. (2000). The effect of pH on growth rate, biochemical composition and extracellular carbohydrate production of the marine diatom Skeletonema costatum. eng. *European journal of phycology* 35.2, pp. 189–194. DOI: 10.1080/09670260010001735781.

[60] Ras, M., Steyer, J.-P. and Bernard, O. (2013). Temperature effect on microalgae: a crucial factor for outdoor production. eng. *Reviews in environmental science and biotechnology* 12.2, pp. 153–164. DOI: 10.1007/s11157-013-9310-6.

[61] Chen, Y. and Vaidyanathan, S. (2012). A simple, reproducible and sensitive spectrophotometric method to estimate microalgal lipids. *Analytica Chimica Acta* 724, pp. 67–72. DOI: 10.1016/j.aca.2012.02.049.

[62] Collos, Y., Mornet, F., Sciandra, A., Waser, N., Larson, A. and Harrison, P. (1999). An optical method for the rapid measurement of micromolar concentrations of nitrate in marine phytoplankton cultures. eng. *Journal of applied phycology* 11.2, pp. 179–184.

[63] Jia, F., Kacira, M. and Ogden, K. L. (2015). Multi-Wavelength Based Optical Density Sensor for Autonomous Monitoring of Microalgae. eng. *Sensors (Basel, Switzerland)* 15.9, pp. 22234–22248.

[64] Mutterer, J. and Zinck, E. (2013). Quick-and-clean article figures with FigureJ. eng. *Journal of microscopy (Oxford)* 252.1, pp. 89–91. DOI: 10.1111/jmi.12069.

Appendix

A Growth medium

A.1 Conwy Concentrate Medium, C-Feed version

- $NaNO_3$ $100.0\,g\,L^{-1}$
- Na−EDTA $30.0\,g\,L^{-1}$
- $NaH_2PO_4 \cdot 2\,H_2O$ $17.4\,g\,L^{-1}$
- $FeCl_3 \cdot 6\,H_2O$ $1.3\,g\,L^{-1}$
- $MnCl_2 \cdot 4\,H_2O$ $0.36\,g\,L^{-1}$
- Vitamin B_1 $0.1\,g\,L^{-1}$
- Vitamin B_{12} $0.005\,g\,L^{-1}$
- Trace Metal Solution $2\,mL\,L^{-1}$
  - $ZnCl_2$ $10.5\,g\,L^{-1}$
  - $CuSO_4 \cdot 5\,H_2O$ $10\,g\,L^{-1}$

$$\frac{17.4\,g_{NaH_2PO_4 \cdot 2\,H_2O}}{156\,g/mol_{NaH_2PO_4 \cdot 2\,H_2O}} = 0.11\,mol_{NaH_2PO_4 \cdot 2\,H_2O}$$

$$\frac{100\,g_{NaNO_3}}{85\,g/mol_{NaNO_3}} = 1.18\,mol_{NaNO_3}$$

The N:P ratio in the medium is 10.6.

A.2 Conwy Concentrate Medium, N:P 22 Version

Deviations from the C-Feed version in Section A.1 are listed.

- $NaH_2PO_4 \cdot 2\,H_2O$ $8.4\,g\,L^{-1}$
- Vitamin B_{12} $0.016\,g\,L^{-1}$

$$\frac{8.4\,g_{NaH_2PO_4 \cdot 2\,H_2O}}{156\,g/mol_{NaH_2PO_4 \cdot 2\,H_2O}} = 0.05\,mol_{NaH_2PO_4 \cdot 2\,H_2O}$$

$$\frac{100\,g_{NaNO_3}}{85\,g/mol_{NaNO_3}} = 1.18\,mol_{NaNO_3}$$

The N:P ratio in the medium is 22.

A.3 Conwy Concentrate Medium, Low Nitrate Version

Deviations from the C-Feed version in Section A.1 are listed.

- $NaNO_3$ $10.0\,g\,L^{-1}$
- $NaH_2PO_4 \cdot 2\,H_2O$ $8.4\,g\,L^{-1}$
- Vitamin B_{12} $0.016\,g\,L^{-1}$

$$\frac{8.4\,g_{NaH_2PO_4 \cdot 2\,H_2O}}{156\,g/mol_{NaH_2PO_4 \cdot 2\,H_2O}} = 0.05\,mol_{NaH_2PO_4 \cdot 2\,H_2O}$$

$$\frac{10\,g_{NaNO_3}}{85\,g/mol_{NaNO_3}} = 0.118\,mol_{NaNO_3}$$

The N:P ratio in the medium is 2.

A.4 Conwy Concentrate Medium, Low Phosphate Version

Deviations from the C-Feed version in Section A.1 are listed.

- $NaH_2PO_4 \cdot 2\,H_2O$ $0.84\,g\,L^{-1}$
- Vitamin B_{12} $0.016\,g\,L^{-1}$

Add 1 mL per liter AFSW.

$$\frac{0.84\,g_{NaH_2PO_4 \cdot 2\,H_2O}}{156\,g/mol_{NaH_2PO_4 \cdot 2\,H_2O}} = 0.005\,mol_{NaH_2PO_4 \cdot 2\,H_2O}$$

$$\frac{100\,g_{NaNO_3}}{85\,g/mol_{NaNO_3}} = 1.18\,mol_{NaNO_3}$$

The N:P ratio in the medium is 236.

B Nanocosm Adjustment Data

In order to find the relation between different parameters fed to the Nanocosm and the PFD, several measurements were taken at different brightness and byte (Table B.1).

Table B.1: Measurements used to compute the equations (2.1) and (2.2). Values for Red, Green, and Blue are given as the PDF [µmol/m^2s]. As there are differences between LEDs, the measurement was performed in two well positions.

Byte	Red	Green	Blue	Brightness	Well
0	0.1	0.1	0.1	140	G2
0	0.1	0.1	0.1	140	B4
2	0.1	0.2	0.2	140	G2
2	0.2	0.2	0.2	140	B4
5	0.8	0.8	1.3	140	G2
5	0.9	0.9	1.4	140	B4
10	2.5	2.6	4.3	140	G2
10	2.6	2.8	4.3	140	B4
20	7.4	7.8	12.8	140	G2
20	7.8	8.0	13.3	140	B4
30	13.4	13.8	23.0	140	G2
30	14.2	14.2	23.8	140	B4
50	32.7	35.0	57.5	140	G2
50	35.3	35.2	57.7	140	B4
50	7.3	7.8	12.6	60	G2
50	7.7	8.1	12.4	60	B4
50	16.4	16.9	28.5	100	G2
50	17.4	18.0	28.6	100	B4
70	57.5	60.2	99.1	140	G2
70	61.1	62.5	98.5	140	B4
110	107.0	113.0	186.2	140	G2
110	113.0	116.6	190.6	140	B4

C Raw Data for Standard Curves

By applying spectrophotometric analysis, there can be found multiple relations between optical density and content of lipids, nutrients and biomass concentrations in an microalgae culture[61–63]. A linear correlation between biomass or cell density and optical density was expected[63] and standard curves were made on the basis of OD and AFDW (Table C.1), and cell concentration, OD and IVF (Table C.2).

Table C.1: Raw data for the standard curve based on OD and AFDW.

Sample	OD750	AFDW [$g\,L^{-1}$]
24	0.017	0.119
25	0.040	0.132
26	0.037	0.115
27	0.018	0.137
28	0.056	0.207
29	0.051	0.243
30	0.057	0.183
31	0.058	0.230
32	0.140	0.447
33	0.128	0.452
34	0.125	0.436
35	0.136	0.420
36	0.281	0.910
37	0.292	0.849
38	0.294	0.886
39	0.243	0.919
40	-0.015	-0.009
41	0.012	0.006
42	-0.013	0.004

Table C.2: Raw data for the standard curve based on OD, IVF and the cell density.

Sample	Cells [$1 \times 10^3\,mL^{-1}$]	OD750	IVF
C1	0	0.0406	25
C2	131.27	0.0759	1723
C3	311.42	0.1107	3316
C4	437.12	0.1410	4284
D1	0.01	0.0406	25
D2	136.69	0.0763	1717
D3	301.01	0.1092	2968
D4	470.02	0.1435	4328
E1	0	0.0413	24
E2	150.23	0.0758	1716
E3	312.13	0.1064	2959
E4	501.58	0.1480	4490

D Extra Results

D.1 Growth in WP-2 and WP-4

Growth was monitored for WP-2 (Figure D.1) and WP-4 (Figure D.2), and growth rate was computed.

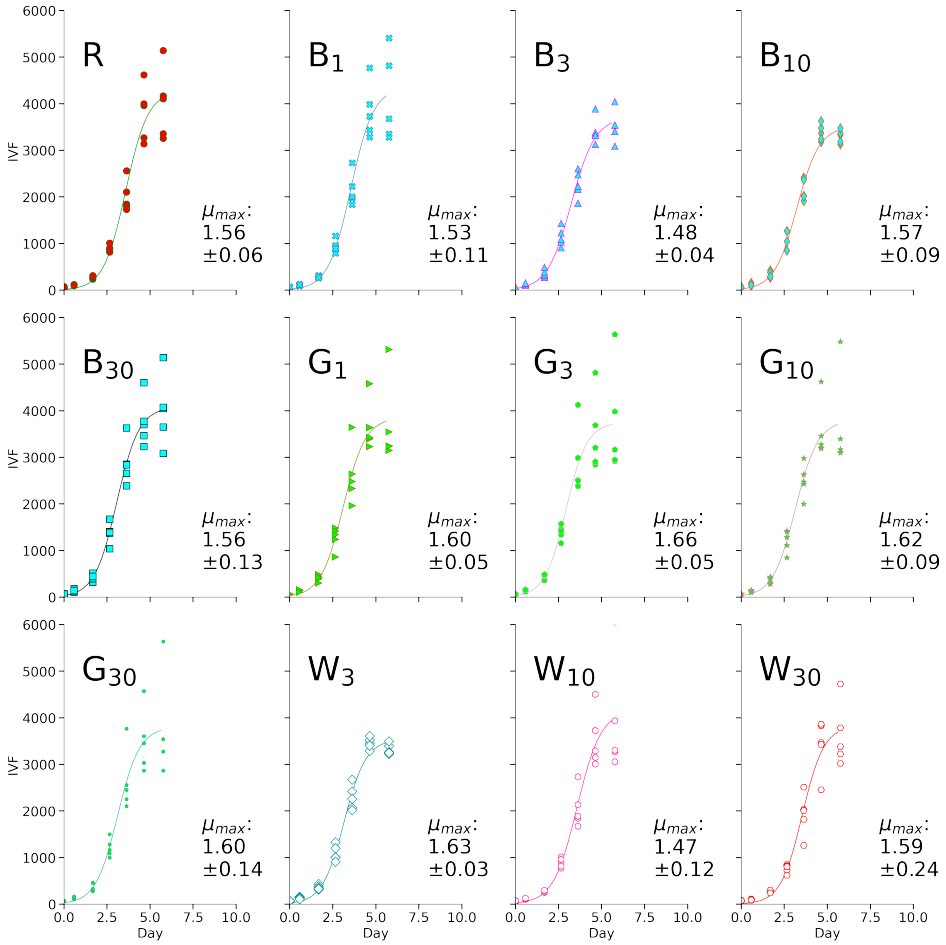

Figure D.1: Growth and μ_{max} for WP-2. μ_{max} (mean ± STD) was calculated from curve fitting each well to a growth curve.

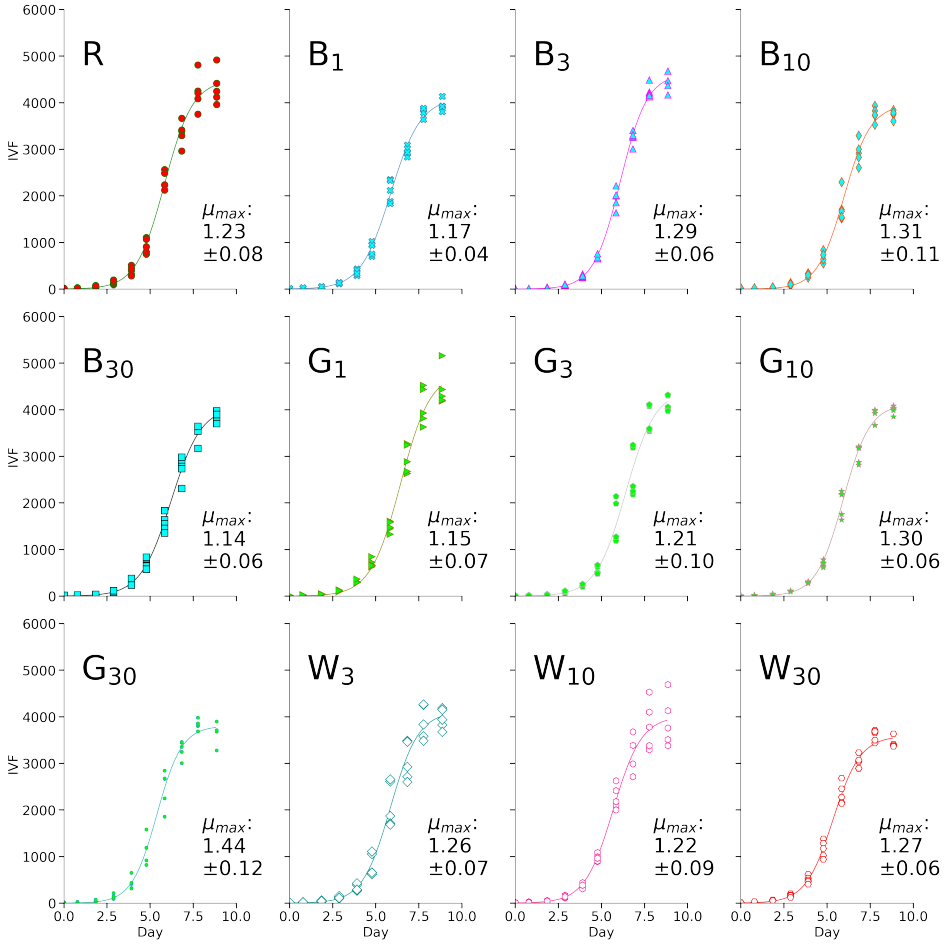

Figure D.2: Growth and μ_{max} for WP-4. μ_{max} (mean ± STD) was calculated from curve fitting each well to a growth curve.

D.2 Maximum Growth Rate by Linear Regression

The values for μ_{max} was calculated as the mean ± STD of linear regression for each well in the different light regimes, see Table D.1.

Table D.1: Maximum growth rate, μ_{max} [d^{-1}] (mean ± STD) for *R. baltica* computed using linear regression.

Light mix	WP-1	WP-2	WP-3	WP-4
R	0.97 ± 0.14	0.98 ± 0.04	0.92 ± 0.02	1.00 ± 0.06
B_1	1.03 ± 0.19	1.00 ± 0.05	0.96 ± 0.06	1.00 ± 0.05
B_3	1.27 ± 0.04	0.97 ± 0.03	0.99 ± 0.09	1.03 ± 0.04
B_{10}	1.30 ± 0.06	0.96 ± 0.02	**1.08 ± 0.09**	1.00 ± 0.05
B_{30}	**1.39 ± 0.06**	**1.01 ± 0.02**	0.99 ± 0.02	1.04 ± 0.03
G_1	1.29 ± 0.04	0.97 ± 0.05	0.93 ± 0.04	0.98 ± 0.08
G_3	1.31 ± 0.05	0.98 ± 0.06	0.95 ± 0.02	0.97 ± 0.06
G_{10}	1.31 ± 0.03	1.00 ± 0.05	0.99 ± 0.02	0.97 ± 0.05
G_{30}	1.32 ± 0.07	0.99 ± 0.05	1.00 ± 0.03	**1.14 ± 0.07**
W_3	1.33 ± 0.01	0.94 ± 0.02	1.02 ± 0.02	0.99 ± 0.06
W_{10}	1.31 ± 0.04	0.96 ± 0.04	0.99 ± 0.04	1.01 ± 0.08
W_{30}	1.30 ± 0.03	0.97 ± 0.07	1.07 ± 0.04	1.03 ± 0.04

D.3 Statistics for Maximum Specific Growth Rate by Curve Fitting

The values for μ_{max} found by curve fitting are listed in Table 3.5. Significance test for the experiment WP-1, WP-3 and WP-4 (Figure D.3, D.4 and D.5) showed a significant difference (ANOVA, $p < 0.001$), but no difference was found in WP-2 (ANOVA, $p = 0.5$).

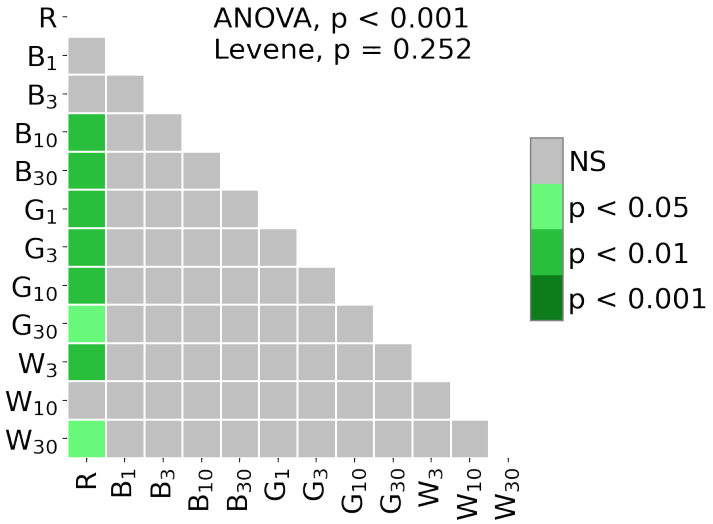

Figure D.3: ANOVA and Levene's test followed by the MCT Tukey for μ_{max} in WP-1.

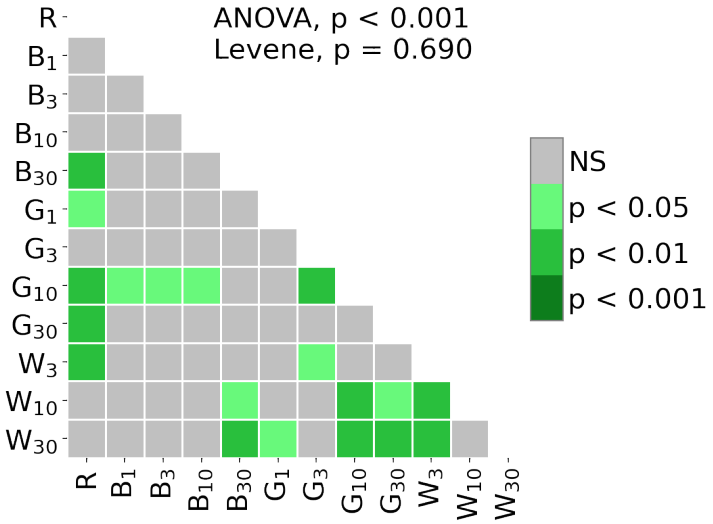

Figure D.4: ANOVA and Levene's test followed by the MCT Tukey for μ_{max} in WP-3.

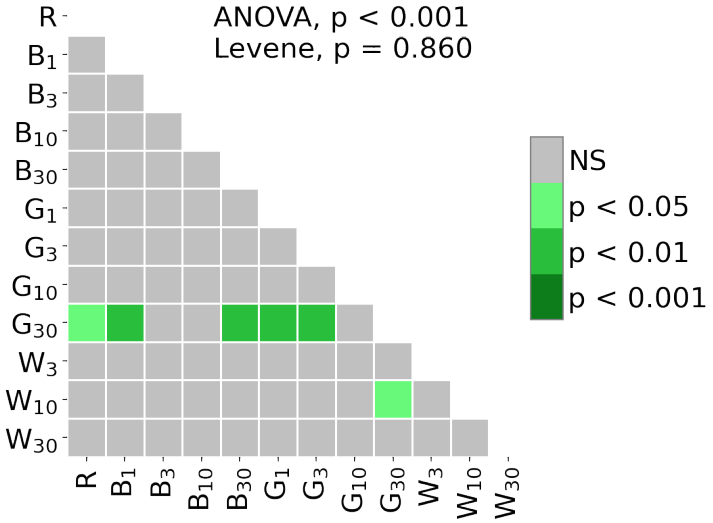

Figure D.5: ANOVA and Levene's test followed by the MCT Tukey for μ_{max} in WP-4.

D.4 Maximum Growth Rate per Intensity

The intensity specific values for μ_{max} [$d^{-1}W^{-1}m^2$] (Table D.2) was different within the experiment WP-1, WP-3 and WP-4 (Figure D.6, D.7 and D.8) (ANOVA, $p < 0.001$), but no difference was found in WP-2 (ANOVA, $p = 0.2$).

Table D.2: Light intensity specific maximum growth rate, μ_{max} [$1 \times 10^{-2}\, d^{-1}W^{-1}m^2$] (mean ± STD) for *R. baltica*. Growth was calculated using curve fitting, and intensity was calculated using Equation (2.3).

Light mix	WP-1	WP-2	WP-3	WP-4
R	7.1 ± 0.6	8.1 ± 0.3	4.6 ± 0.6	6.4 ± 0.4
B_1	8.8 ± 1.7	8.0 ± 0.6	5.4 ± 0.5	6.0 ± 0.2
B_3	9.0 ± 0.7	7.6 ± 0.2	5.3 ± 0.3	6.6 ± 0.3
B_{10}	9.4 ± 0.4	7.9 ± 0.5	5.2 ± 0.5	6.6 ± 0.5
B_{30}	9.4 ± 1.1	7.5 ± 0.7	5.4 ± 0.3	5.4 ± 0.3
G_1	9.9 ± 0.4	8.3 ± 0.2	5.8 ± 0.2	6.0 ± 0.4
G_3	9.9 ± 0.8	**8.5 ± 0.3**	5.1 ± 0.6	6.2 ± 0.5
G_{10}	9.8 ± 1.3	8.2 ± 0.5	**6.3 ± 0.2**	6.7 ± 0.3
G_{30}	8.9 ± 0.5	7.8 ± 0.7	5.6 ± 0.2	**7.1 ± 0.6**
W_3	**10.0± 0.7**	8.2 ± 0.1	6.0 ± 0.3	6.4 ± 0.3
W_{10}	8.4 ± 0.4	7.5 ± 0.6	4.9 ± 0.4	6.3 ± 0.5
W_{30}	8.7 ± 0.4	7.7 ± 1.2	4.4 ± 0.5	6.1 ± 0.3

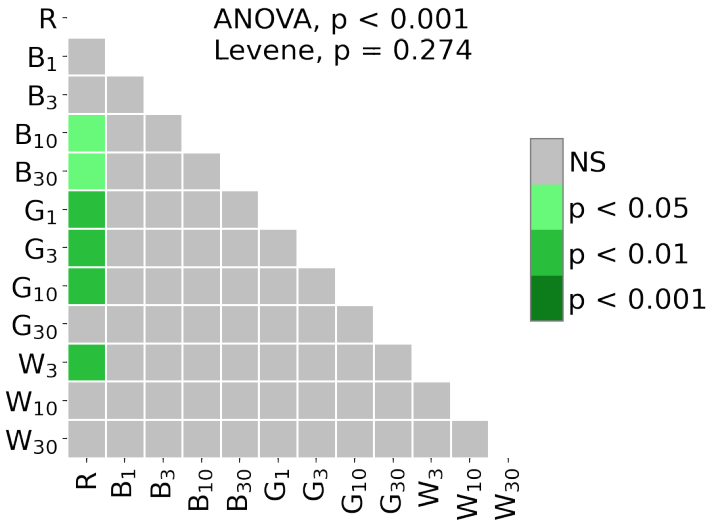

Figure D.6: ANOVA and Levene's test followed by the MCT Tukey for μ_{max} in WP-1.

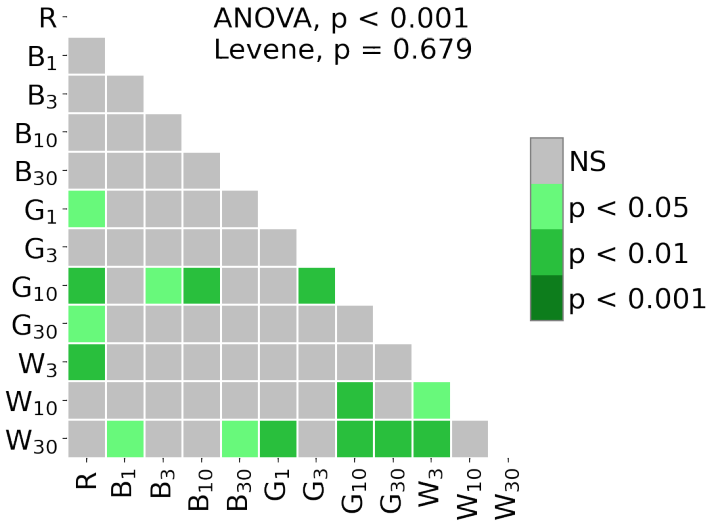

Figure D.7: ANOVA and Levene's test followed by the MCT Tukey for μ_{max} in WP-3.

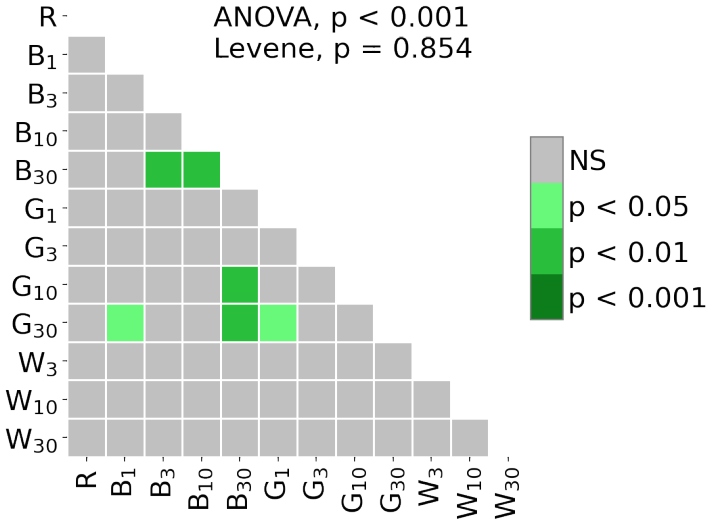

Figure D.8: ANOVA and Levene's test followed by the MCT Tukey for μ_{max} in WP-4.

D.5 Statistics for Carrying Capacity K

Statistics for the relative carrying capacity measured in WP-1 (Figure D.9), WP-3 (Figure D.10), and WP-4 (Figure D.11).

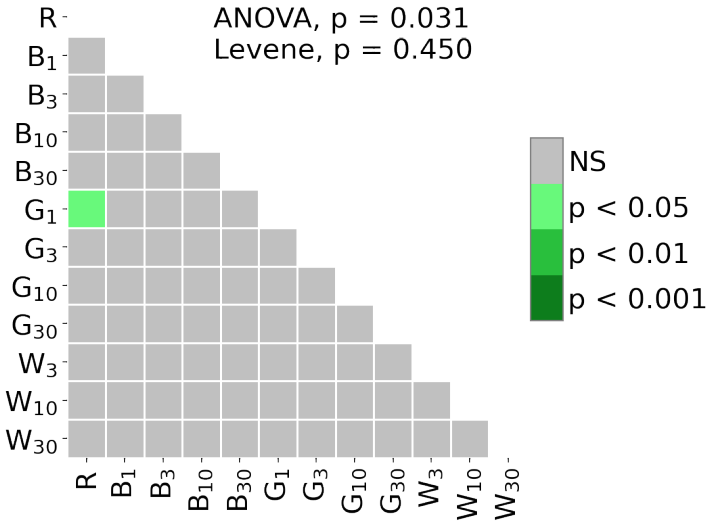

Figure D.9: ANOVA and Levene's test followed by the MCT Tukey for K in WP-1.

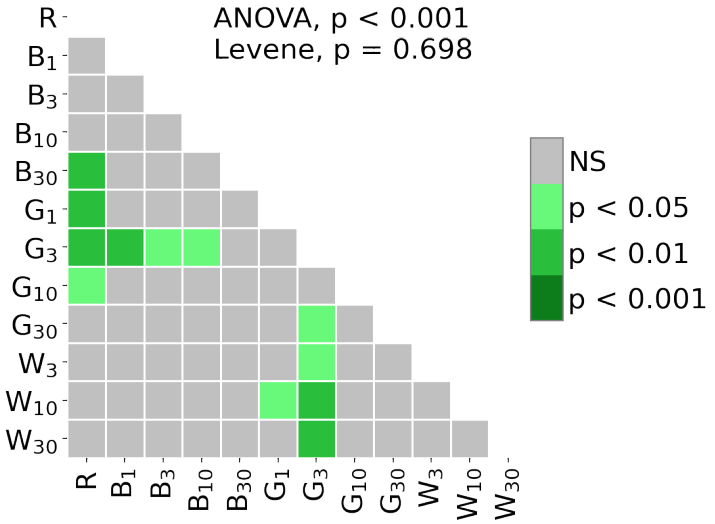

Figure D.10: ANOVA and Levene's test followed by the MCT Tukey for K in WP-3.

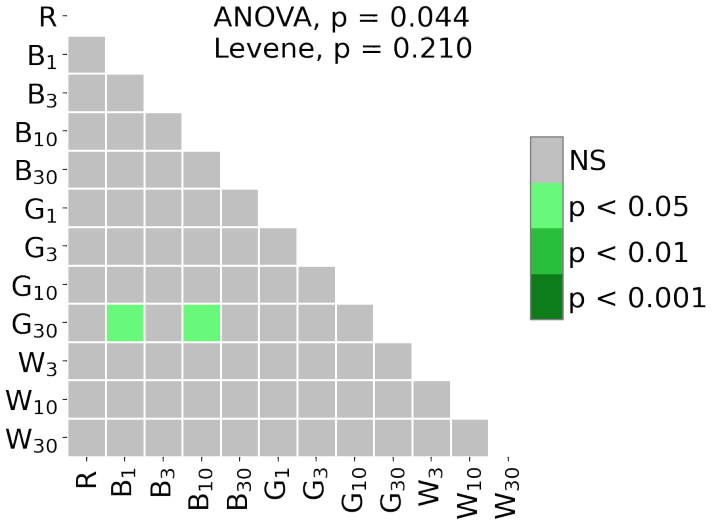

Figure D.11: ANOVA and Levene's test followed by the MCT Tukey for K in WP-4.

D.6 Frequency Table

In order to quantify the consistency of the results, a frequency table was made (Table D.3). Here the top ranking results from WP-1, WP-2, WP-3 and WP-4 on the basis of μ_{max} and K were compared.

Table D.3: Frequency table for μ_{max} computed by Curve Fit (CF) (Table 3.5) and LinReg (LR) (Table D.1), and for the carrying capacity (K). The five highest (T 5) or five lowest (B 5) ranking light regimes in each experiment were given one point in the category Top 5 or Bottom 5 respectively. When the mean was equal, the lowest STD gave a higher rank. In the case of equal mean and STD, both were given a point.

Light mix	T 5 CF	B 5 CF	T 5 LR	B 5 LR	T 5 K	B 5 K
R	0	3	1	3	2	2
B_1	0	3	2	2	1	3
B_3	1	3	0	2	3	1
B_{10}	1	1	1	2	0	3
B_{30}	2	2	4	0	2	2
G_1	3	1	0	4	2	1
G_3	2	2	0	2	1	1
G_{10}	4	0	3	1	3	1
G_{30}	3	0	4	0	4	0
W_3	3	0	2	1	0	3
W_{10}	0	3	2	1	2	0
W_{30}	1	2	2	1	1	2

D.7 Ethanol and PBS Pigment Extraction from WP-3

The extraction using ethanol (Figure D.12) did not obtain PE, but extracted an array of other pigments, see Table 3.8.

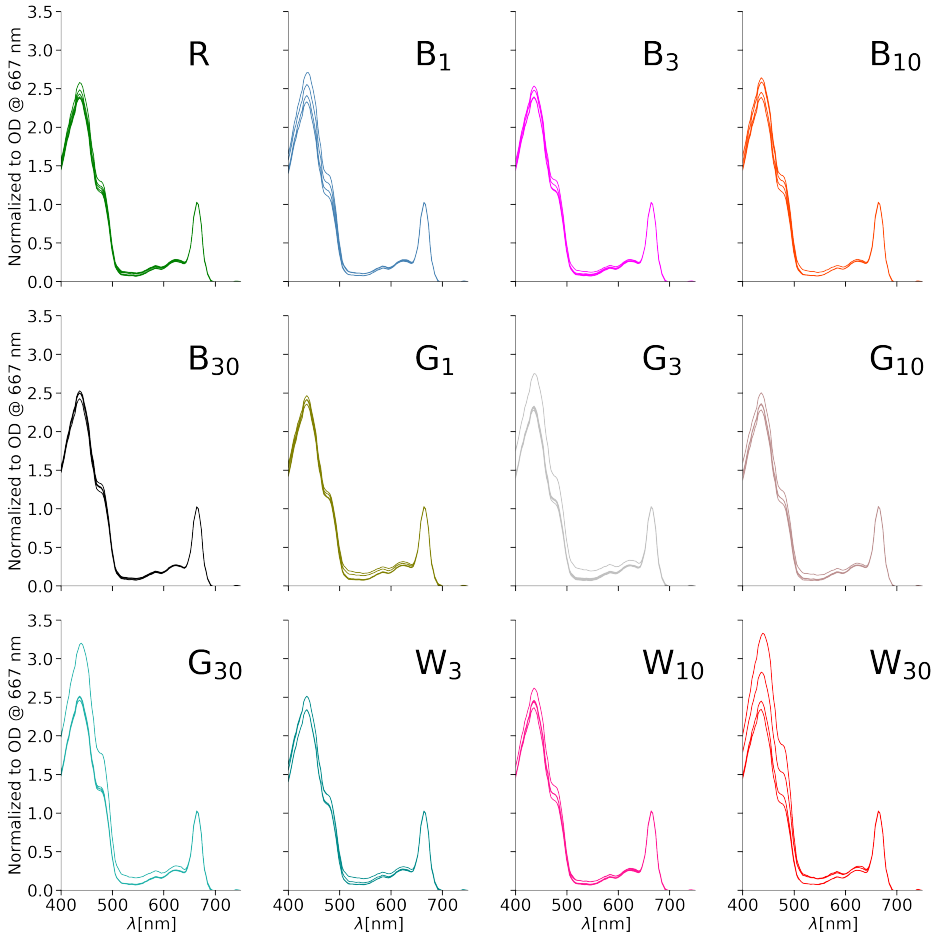

Figure D.12: Absorbance spectre measured from WP-3 after extraction of pigments using ethanol. All values were normalized to the peak at 667 nm.

PE was extracted to assess the relation between light regime and pigment content and composition. Only a few wells showed sign of PE being extracted, see Figure D.13.

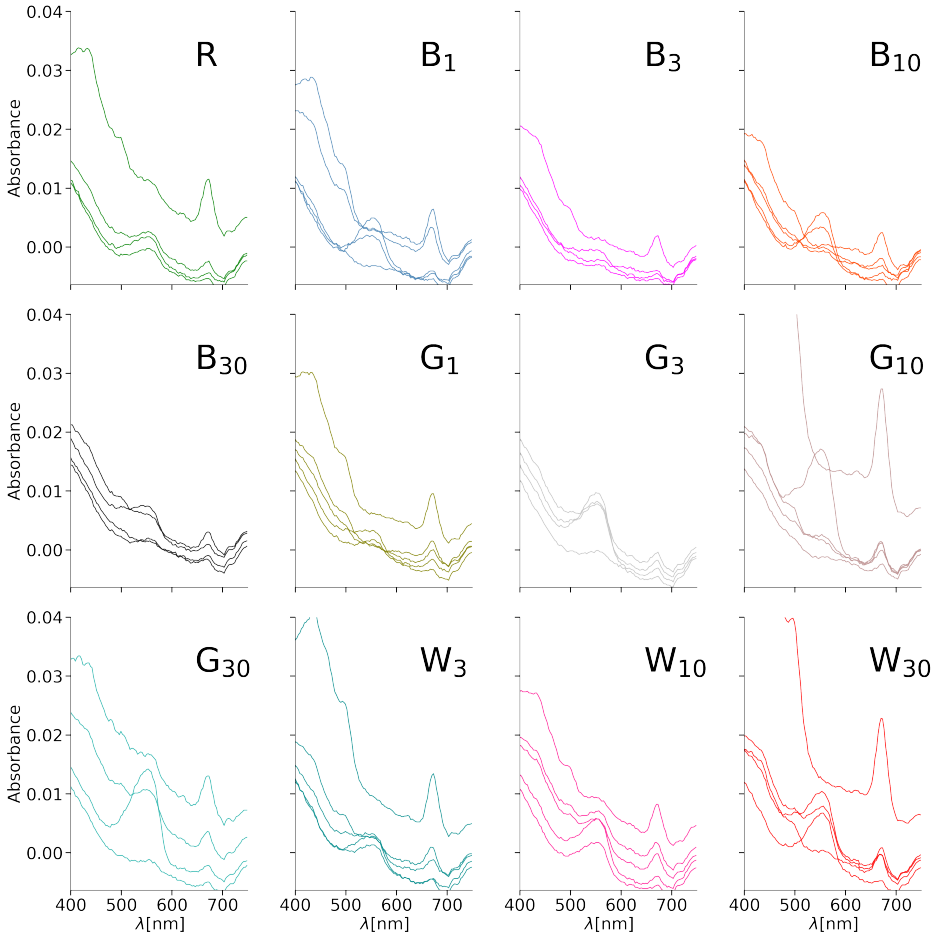

Figure D.13: Absorbance spectre measured from WP-3 after extraction of PE using PBS.

D.8 Estimation of Lipid Content Using Nile Red

As an attempt to determine the lipid content in the algae, Nile Red staining was applied. However, a control experiment showed that the relative fluorescence was only found to be 1% higher than the unstained samples (Figure D.14). As a result the development in fatty acid content was hard, if not impossible, to estimate from the recorded values.

Lipid Staining with Nile Red

In order to evaluate the lipid content, Nile Red staining was applied. To check for an adequate signal from Nile Red stained algae, several control experiments were performed. One such control is represented in Figure D.14.

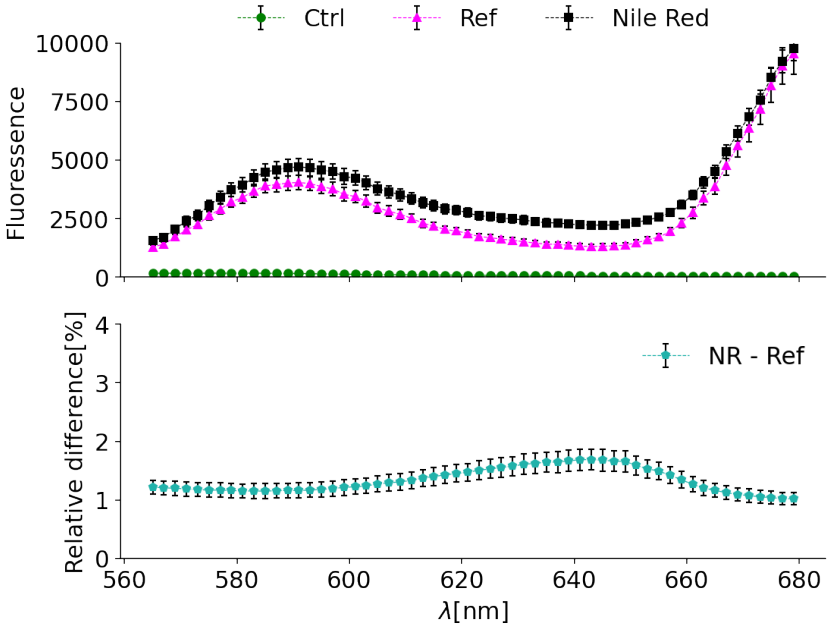

Figure D.14: The measured fluorescence emitted in the range 565-680 nm from *R. baltica* when stained with Nile Red and exited at 490 nm. Ctrl is the salt water control, Ref is the unstained sample, Nile Red is the stained sample, and NR - Ref is the relative increase in fluorescence from Nile Red staining.

The cultures (N:P 22, Low-P, and Low-N) were studied under a fluorescence microscope (ex 559, em 636), searching for any obvious differences. Further, the Nile Red staining was tested. The largest difference was observed between N:P 22 and Low-N (Figure D.15 **c)** and **b)**). Here the fluorescence was much stronger in N:P 22. While no sign of lipid granulates were observed for N:P 22 in Figure D.15 a), there were circular fluorescent granulates observed for Low-N in Figure D.15 **d)**.

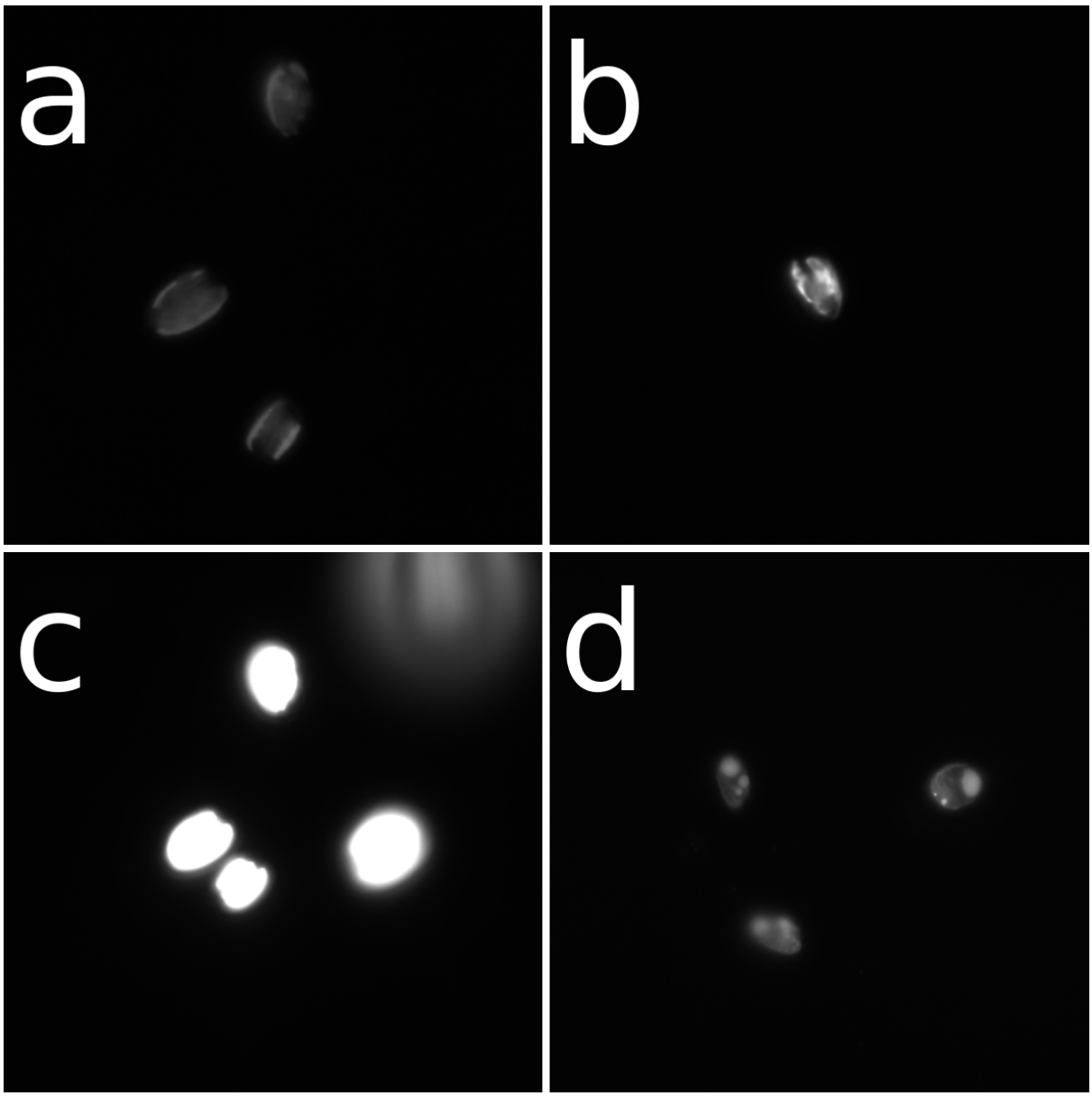

Figure D.15: *R. baltica* was studied (day 8) in a fluorescence microscope during nut_1. Figure made using FigureJ[64]. The images **b**, **c**, and **d** are taken using equal settings. **a)** N:P 22 culture. Exposure adjusted. **b)** Low-N culture. Note the thylakoid membrane. **c)** N:P 22 culture. Overexposure is deliberate to show the relative fluorescence. **d)** Low-N culture stained with Nile Red. Note the circular granulates inside the cells.

E Calculations

E.1 Statistical Script

A general example of how the statistics were calculated follows.

```
#!/usr/bin/env python3
# -*- coding: utf-8 -*-
"""
Statistics:
LEVENES
ANOVA
TUKEY

@author: Tor-Erik Holt Paulen
@contact: tepaulse@stud.ntnu.no
"""
import numpy as np
import pandas as pd
from scipy.stats import f_oneway
from statsmodels.stats.multicomp import pairwise_tukeyhsd
import scipy.stats  as ss

#Sets of data to compare:
Values_1 = [1,2,3]
Values_2 = [4,5,6]
Values_3 = [7,8,9]
Values_4 = [10,11,12]
Values_5 = [13,14,15]

#Sets of data compared:
these = [Values_1, Values_2,
         Values_3, Values_4]

#Name of sets compared:
gr = ["Set_1", "Set_2","Set_3", "Set_4"]

#Create a list containing all values
all_values = []
for t in these:
    for v in t:
        all_values.append(v)

#Performs Levene's test
W, var_score = ss.levene(Values_1, Values_2,
                         Values_3, Values_4,
                         center= 'median')

#Prints result of Levene's test
text = '\n'f'Levene, p = {var_score:.3f}'
print(text)

```

```
#Performs one way ANOVA
resu = f_oneway(Values_1, Values_2,
                Values_3, Values_4)
#Prints result from ANOVA
print(resu)

#Creates DataFrame for post hoc test
DF_stat=pd.DataFrame({'score':all_values,
                      'group':np.repeat(gr,
                                        repeats = len(Values_1))})

#Performs Tukey HSD post hoc test
tukey = pairwise_tukeyhsd(endog=DF_stat['score'],
                          groups=DF_stat['group'],
                          alpha=0.05)
#Prints result
print(tukey)
```

STATS.py

E.2 Maximum Specific Growth Rate Script

A general example of how μ_{max} was calculated using Step, Curve Fit and LinReg follows.

```
#!/usr/bin/env python3
# -*- coding: utf-8 -*-
"""
Maximum specific growth rate:
Step
LinReg
Curve Fit

@author: Tor-Erik Holt Paulen
@contact: tepaulse@stud.ntnu.no
"""
import numpy as np
import scipy.stats  as ss
from scipy.optimize import curve_fit
"""
============================RAW DATA==============================
"""
#Array for three wells
Arrays = np.array(
                [[1,1,1],
                 [2,3,1],
                 [3,4,5],
                 [9,9,8],
                 [16,12,10]]
                )
#Days in the interval
Days = np.array([1,2,3,4,5])

```

```
"""
==========================STEP====================================
"""
#Calculation of growth rate using Step
mus = []
steps = len(Days)-1
for a in range(steps):
    mu1 = np.log(Arrays[a+1]/Arrays[a])/(Days[a+1]-Days[a])
    mus.append(mu1)

#Average mu for each step of the interval
for mu in mus:
    mu_avg = np.mean(mu)
    mu_std = np.std(mu)
    #Prints results
    print(f'{mu_avg:.3f} +/- {mu_std:.3f}')

"""
======================CURVE FIT=================================
"""
#Function defining a sigmoid growth curve
def func(t,K,r,y0):
    return K/(1+((K-y0)/y0)*np.exp(-r*t))

#Sorting of data
wells = ['W1','W2','W3']
organize = {}
day = {}
for w in wells:
    organize[w] = []
    day[w] = []
mu_max_Curve_Fit = []
for d in range(len(Days)):
    for i in range(3):
        day[wells[i]].append(Days[d])
        organize[wells[i]].append(Arrays[d][i])
#Calculation of maximum specific growth rate for each well
for well in wells:
    x = day[well]
    y = organize[well]
    popt, pcov = curve_fit(func, xdata=x,
                           ydata=y, bounds=([0,0,0],
                                            [20000,5,300]))
    #Adds growth rate to list of mu max
    mu_max_Curve_Fit.append(popt[1])
#Computes mean +/- std
mu_avg_L = np.mean(mu_max_Curve_Fit)
mu_std_L = np.std(mu_max_Curve_Fit)
#Prints results
print(f'{mu_avg_L:.3f} +/- {mu_std_L:.3f}')

```

```
"""
======================LINREG=======================================
"""
#Log transform
Arrays = np.log(Arrays)
#Sorting of data
wells = ['W1','W2','W3']
organize = {}
day = {}
for w in wells:
    organize[w] = []
    day[w] = []
mu_LinReg = []
for d in range(len(Days)):
    for i in range(3):
        day[wells[i]].append(Days[d])
        organize[wells[i]].append(Arrays[d][i])
#Calculation of maximum specific growth rate for each well
for well in wells:
    #Perform linear regression
    slope, icept, r, p, se = ss.linregress(day[well],
                                           organize[well])
    #Adds slope to list of mu_max
    mu_max = slope
    mu_LinReg.append(mu_max)
#Computes mean +/- std
mu_avg_L = np.mean(mu_LinReg)
mu_std_L = np.std(mu_LinReg)
#Prints results
print(f'{mu_avg_L:.3f} +/- {mu_std_L:.3f}')
```

Growth_rate_calculation.py

F Pre-inoculum monitoring

The *R. baltica* stem culture was continuously monitored for 104 days. This provide information about the state before the inoculation of all experiments. Most data points consisted of one single sample.

First Batch Experiment (nut_1) - Without Carbon Dioxide

The stem culture was in a stationary phase before inoculation, see Figure F.1. Temperature was 22 °C
and irradiation 150 µmol/m^{2}s.

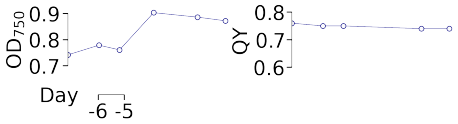

Figure F.1: Stem culture data. Days until inoculum (day 0) is indicated by scale bar.

First Batch Experiment Conwy (nut_1) - Without Carbon Dioxide

The high density stem culture was in a stationary phase before inoculation. Note that QY is only slightly above 0.7 (Figure F.2). Temperature was 22 °C
and irradiation 60 µmol/m^{2}s.

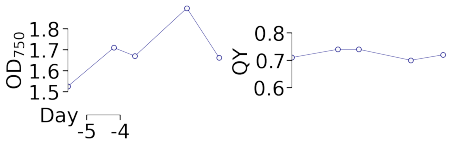

Figure F.2: Stem culture data. Days until inoculum (day 0) is indicated by scale bar.

Second Batch Experiment (nut_2) - With Carbon Dioxide

The stem culture was in a stationary phase before inoculation, but had just recovered from nutrient limitation, see Figure F.3. Temperature was 20 °C
and irradiation 26 µmol/m^{2}s.

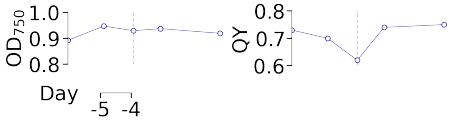

Figure F.3: Stem culture. The dashed line indicate addition of stock. Days until inoculum (day 0) is indicated by scale bar.

WP-1, pre-inoculum data

The stem culture was from the batch experiment with Conwy stock solution, and in exponential growth before inoculum, see Figure F.4. Temperature was 22.5 °C
and irradiation 100 µmol/m^{2}s 20 days prior.

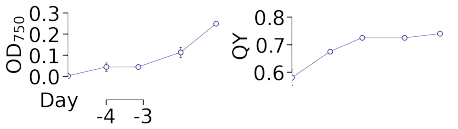

Figure F.4: Stem culture. Days until inoculum (day 0) is indicated by scale bar.

WP-2, pre-inoculum data

The stem culture was from a stationary culture that had recovered from nutrient limitation, see Figure F.5. Temperature was 20 °C and irradiation 26 µmol/m^{2}s 5 days prior.

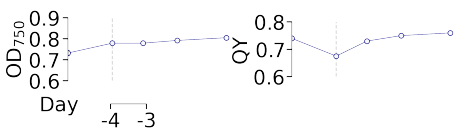

Figure F.5: Stem culture. The dashed line indicate addition of stock. Days until inoculum (day 0) is indicated by scale bar.

WP-3, pre-inoculum data

The stem culture was from a stationary culture that had recovered from nutrient limitation, see Figure F.6. Temperature was 20 °C and irradiation 26 µmol/m^{2}s 14 days prior.

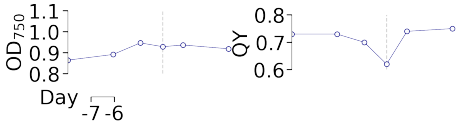

Figure F.6: Stem culture. The dashed line indicate addition of stock. Days until inoculum (day 0) is indicated by scale bar.

WP-4 & WP-C, pre-inoculum data

The stem culture was adapted to low light and had a drop in QY the day of inoculation, see Figure F.7. Temperature was 22.5 °C and irradiation 20 µmol/m^{2}s 16 days prior.

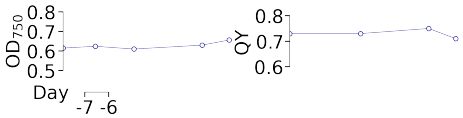

Figure F.7: Stem culture data. The dashed line indicate addition of stock. Days until inoculum (day 0) is indicated by scale bar.

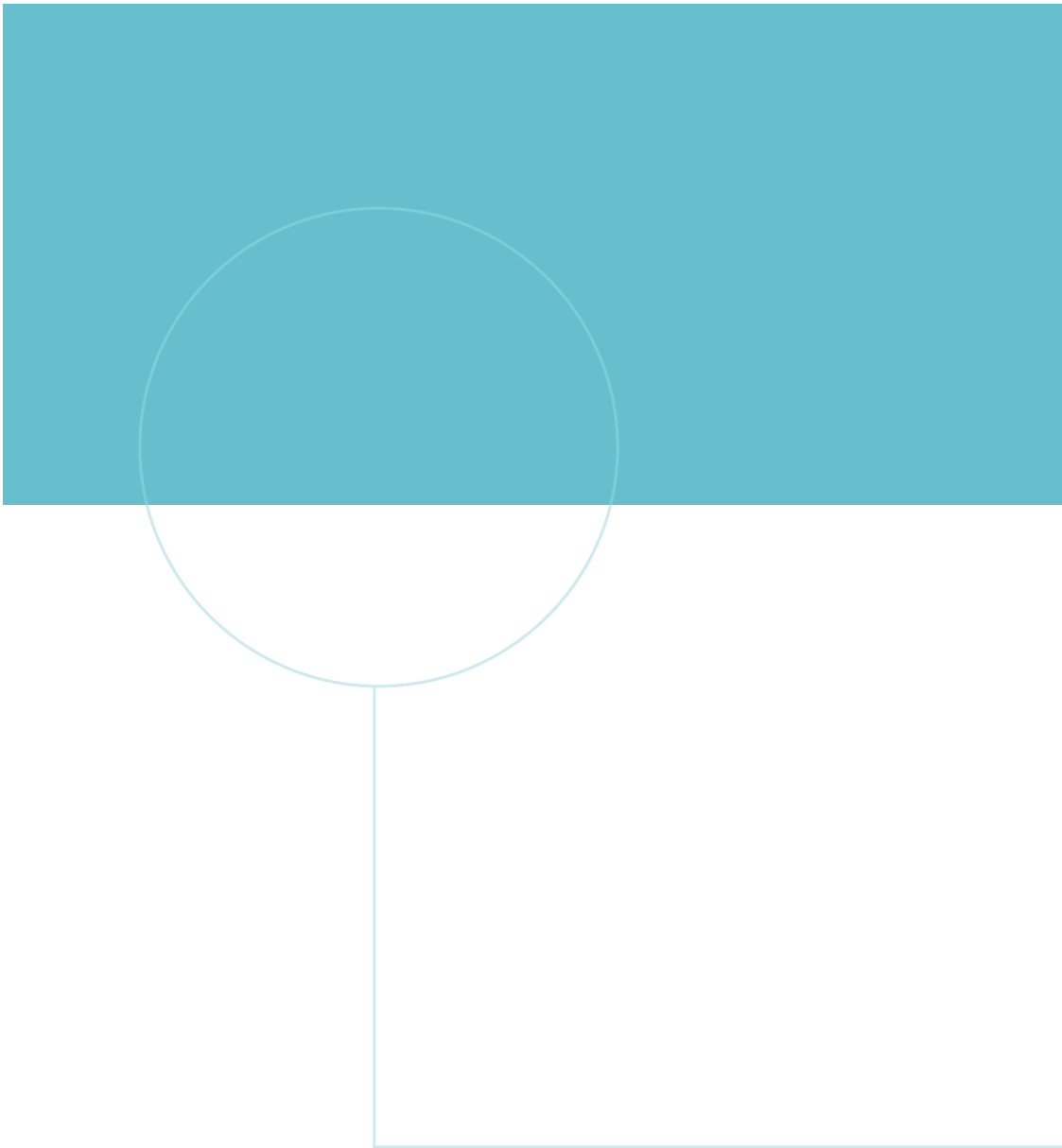

NTNU
Kunnskap for en bedre verden

CFEED